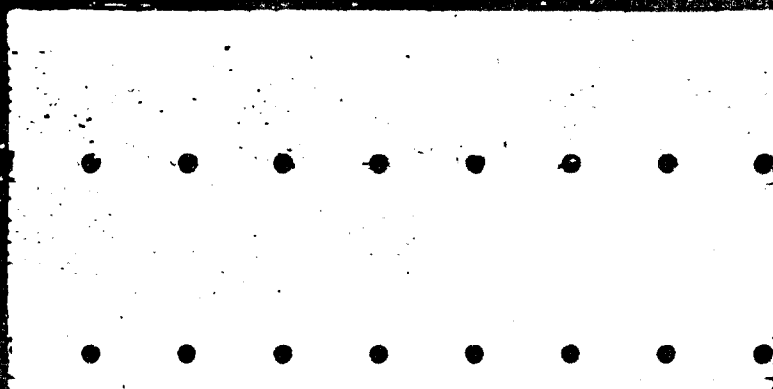POST-FLIGHT TRAJECTORY RECONSTRUC-

TION OF A MANEUVERING REENTRY

VEHICLE FROM RADAR MEASUREMENTS

THESIS

AFIT/GA/AA/82D-5   Larry N. Lillard

Approved for public release; distribution unlimited

POST-FLIGHT TRAJECTORY RECONSTRUCTION OF A

MANEUVERING REENTRY VEHICLE FROM RADAR MEASUREMENTS

THESIS

Presented to the Faculty of the School of Engineering

of the Air Force Institute of Technology

Air University

In Partial Fulfillment of the

Requirements for the Degree of

Master of Science

by

Larry N. Lillard, B.S., M.S.

Graduate Astronautical Engineering

December 1982

Acknowledgments

The ideas which are incorporated in the development of this thesis are the result of a number of authors who have addressed the subject of trajectory estimation either directly or indirectly. I have included in the bibliography a list of those authors whose publications have been most helpful; however, I would especially like to acknowledge my indebtedness to my thesis advisor, Dr. Bill Wiesel, for his generously giving of his time, his willingness to listen, and for his many helpful suggestions. I am also especially thankful for having had the opportunity to study estimation theory under Dr. Peter Maybeck.

Lastly I wish to thank my employer, the Air Force Foreign Technology Division for allowing me the time to do this research.

Contents

iii

List of Figures

List of Tables

Abstract

A technique for determining the aerodynamic parameters of a maneuvering reentry vehicle (MaRV) from post-flight analys's of radar tracking data was developed. The technique uses a sequential weighted least squares estimator which steps through the data processing batches of data sequentially. The observations consisted of angle and range measurements from a precision tracking radar located in the vicinity of the impact area. A six dimension estimator consisting of three position and three velocity components was designed for estimating the state of the RV during free flight. Two reentry estimators were developed. One, a seven dimension estimator consisting of the six elements of the free-flight estimator plus the ballistic coefficient, was designed to estimate the state during ballistic reentry. The second is the nine element MaRV estimator used once a maneuver is begun. An algorithm based on measurement residual monitoring was developed to switch adaptively from the six-state estimator to the seven-state estimator and then to the nine-state estimator. A series of numerical simulations was performed to validate the technique and its programming. Monte Carlo simulations were used to verify the accuracy of the estimator covariance matrix.

POST-FLIGHT TRAJECTORY RECONSTRUCTION OF A
MANEUVERING REENTRY VEHICLE FROM
RADAR MEASUREMENTS

I   Introduction

Objective and Scope

The objective of this thesis was to develop a technique for the efficient and accurate post-mission analysis of radar tracking data collected on the reentry vehicle (RV) of a ballistic missile. The RV was assumed to have the capability of maneuvering in the atmosphere by controlling the direction and magnitude of its lift vector. This ignores the case of a maneuverable reentry vehicle (MaRV) which might be designed to maneuver by thrusting; and therefore, could conceivably maneuver even above the atmosphere. In general, the technique which was developed and which is described in this report would not be applicable to such an RV. It was further assumed that a single radar was ideally located in the vicinity of the impact area and that the radar tracked the RV from near hori-zon break (~0° elevation) to very near impact. The accura-cies of the radar tracking data, which consists of time-tagged range, azimuth, and elevation measurements, were assumed to be consistent with those of a state-of-the-art, precision, phased-array tracking radar. The data rates were also con-sidered to be within the capability of such a radar. All of the data which were used for this investigation were

simulated. Table I lists the pertinent information relative to the simulated data where the noise on the data was simulated as zero-mean white Gaussian noise.

Table I-1

Description of Simulated Data Used in Numerical Examples

Data Rates:	
Range	1 point per second above
Azimuth	120 km and 10 points per
Elevation	second below 120 km
Data 1-σ Errors	
Range	5 m
Azimuth	$0.016°$
Elevation	$0.020°$

A further assumption is that all parameters other than those being estimated are perfectly known. This is equivalent to saying that there are no "Q-parameters", where Q-parameters are defined by Day (Ref 11) and others as those parameters affecting the observations but which, for some reason or another, are not or cannot be estimated. These include, among others, station location, biases, and a most important one for the technique developed, atmospheric density. This is not a limitation on the technique itself but on the interpretation of the covariance matrices which result.

The Research Approach

The problem of real-time tracking of a reentry vehicle based on its radar measurements has received considerable attention in the literature over the past 2-3 decades. It has been described by various authors (25) and (10) as a highly complex problem in nonlinear filtering. Since 1960, following the important work of Kalman and Bucy (Ref 20), the extended Kalman filter (EKF) has found wide application for both the ballistic reentry vehicle (BRV) tracking problem (22), (14) and later the maneuvering reentry vehicle tracking problem (10). This is owing to the real time nature of the problem where measurements need to be processed as they become available so as to "point" the radar for the next measurement. Here the primary emphasis is on maintaining track on the target.

The post-flight analysis problem is very similar to the tracking problem, but it differs in two important aspects. The similarity is that the true equations of motion governing the flight of the RV being tracked are the same in both cases. The differences involve 1), the time constraint and 2), the emphasis. In the post-flight analysis, there is virtually no time constraint and the emphasis is on accuracy. That is to say that we are interested in determining the RV state varia-bles at some epoch time* (or possibly a series of epoch times) with as much accuracy as the data will permit. It should, after all, be the data which limit the accuracy of our esti-mates and not our model. In the tracking problem, out of necessity imposed by the time constraint, many simplifying

---

*Defined as the time at which state variables are estimated.

assumptions about the dynamics model are made, e.g., a flat, nonrotating earth may be assumed. In the post-mission analysis problem, even a rotating, spherical earth is not of sufficient accuracy. Because of this emphasis on accuracy, much attention to detail is given in the later sections of this report which deal with modeling the flight of the MaRV. It should be pointed out that the term "state of the RV" as used above implies the RV state vector which consists of position, velocity, and zero, one, or three aerodynamic parameters depending respectively on whether the RV is in free flight, ballistic flight, or maneuvering flight. Quite often, in missile analysis, the aerodynamic parameters are the ones we are most interested in estimating in post-mission trajectory reconstruction.

Another advantage we have in the post-flight analysis problem over the real-time tracking problem is that we have all the data at hand to treat simultaneously, if we desire; or one point at a time, if we desire. This gives us great flexibility in designing the estimator for the post-flight analysis problem. It also forces us to make a choice. Chang et al., (Ref 8) have applied a fixed interval smoother, which consists of combining the outputs of a forward pass of an extended Kalman filter with a backward pass of the extended Kalman filter, to solve the problem. Gauss invented the method of weighted least squares (WLS) in 1795 to solve an astrodynamical problem by treating all of the available observations simultaneously. The technique, which was developed

4

for this research is a very flexible algorithm which is based
on the method of WLS. The user, by specifying the batch size
(i.e., the number of observations to process in a given batch),
can operate the program in either a batch WLS mode where
all data are treated simultaneously; or as an EKF treating
each data point (range, azimuth, and elevation at a single
time) separately; or any place in between as a sequential WLS
estimator.

Novel Features

The algorithm which was developed and programmed for
this thesis research is presented in detail in the remaining
chapters of this report. It has two novel features. One is
the way in which the trajectory partials, which are required
in the weighted-least-squares-differential-correction process,
are calculated. The other is a technique for adaptively
switching from the six-element state vector used for free-
flight estimation to the seven-element state vector used for
ballistic-reentry-flight and then from the seven-element state
vector to the nine-element MaRV state vector.

The standard technique for calculating trajectory par-
tials in both satellite and missile trajectory reconstruction
is to integrate numerically a set of second order, ordinary
differential equations called variational equations. See for
example Refs (1), (27) and (34). The variational equations
have as their dependent variables the partial derivatives of
the total acceleration with respect to the parameters to be
estimated. There are at least (free-flight) 18 of these second

5

order (corresponding to 36 first order) differential equations to be integrated. They are typically passed to the same integration routine which integrates the equations of motion. This represents a significant computational burden on a technique, whether batch or sequential, which is at best slow; however, because the WLS differential correction technique is inherently iterative, the accuracies of the partials need not be as great as those of the state variable themselves. The validity of this claim is demonstrated in Chapter IV of this report where it is shown that the batch least squares estimator converges in two or three iterations with good initial, estimates of the state variables.

As an example, a spherical harmonic series of zonal harmonics, representing the potential of an oblote spheroid, is used for accurately modeling the missile's acceleration due to gravity; whereas, the predominate term of this series, that due to a spherical earth, is quite adequate for partials calculations. As a result of this less demanding requirement on the partials' accuracies, a very simple Taylor's series expansion is used to equate the state, X_{i+1} at some time t_{i+1} with the state, X_i at some earlier time t_i (i.e., numerically integrate $\dot{X}_i$). This is then used in calculating the state transition matrix, $\Phi(t_{i+1}, t_i)$ which is central to the trajectory partials' calculations as well as to propagating the state covariance matrix in time. The approximations mentioned above, as well as others used in the partials calculations, are given in complete detail in Appendix B along with all the partials

6

used in the development of the state transition matrix. It should be emphasized that these approximations are only used in partials calculations.

The other unique feature of the technique which was developed is a method for adaptively sensing when a higher order estimator is required and then switching to the higher order estimator. As was mentioned earlier, it was assumed that the data collection began as the RV broke the radar's horizon meaning that several minutes of free-flight data were collected. Free-flight is that phase of the trajectory after booster burnout and prior to reentry when the RV is accelerated only by the force of the earth's gravity. During this phase of flight, the RV state vector is given as

$$\underline{X} = (X, Y, Z, \dot{X}, \dot{Y}, \dot{Z})^T$$

where X, Y, and Z are coordinates of the RV's position vector and $\dot{X}$, $\dot{Y}$, and $\dot{Z}$ are coordinates of the RV's velocity in some arbitrarily chosen cartesian coordinate system. In this context, the state vector is a vector of those parameters we wish to estimate at some given time called the epoch time such that given the state vector at epoch and the equation of motion for each state variable, we can predict the state at any other time within the interval during which the equations are valid. After reentering the earth's atmosphere, the RV begins to experience an additional force, that due to atmospheric drag. During this ballistic-reentry-phase* the RV's

_____
*Even a MaRV initially reenter along a ballistic trajectory. The MaRV state vector is given in later sections of this report.

7

state vector is given as

$$\underline{X} = (X,Y,Z,\dot{X},\dot{Y},\dot{Z},\beta)^T$$

where β is a parameter associated with the drag called the ballistic coefficient. During free-flight, the ballistic coefficient is completely unobservable (meaning it can not be estimated from the data). The transition from free-flight to reentry, where β *is* observable, is a gradual one with no clear cut demarcation; therefore, if one is using a sequential estimator to step through the data, there must be a way to determine when this transition from free-flight to ballistic-reentry-flight has occurred. In Chapter III of this report, a method based on monitoring the root-mean-square (RMS) error of the data residuals is presented for this purpose.

Report Organization

The remaining sections of this report describe in detail the necessary calculations for the post-flight analysis of radar tracking data collected on a maneuvering reentry vehicle. Chapter II presents the equations necessary for accurately modeling the flight of a MaRV. These include the equations of motion, various transformations need, and models of the earth's atmosphere and the RV's drag. In Chapter III, the algorithm for estimating the trajectory and aerodynamic parameters from the noise corrupted radar measurements is developed. This starts with the basic weighted least squares (WLS) estimator for nonlinear equations and shows how this is related to the minimum variance (MV) and maximum likelihood

8

(ML) estimators. A sequential estimator with and without a priori covariance on the initial conditions is presented. A technique for adaptively switching from the free-flight estimator to the BRV estimator, to the MaRV estimator is given, and a method for determining close initial estimates is suggested. Chapter IV discusses the numerical simulations that went into developing and testing the computer program which was developed. Two numerical examples are presented in detail which demonstrate the operation of the program using simulated data. Chapter V presents a brief summary and suggests some areas where further study is required. Two appendices are also included. Appendix A describes the oblate spheroid which is used as the model of the geometric shape of the earth. Appendix B defines the state transition matrix and presents the equations used in deriving the partial derivatives of the state transition matrix, and then lists all the partials thus derived.

9

II Trajectory Generation Equations and Methods

This chapter presents the equations necessary for accurately modeling the flight of a ballistic missile's MaRV. These include the differential equations of motion and a numerical integration scheme for propagating the MaRV's state vector in time. Also included are the equations for transforming the position of the MaRV in the computational coordinate system, the one in which the equations of motion are expressed and integrated, to radar range, azimuth, and elevation for a given radar station. This transformation will be necessary for the least squares-differential correction algorithm presented in Chapter III which compares the observed radar measurements to the calculated radar measurements based on an assumed or estimated state vector for the MaRV. Also included in this chapter are models of the earth's atmosphere and the drag model for a class of sphere-cone shaped RV's.

Coordinate Systems and Transformations

Several different coordinate systems are useful for expressing the trajectory and radar related equations. The most important ones are described in this section. The computational coordinate system, the one in which the equations of motion are expressed and integrated, is the earth-centered-inertial (ECI) cartesian coordinate system depicted in Figure II-1. The origin of this coordinate system is at the center of

10
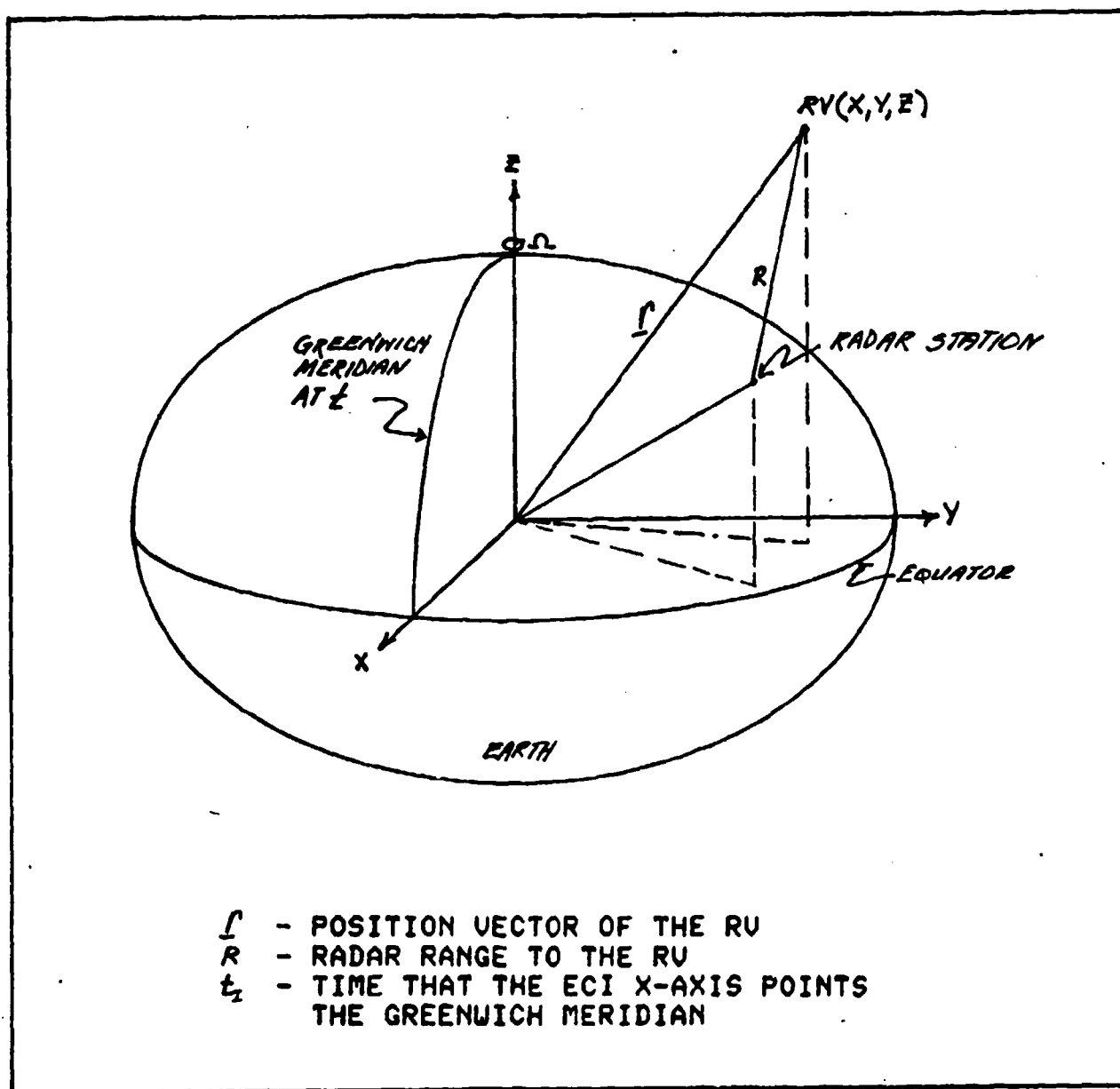
FIG II-1   ECI COORDINATES AND RV-RADAR GEOMETRY

the ellipsoidal earth model*; the X-Y plane is the equatorial plane of the earth; and the Z-axis is coincident with the earth's axis of rotation. This coordinate system is fixed in inertial space with the X-axis passing through the Greenwich meridian at some arbitrarily chosen initialization time, t_I. For this analysis, t_I is taken as the time of the first radar observation.

Figure II-1 also shows the radar-RV geometry. The radar location is typically expressed in geographic coordinates-geodetic latitude (ϕ^*), longitude (λ), and height (h) above the earth's surface. These coordinates are also convenient for displaying and plotting the RV's position as a function of time. Figure II-2 identifies the geographic coordinates of the radar station.

Two other coordinate systems which are useful in describing the trajectory estimation problem are two radar coordinate systems which are shown in Figure II-3. One is a left-handed cartesian coordinate system (x,y,z) called the north-east-up (NEU) system and the other is a spherical coordinate system (R,Az,E). The origin of these two coordinate systems is the radar. The z-axis is along the local geodetic vertical and azimuth an elevation are measured as shown in the figure.

The final coordinate system to be described in this section is the earth-centered-rotating (ECR) system. It

---

*See Appendix A for a description of the reference ellipsoid used to model the earth.

12

h_s - ALTITUDE OF THE RADAR STATION
ϕ_s' - GEOCENTRIC LATITUDE OF THE RADAR STATION
ϕ_s - GEODETIC LATITUDE OF THE RADAR STATION
λ - LONGITUDE OF THE RADAR STATION
R - RADAR RANGE TO THE RV
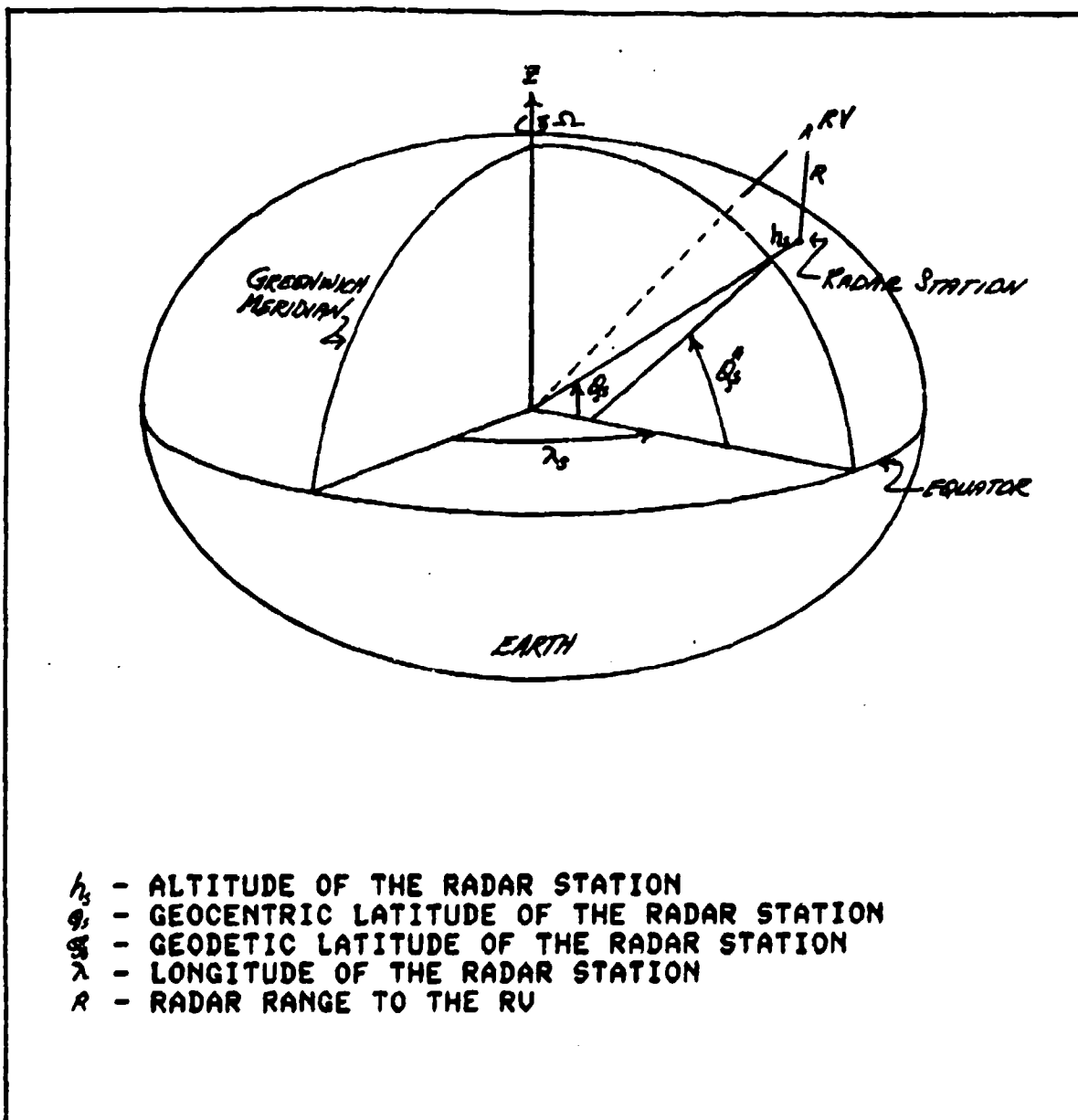
FIG II-2   GEOCENTRIC COORDINATES OF THE RADAR STATION

$$R = (x^2 + y^2 + z^2)^{1/2}$$

$$A_z = TAN^{-1}(y/x)$$

$$E = SIN^{-1}(z/R)$$

$x = R \cos E \cos A_z$
$y = R \cos E \sin A_z$
$z = R \sin E$

RADAR STATION

z (GEODETIC UP)

RV (x, y, z)
(R, A_z, E)

x (NORTH)

y (EAST)

R
E
A_z

R — RADAR RANGE
A_z — RADAR AZIMUTH
E — RADAR ELEVATION
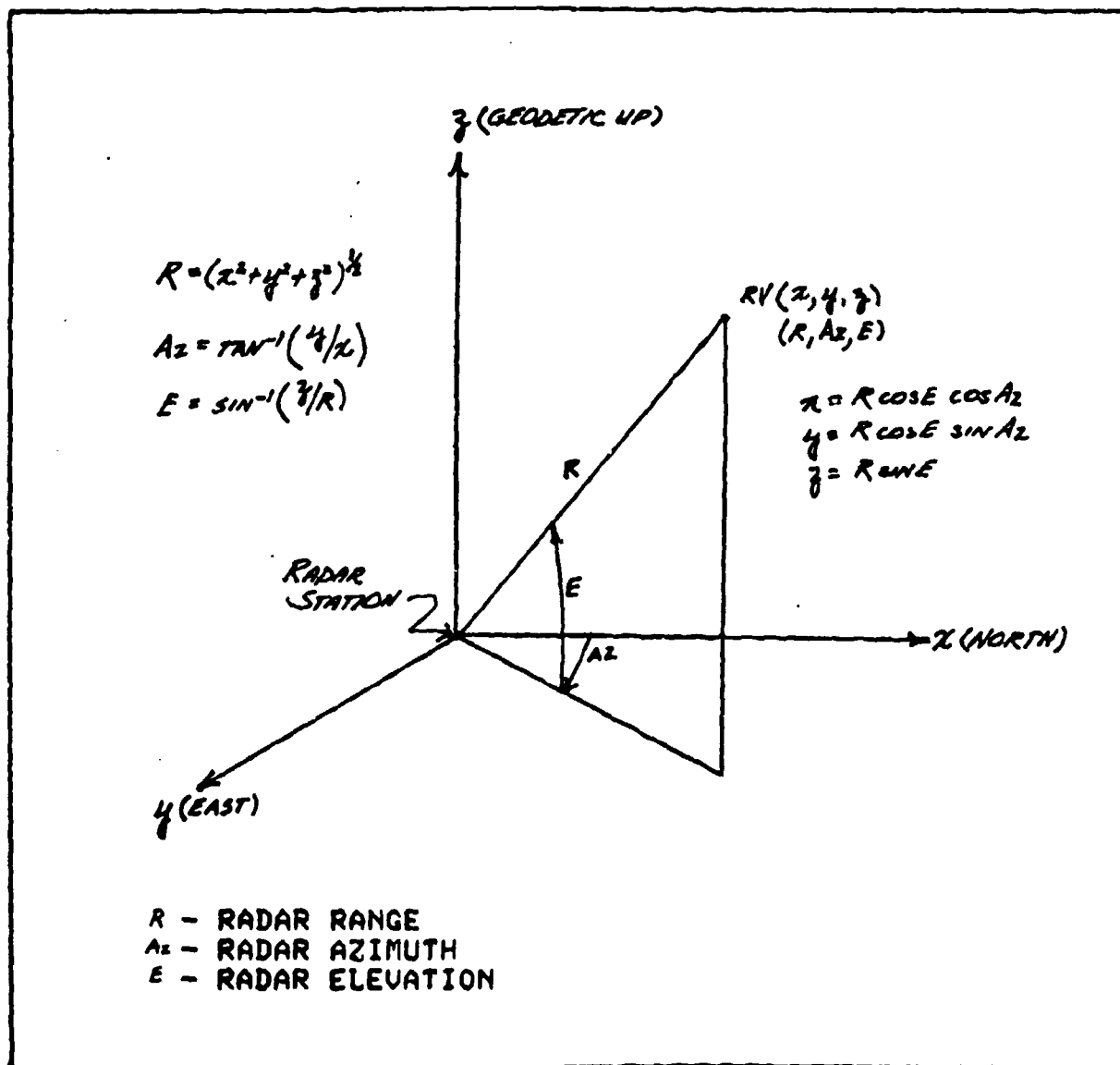
FIG II-3   RADAR STATION COORDINATES

differs from the ECI coordinate system only in that the X_R-axis always points out the Greenwich meridian. The ECI and ECR coordinate are related by the following transformation at any given time t_i.

$$\begin{bmatrix} X_R \\ Y_R \\ Z_R \end{bmatrix} = \begin{bmatrix} \cos(\Delta t \cdot \Omega) & \sin(\Delta t \cdot \Omega) & 0 \\ -\sin(\Delta t \cdot \Omega) & \cos(\Delta t \cdot \Omega) & 0 \\ 0 & 0 & 1 \end{bmatrix} \begin{bmatrix} X \\ Y \\ Z \end{bmatrix} \qquad \text{(II-1)}$$

where

$\Delta t = t_i - t_I$

Ω is the earth's rotation rate and

X_R, Y_R, Z_R are coordinates in the ECR reference frame

The geographic coordinates (φ^*, λ, h) are related to the ECR coordinates by the following equations.

$$X_R = (r_e + h) \cos\varphi \cdot \cos\lambda \qquad \text{(II-2)}$$

$$Y_R = (r_e + h) \cos\varphi \sin\lambda \qquad \text{(II-3)}$$

$$Z = (r_e + h) \sin\varphi \qquad \text{(II-4)}$$

$$h = \left(X_R^2 + Y_R^2 + Z^2\right)^{1/2} - r_e \qquad \text{(II-5)}$$

$$\varphi = \sin^{-1}(Z/r) \qquad \text{(II-6)}$$

$$\lambda = \tan^{-1}(Y_R / X_R) \qquad \text{(II-7)}$$

15

and

$$\varphi^* = \tan^{-1}\left(\frac{a^2}{b^2} \tan \varphi\right) \qquad (\text{II-8})$$

$$r_e = b/(1 - e^2 \cos^2 \varphi)^{\frac{1}{2}} \qquad (\text{II-9})$$

where

φ is the geocentric latitude

r_e is the local radius of the earth

a is the semi-major axis of the ellipsoidal earth model

b is the semi-minor axis of the ellipsoidal earth model, and

e is the eccentricity of the ellipsoidal earth model.

Equations (II-8) and (II-9) are derived in Appendix A. Appendix A, which describes in detail the reference ellipsoid used to model the shape of the earth, also gives the numerical values of the constants a, b, and e.

The final transformation which will be necessary to transform the ECI coordinates of the RV to radar observation coordinates (R, Az, and E) is the following

$$\begin{bmatrix} x \\ y \\ z \end{bmatrix} = \begin{bmatrix} -\sin \varphi_s^* \cos \lambda_s & -\sin \varphi_s^* \sin \lambda_s & \cos \varphi_s^* \\ -\sin \lambda_s & \cos \lambda_s & 0 \\ \cos \varphi_s^* \cos \lambda_s & \cos \varphi_s^* \sin \lambda_s & \sin \varphi_s^* \end{bmatrix} \begin{bmatrix} X_R - X_s \\ Y_R - Y_s \\ Z - Z_s \end{bmatrix}$$

where φ_s^*, λ_s, and h_s are the geographic coordinates of the radar station (Fig II-2) and X_s, Y_s and Z_s are the

coordinates of the radar station in the ECR reference frame given by

$$X_s = (h_s + r_{e_s}) \cos \varphi_s \cos \lambda_s \qquad (II-11)$$

$$Y_s = (h_s + r_{e_s}) \cos \varphi_s \sin \lambda_s \qquad (II-12)$$

$$Z_s = (h_s + r_{e_s}) \sin \varphi_s \qquad (II-13)$$

where r_{es} is the radius of the earth at the radar station and φ_s is the geocentric latitude of the radar station. φ_s and r_{es} are determined from φ_s^* using (II-8) and (II-9). Then

$$R = (x^2 + y^2 + z^2)^{\frac{1}{2}} \qquad (II-14)$$

$$Az = \tan^{-1}(y/x) \qquad (II-15)$$

$$E = \sin^{-1}(y/R)$$
$$\qquad (II-16)$$

Free-Flight Equations of Motion

For a reentry vehicle, unpowered and still above the earth's atmosphere, the only significant force acting on it is that due to the earth's gravity. The acceleration due to gravity is typically derived from the gravity potential. Wolaver (Ref 38) shows that the earth's gravity potential, U is a solution to Laplaces equation

$$\frac{\partial^2 U}{\partial X^2} + \frac{\partial^2 U}{\partial Y^2} + \frac{\partial^2 U}{\partial Z^2} = 0 \qquad\qquad (II-17)$$

The most general solution to Eq (II-17) for a unit mass exterior to the earth is given as an infinite spherical harmonic series which is a function of r, the distance from the earth's center; φ, the geocentric latitude; and λ, the longitude

$$U = \mu/r \left[1 - \sum_{N=2}^{\infty} \left(\frac{a}{r}\right)^N J_N P_N(sin\varphi) - \sum_{N=2}^{\infty}\sum_{M=1}^{N} J_N^M \left(\frac{a}{r}\right)^N P_N^M(sin\varphi)\cos(\lambda - \lambda_N^M) \right] \qquad (II-18)$$

where,

  μ is the earth's mass times the universal gravity constant

  a is the mean equitorial radius

  $P_n(sin\varphi)$, $P_N^M(sin\varphi)$ are the Legendre polynomials and

  J_N, J_N^M, λ_N^M are constants determined from satellite data.

Typically, some truncated form of Eq (II-18) is used for satellite and missile trajectory simulation and analysis depending on the accuracy which is required. A particularly convenient form is one which assumes the dependence on longitude to be negligible. This truncated expression (Ref 5)

$$U = \mu/r \left[1 - \sum_{N=2}^{\infty} J_N \left(\frac{a}{r}\right)^N P_N(sin\varphi) \right] \qquad\qquad (II-19)$$

is called the zonal potential. The first four terms of the zonal potential were used in this investigation to model the

18

earth's gravity. Values of the constants used and the first
three Legendre polynomials are given below

$$P_2(\sin\varphi) = 0.5(3\sin^2\varphi - 1) \tag{II-20}$$

$$P_3(\sin\varphi) = 0.5\sin\varphi(5\sin^2\varphi - 3) \tag{II-21}$$

$$P_4(\sin\varphi) = \frac{1}{8}(35\sin^4\varphi - 30\sin^2\varphi + 3) \tag{II-22}$$

$$a = 6378135.\ m \tag{II-23}$$

$$J_2 = 1082.616 \times 10^{-6} \tag{II-24}$$

$$J_3 = -2.53 \times 10^{-6} \tag{II-25}$$

$$J_4 = -1.66 \times 10^{-6} \tag{II-26}$$

$$\mu = 398600.8\ km^3/sec^2 \tag{II-27}$$

The zonal potential is considered sufficiently accurate for
the application being considered here and the advantage is
that by setting

$$\sin\varphi = z/r \tag{II-28}$$

it can be written completely in terms of the computational
coordinate system. This eliminates the need to transform from
a non-inertial system to the inertial system at each integra-
tion step as would be required if the time dependent terms

19

were retained. The disadvantage of using this potential function is that the $J_2{}^2$ term is neglected. The magnitude of the $J_2{}^2$ term, which represents the Earth's equatorial ellipticity, has the same order as the J_3 zonal harmonic and perturbs motion as much as any zonal harmonic except J_2. Thus for other applications, the potential represented by Eq (II-19) may not give sufficient accuracy.

The acceleration due to gravity is given as the negative of the gradient of the potential function.

$$\underline{g} = - \nabla U \tag{II-29}$$

In the ECI reference frame, the components of the acceleration due to gravity become

$$\ddot{X}_g = -\frac{\mu X}{r^3}\left[1 + J_2\left(\frac{a}{r}\right)^2 \frac{3}{2}\left(1 - 5\frac{Z^2}{r^2}\right) + J_3 \frac{a}{r}\left(\frac{a}{r}\right)^3 \frac{5}{2}\left(3 - 7\frac{Z^2}{r^2}\right) \right.$$
$$\left. + J_4\left(\frac{a}{r}\right)^4 \frac{5}{8}\left(-3 + 42\frac{Z^2}{r^2} - 63\frac{Z^4}{r^4}\right) \right] \tag{II-30}$$

$$\ddot{Y}_g = \ddot{X}_g \frac{Y}{X} \tag{II-31}$$

$$\ddot{Z}_g = -\frac{\mu Z}{r^3}\left[1 + J_2\left(\frac{a}{r}\right)^2 \frac{3}{2}\left(3 - 5\frac{Z^2}{r^2}\right) + J_3 \left(\frac{a}{r}\right)^3 \frac{5}{2}\frac{3}{2}\left(-1 + 10\frac{Z^2}{r^2} - \frac{35}{3}\frac{Z^4}{r^4}\right) \right.$$
$$\left. + J_4\left(\frac{a}{r}\right)^4 \frac{5}{8}\left(-15 + 70\frac{Z^2}{r^2} - 63\frac{Z^4}{r^4}\right) \right] \tag{II-32}$$

The RV state vector during free flight then contains the six elements of position and velocity

$$\underline{X} = \left(X, Y, Z, \dot{X}, \dot{Y}, \dot{Z}\right)^T \tag{II-33}$$

20

where the state at any time is determined by numerically integrating Eqs (II-30), (II-31), and (II-32) from some initial state.

BRV Equations of Motion

Once the RV reenters the earth's atmosphere, somewhere below 120 km altitude, it begins to experience an additional force due to aerodynamic drag. Even a MaRV reenters along a ballistic trajectory, so that for a portion of its flight the equations of motion of a MaRV are the same as those of a BRV. The aerodynamic drag force acts opposite to the air relative velocity vector and is calculated as the product of three quantities:

    (i)   the dynamic pressure, q

    (ii)   the nondimensional drag force coefficient, C_D and

    (iii) a reference area, A

The dynamic pressure, q depends on the air density, ρ and the relative velocity between the RV and surrounding air, V_a^* in the following manner

$$q = \frac{1}{2}\rho V_a^2 \qquad (\text{II-34})$$

Choosing A as the cross sectional area of the RV and defining the ballistic coefficient, β as

$$\beta = \frac{m}{C_D A} \qquad (\text{II-35})$$

---

*In this analysis, winds are assumed to be negligible, so that air relative velocity is velocity relative to the rotating earth.

21

where

m is the mass of the RV,

the acceleration due to the drag force is given by the vector equation

$$\underline{A}_D = -g \frac{1}{\beta} \hat{e}_v \qquad (II-36)$$

where

$\hat{e}_v$ is the unit vector in the direction of $\underline{V}_a$.

In the ECI reference frame, the components of the drag acceleration are determined to be

$$\ddot{X}_D = -\frac{\rho V_a}{2\beta} \dot{X}_a \qquad (II-37)$$

$$\ddot{Y}_D = -\frac{\rho V_a}{2\beta} \dot{Y}_a \qquad (II-38)$$

$$\ddot{Z}_D = -\frac{\rho V_a}{2\beta} \dot{Z}_a \qquad (II-39)$$

where $\dot{X}_a$, $\dot{Y}_a$, and $\dot{Z}_a^*$ are the components of the air relative velocity in the ECI reference frame given by

$$\dot{X}_a = \dot{X} + \Omega Y \qquad (II-40)$$

$$\dot{Y}_a = \dot{Y} - \Omega X \qquad (II-41)$$

$$V_a = \left[(\dot{X} + \Omega Y)^2 + (\dot{Y} - \Omega X)^2 + \dot{Z}^2 \right]^{\frac{1}{2}} \qquad (II-42)$$

where $\dot{X}$, $\dot{Y}$, and $\dot{Z}$ are the components of the inertial velocity

---

$* \quad \dot{Z}_a \equiv \dot{Z}$

22

in the ECI coordinate system and X, Y, and Ω are as previously defined.

The total acceleration of the BRV is the sum of the gravity acceleration and the drag acceleration. So the equations of motion of the BRV in ECI coordinates are given as

$$\ddot{X} = \ddot{X}_g - \rho \frac{V_a}{2\beta} \dot{X}_a \qquad (\text{II-43})$$

$$\ddot{Y} = \ddot{Y}_g - \rho \frac{V_a}{2\beta} \dot{Y}_a \qquad (\text{II-44})$$

$$\ddot{Z} = \ddot{Z}_g - \rho \frac{V_a}{2\beta} \dot{Z} \qquad (\text{II-45})$$

where $\ddot{X}_g$, $\ddot{Y}_g$, and $\ddot{Z}_g$ are given by Eqs (II-30), (II-31), and (II-32).

Although BRV flight is somewhat idealized in that there is almost always some lift due to non-zero angle of attack or asymmetric ablation, the net effect is usually assumed to be negligible in the motion model of high performance ballistic RV's. The state vector for the reentry of a ballistic RV is

$$\underline{X} = \left(X, Y, Z, \dot{X}, \dot{Y}, \dot{Z}, \beta \right)^T \qquad (\text{II-46})$$

If the unintentional lift mentioned above becomes significant, then the ballistic RV model must be modified and will be the same as that of a MaRV.

MaRV Equations of Motion

When the reentry vehicle undertakes a maneuver, a third force, aerodynamic lift is introduced. The lift force

23

is in a plane perpendicular to the air relative velocity.
One method which allows the lift acceleration to be formulated
in a manner similar to the drag acceleration is to decompose
the lift force into two orthogonal components. One component
is chosen to be in a direction whose unit vector, $\hat{e}_T$ is given
as (see Fig II-4)

$$\hat{e}_T = \frac{\underline{r} \times \underline{V}_a}{|\underline{r} \times \underline{V}_a|} \qquad (II-47)$$

The other component is chosen to be in a direction whose unit
vector, $\hat{e}_c$ is given as

$$\hat{e}_c = \frac{\underline{V}_a}{|\underline{V}_a|} \times \hat{e}_T \qquad (II-48)$$

These two components of the lift force are called turn, F_T and
climb, F_c. Figure II-4 shows the geometry of the lift compo-
nents in relationship to $\underline{V}_a$ and the drag force, $\underline{F}_D$. With
these definitions, turn acceleration and climb acceleration
are given as

$$\underline{A}_T = g \frac{C_T^* A}{m} \hat{e}_T \qquad (II-49)$$

$$\underline{A}_c = g \frac{C_c^* A}{m} \hat{e}_c \qquad (II-50)$$

where

C_T^* is the non-dimensional turn force coefficient, and

C_c^* is the non-dimensional climb force coefficient

To simplify the notation, two new terms are introduced, C_T,

24
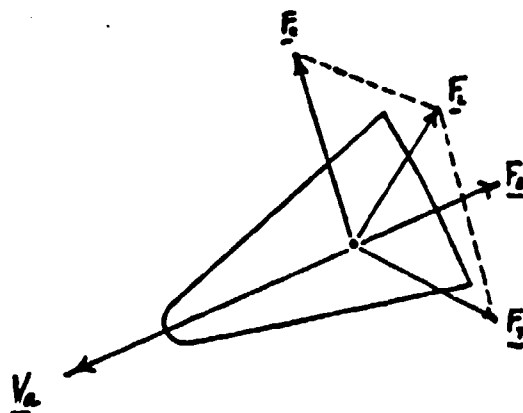
LIFT, F_L IS NORMAL TO THE VELOCITY V_a

TURN, F_T AND CLIMB, F_C ARE COMPONENTS OF LIFT

TURN IS IN THE LOCAL HORIZONTAL PLANE

CLIMB IS NORMAL TO BOTH F_T AND V_a

DRAG, F_D IS OPPOSITE TO V_a

FIG II-4   GEOMETRY OF THE AERODYNAMIC FORCES, DRAG AND LIFT

25

the turn parameter, and C_c, the climb parameter, defined below

$$C_T = \frac{C_T^\bullet A}{2m} \tag{II-51}$$

$$C_c = \frac{C_c^\bullet A}{2m} \tag{II-52}$$

The ECI components of the turn and climb accelerations may then be written as

$$\ddot{X}_T = \rho V_a^2 C_T \frac{(Y\dot{Z} - Z\dot{Y}_a)}{T} \tag{II-53}$$

$$\ddot{Y}_T = \rho V_a^2 C_T \frac{(Z\dot{X}_a - XZ)}{T} \tag{II-54}$$

$$\ddot{Z}_T = \rho V_a^2 C_T \frac{(X\dot{Y}_a - Y\dot{X}_a)}{T} \tag{II-55}$$

$$\ddot{X}_c = \rho V_a C_c \left[\frac{\dot{Y}_a(X\dot{Y}_a - Y\dot{X}_a) - \dot{Z}(Z\dot{X}_a - XZ)}{T} \right] \tag{II-56}$$

$$\ddot{Y}_c = \rho V_a C_c \left[\frac{\dot{Z}(Y\dot{Z} - Z\dot{Y}_a) - \dot{X}_a(X\dot{Y}_a - Y\dot{X}_a)}{T} \right] \tag{II-57}$$

$$\ddot{Z}_c = \rho V_a C_c \left[\frac{\dot{X}_a(Z\dot{X}_a - X\dot{Z}) - \dot{Y}_a(Y\dot{Z} - Z\dot{Y}_a)}{T} \right] \tag{II-58}$$

where

$$T = \left[(Y\dot{Z} - \dot{Y}_a Z)^2 + (Z\dot{X}_a - X\dot{Z})^2 + (X\dot{Y}_a - Z\dot{X}_a)^2 \right]^{\frac{1}{2}} \tag{II-59}$$

Now all the equations necessary for representing the equations of motion of the MaRV completely in the computational-ECI reference frame have been given. In some cases

26

the accelerations have been expressed in terms of air rela-
tive coordinates because of the convenience of notation;
however, in those cases, expressions relating the air rela-
tive coordinates to inertial coordinates have been given.
Symbolically then, the equations of motion for a MaRV in the
ECI reference frame are given as

$$\ddot{X} = \ddot{X}_g + \ddot{X}_D + \ddot{X}_r + \ddot{X}_c \tag{II-60}$$

$$\ddot{Y} = \ddot{Y}_g + \ddot{Y}_D + \ddot{Y}_r + \ddot{Y}_c \tag{II-61}$$

$$\ddot{Z} = \ddot{Z}_g + \ddot{Z}_D + \ddot{Z}_r + \ddot{Z}_c \tag{II-62}$$

where $\ddot{X}_g$, $\ddot{Y}_g$, and $\ddot{Z}_g$ are given by Eqs (II-30), (II-31), and
(II-32); $\ddot{X}_D$, $\ddot{Y}_D$, and $\ddot{Z}_D$ are given by Eqs (II-37), (II-38), and
(II-39); $\ddot{X}_T$, $\ddot{Y}_T$, and $\ddot{Z}_T$ are given by Eqs (II-53), (II-54), and
(II-55); and $\ddot{X}_c$, $\ddot{Y}_c$, and $\ddot{Z}_c$ are given by Eqs (II-56), (II-57),
and (II-58).

Numerical Integration of Equations of Motion

The equations of motion given by Eqs (II-60), (II-61)
and (II-62) represent a system of coupled, second order, non-
linear ordinary differential equations which cannot be solved
in closed form. They must be numerically integrated from
some initial conditions on X, Y, Z, $\dot{X}$, $\dot{Y}$, and $\dot{Z}$ to give the
position and velocity at any other time. A numerical inte-
gration scheme which is used extensively in ballistic missile
trajectory simulation and estimation is a fourth-order

27

Runge-Kutta method modified by Nyström to handle the second order equation. Kreyszig (Ref 21) calls this the Runge-Kutta-Nyström method. Its popularity for propagating the state of a ballistic missile is due to the fact that it is self starting; it has small round off error for small step size; the step size may be varied at will from step to step; and it is straightforward to implement. The following description follows essentially that of (Ref 33).

Let the equations of motion given in the previous section be represented by the functional relationship

$$\ddot{r} = f(t, r, \dot{r})$$

(II-63)

where

$$\ddot{r} \equiv \begin{bmatrix} \ddot{X} \\ \ddot{Y} \\ \ddot{Z} \end{bmatrix}, \quad \dot{r} \equiv \begin{bmatrix} \dot{X} \\ \dot{Y} \\ \dot{Z} \end{bmatrix}, \quad r \equiv \begin{bmatrix} X \\ Y \\ Z \end{bmatrix}$$

(II-64)

Furthermore, let $r(t)$ denote the solution of Eq (II-63) corresponding to the initial conditions $r(t_o) = r_o$ and $\dot{r}(t_o) = \dot{r}_o$. Let r_j and $\dot{r}_j$ denote approximations to $r(t_j)$ and $\dot{r}(t_j)$ and set $h = t_{j+1} - t_j$. To obtain the approximations r_{j+1} and $\dot{r}_{j+1}$ we calculate as follows

$$K_1 = h f(t_j, r_j, \dot{r}_j)$$

(II-65)

28

$$\underline{K}_2 = h\underline{f}\left(t_j + \frac{h}{2}, \underline{r}_j + \frac{h}{2}\dot{\underline{r}}_j + \frac{h}{8}\underline{K}_1, \dot{\underline{r}}_j + \frac{1}{2}\underline{K}_1\right) \qquad \text{(II-66)}$$

$$\underline{K}_3 = h\underline{f}\left(t_j + \frac{h}{2}, \underline{r}_j + \frac{h}{2}\dot{\underline{r}}_j + \frac{h}{8}\underline{K}_1, \dot{\underline{r}}_j + \frac{1}{2}\underline{K}_2\right) \qquad \text{(II-67)}$$

$$\underline{K}_4 = h\underline{f}\left(t_j + h, \underline{r}_j + h\dot{\underline{r}}_j + \frac{h}{2}\underline{K}_3, \dot{\underline{r}}_j + \underline{K}_3\right) \qquad \text{(II-68)}$$

After the above are computed, the new values $\underline{r}_{j+1}$ and $\dot{\underline{r}}_{j+1}$ are then obtained as

$$\underline{r}_{j+1} = \underline{r}_j + h\left[\dot{\underline{r}}_j + \frac{1}{6}\left(\underline{K}_1 + \underline{K}_2 + \underline{K}_3\right)\right] \qquad \text{(II-69)}$$

$$\dot{\underline{r}}_{j+1} = \dot{\underline{r}}_j + \frac{1}{6}\left[\underline{K}_1 + 2\underline{K}_2 + 2\underline{K}_3 + \underline{K}_4\right] \qquad \text{(II-70)}$$

Thus, starting with $\underline{r}_o$ and $\dot{\underline{r}}_o$ as known quantities the integration subroutine which consists basically of Eqs (II-65) through (II-70), repeats itself cyclically until as many steps, h as may be desired have been completed.

Drag Models

As Athans (Ref 3) states, the ballistic coefficient is an important parameter for several reasons. This parameter physically represents the ratio between the mass of the RV and the effective drag area along the velocity vector. Thus, knowledge of this coefficient reveals some telltale characteristics about the missile. In addition, an accurate ß-estimate generally imposes a more stringent requirement than

29

do other criteria on the estimator performance and, therefore, offers to us a convenient method of evaluating estimator accuracy or comparing estimator results.

The ballistic coefficient given in Eq (II-35)

$$\beta = m/C_D A \tag{II-35}$$

is not a constant because the drag coefficient, C_D varies with Mach number for an RV of given geometric shape. For sphere-cone RV's, C_D is parameterized as functions of the vehicle half-cone angle, bluntness-ratio (radius of nose/radius of base); and Mach number. A series of unpublished tables from wind tunnel test of sphere-cone RV's is stored internal to the program and the user supplies an estimate of the half cone angle and bluntness ratio. Figure II-5 shows the theoretical drag curve reproduced from Ref (35) for a 6° half-cone-angle, 0.21-bluntness-ratio, sphere-cone RV.

Since tables don't lend themselves readily to analytic differentiation, an analytic expression for drag is needed for the partials necessary in the differential correction process. The drag model used for this purpose is (Ref 34)

$$C_D = k_1 + \frac{k_2}{M_1} + \frac{k_3}{M^2} \tag{II-71}$$

where M is Mach Number and k_1, k_2 and k_3 are related to the RV half-cone angle and bluntness ratio and are determined from least squares fits of the drag tables to Eq (II-71).
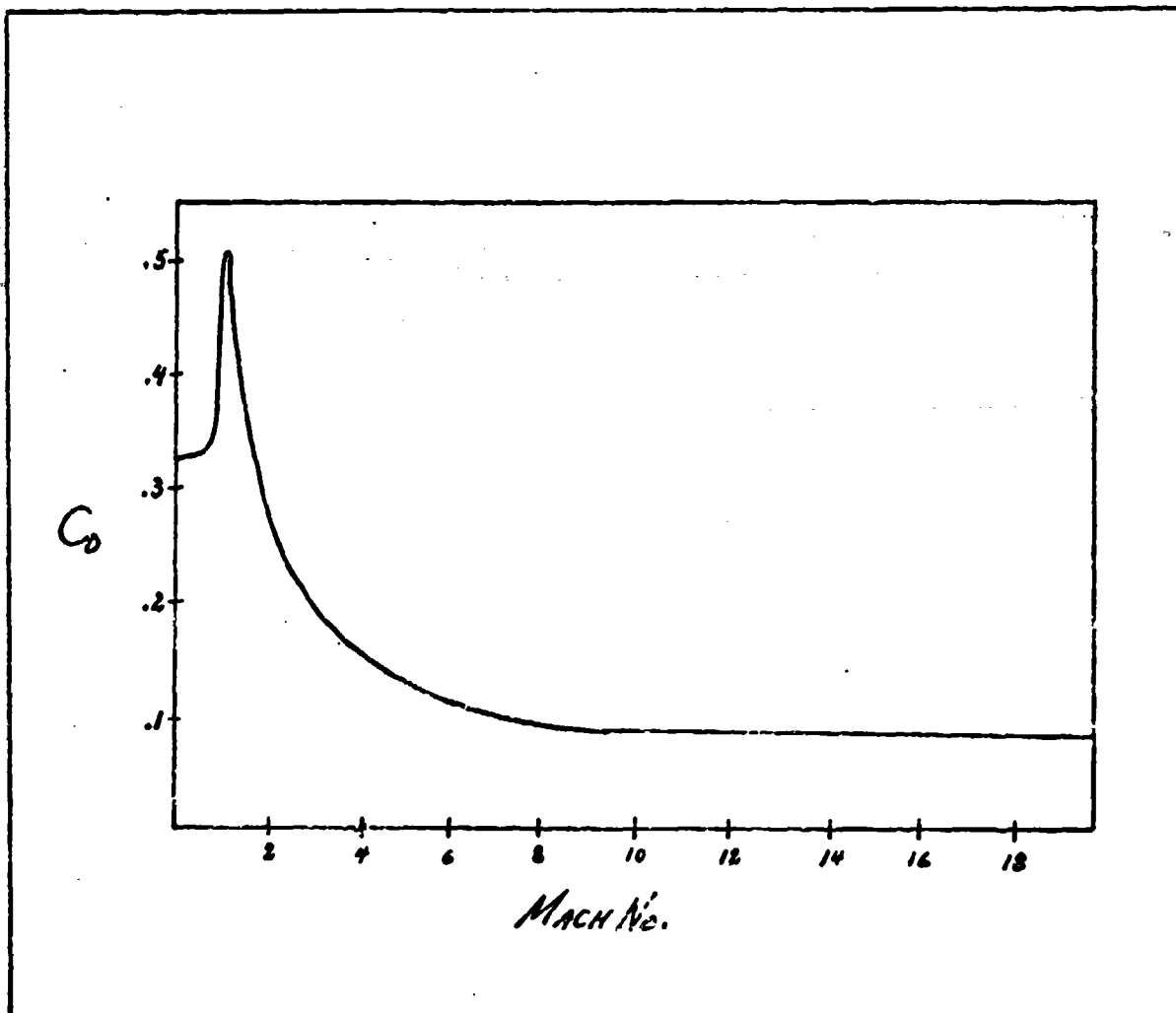
FIG II-5

DRAG COEFFICIENT VS MACH NO. FOR A SPHERE-CONE RV WITH A
HALF CONE ANGLE OF 6 DEG AND A BLUNTNESS RATIO OF 0.21

Although Eq (II-71) doesn't represent all Mach Numbers shown in Fig II-5, it represents quite adequately the region in which we are interested, down to about Mach 3.[*]

Models of the Atmosphere

Models of the atmospheric density and temperature are required for accurate trajectory simulation and estimation. The density is required for calculating the dynamic pressure, and temperature is required for Mach number calculation.

$$q = \frac{1}{2} \rho V_a^2 \tag{II-34}$$

$$M = \frac{V_a\,(mps)}{20 \sqrt{Temp\,(°K)}} \tag{II-73}$$

The importance of accurate density information for accurate β calculation is seen by the fact that a percent error in density transforms directly into a percent error in β owing to the linear relationship between β and ρ

$$\beta = \frac{\frac{1}{2} \rho V_a^2}{|A_D|} \tag{II-74}$$

Thus, the program provides for the input of the local density and temperature tables as functions of altitude. In addition, for simulation purposes, tables from the 1962 U.S. Standard Atmosphere, are stored internal to the program. Again,

---

[*]For ICBM ranges, a high performance RV ($\beta > 7000 kg/m^2$) impacts about Mach 3.

however, tables don't lend themselves to analytic differentiation. Thus, an analytic expression for density is required.
The density model which is used for the partials needed in
the differential correction process is (Ref 7)

$$\rho = \rho_o e^{-\frac{h}{s.h.}} \tag{II-75}$$

where

ρ_o = (1.226kg/m^3) the atmospheric density at h = 0

e = the constant 2.7182818

s.h. = the scale height ($\sim$ 7000m)

III The Estimator Equations

In the previous chapter, equations were given for propagating the state of a MaRV forward[*] in time. These were expressed in terms of the differential equations of motion along with an algorithm for numerically integrating the equations of motion. Additional equations were given for transforming the position of the RV at any time, t_i from ECI coordinates, (X_i, Y_i, Z_i) to spherical radar coordinates, (R_i, Az_i, E_i).

In this chapter, equations for estimating the state of a MaRV at some epoch time, t_o, based on the observed radar measurements and the equations given in the previous chapter, are given. These estimator equations are based on the classical method of weighted least-squares, which is generally agreed to have been invented first by Gauss for his astronomical studies in 1795. He was 18 years old at the time. There are two others, Legendre in France in 1806 and Adrain of America in 1808, who independently developed the method. Since these early times, there has been a vast literature on various aspects of the least-squares method just as Gauss predicted there would be. For details of the very interesting

---

[*]The equations given will allow for the propagation to be forward or backward in time with equal ease; however, all propagations of the state in this report will be forward in time.

history of estimation theory, the reader is referred to the excellent survey papers listed in Refs (19) and (30) in the bibliography.

The basic weighted-least-squares differential correction procedure is developed first. Then the relationship between WLS estimation and minimum variance and maximum likelihood estimation is discussed. The estimator with and without apriori statistics is described. Sequential estimation and an algorithm for deciding when to switch to a higher order estimator are discussed. A method for obtaining initial conditions is also suggested.

Weighted Least-Squares Differential Correction

The method of least squares is concerned with estimating the values of a set of parameters of the measurement model, which relates the measurements to the parameters, by minimizing the sum of the squares of the residuals. The residuals are defined to be the differences between the observed measurements and the corresponding measurements computed from the mathematical model using some set of estimates of the parameters. The set of estimates which renders the sum of squared residuals a minimum is said to be optimal in the least-squares sense. To put this in terms of the problem at hand, the observed measurements are the ranges, azimuths, and elevations from the tracking data and the corresponding computed measurements are determined from the equations in Chapter II. That is to say that the equations of Chapter II constitute our measurement model. The parameters we want to

estimate are the RV state variables at some fixed time, t_o called the epoch time. If we let the vector z_i represent the set of observed measurements of range, azimuth, and elevation at any given time, t_i, $(t_i > t_o)$ the measurement model may be represented notationally as

$$z_i = h_i(X_o, t_o) + \epsilon_i \quad , \quad i = 1, 2, \cdots, n \qquad \text{(III-1)}$$

where

  n = the total number of measurement times

  X_o = the true (but unknown) RV state vector at epoch

  h_i = the vector of nonlinear functions relating X_o to z_i

  ϵ_i = the vector of errors in the observed measurements
    at t_i

In component form, the measurement model is given as

$$R_{o_i} = R_i(X_o, t_o) + \epsilon_{R_i} \qquad \text{(III-2)}$$

$$Az_{o_i} = Az_i(X_o, t_o) + \epsilon_{A_i} \qquad \text{(III-3)}$$

$$E_{o_i} = E_i(X_o, t_o) + \epsilon_{E_i} \qquad \text{(III-4)}$$

where ϵ_{Ri}, ϵ_{Ai}, and ϵ_{Ei} are the measurement errors in range, azimuth, and elevation respectively at t_i and the o subscript on R_{oi}, Az_{oi}, and E_{oi} is to identify them as the observed values at t_i.

The most general state vector for a MaRV contains nine elements-three positions elements, three velocity elements, and three aerodynamic parameters. Thus, the state vector at epoch may be given as

$$\underline{X}_o = \left(X_o, Y_o, Z_o, \dot{X}_o, \dot{Y}_o, \dot{Z}_o, \beta_o, C_T, C_c \right)$$ (III-5)

this would represent the MaRV during maneuvering provided C_T and C_c are not zero. Ballistic-flight is modeled by setting C_T and C_c to zero and free-flight is modeled by setting $1/\beta_o$, C_T, and C_c to zero.

The set of equations given by Eqs (III-2) - (III-4) are the observation equations. If they were linear, we could take any ℓ of them and solve for the unknowns, where ℓ is the number of unknown state variables (i.e., $\ell = 6$, 7, or 9). (Here we have assumed that $\ell \geq 3$ n) The problem is the non-linearity of the observation equations. There is no direct method for simultaneously solving a set of nonlinear equations; therefore, an iterative approach must be taken. The iterative approach when applied to the least-squares observation equations is typically called differential correction. It consists of "linearizing" Eq (III-1) by expanding it in a Taylor's series about some initial guess or estimate of $\underline{X}_o$; truncating it by ignoring all terms of order two or higher; and solving for the resulting differentials which minimize the sum of the squared residuals determined from using the initial estimate. This optimal set of differentials is then

37

added to the initial estimate to form a better estimate, and the process is repeated until some convergence criterion is met (e.g., all of the differentials become essentially zero). This is explained in more detail in what follows where the weighted-least-squares estimate is derived.

Let $\overset{\wedge}{\underline{X}}_o$ be an estimate of $\underline{X}_o$, then the Taylor's series expansion of Eqs (III-2) - (III-4) are given as

$$\epsilon_{R_i} = R_{o_i} - R_i(\hat{\underline{X}}_o, t_o) - \frac{\partial R_i}{\partial \underline{X}_o}\Big|_{\underline{X}_o = \hat{\underline{X}}_o} \Delta X + h.o.t. \qquad (III-6)$$

$$\epsilon_{A_i} = A_{zo_i} - A_{z_i}(\hat{\underline{X}}_o, t_o) - \frac{\partial A_{z_i}}{\partial \underline{X}_o}\Big|_{\underline{X}_o = \hat{\underline{X}}_o} \Delta X + h.o.t. \qquad (III-7)$$

$$\epsilon_{E_i} = E_{o_i} - E_i(\hat{\underline{X}}_o, t_o) - \frac{\partial E_i}{\partial \underline{X}_o}\Big|_{\underline{X}_o = \hat{\underline{X}}_o} \Delta X + h.o.t. \qquad (III-8)$$

where the vector of differentials, $\underline{\Delta X}$ for the free-flight case is given as

$$\underline{\Delta X} = \begin{bmatrix} X_o - \hat{X}_o \\ Y_o - \hat{Y}_o \\ Z_o - \hat{Z}_o \\ \dot{X}_o - \hat{\dot{X}}_o \\ \dot{Y}_o - \hat{\dot{Y}}_o \\ \dot{Z}_o - \hat{\dot{Z}}_o \end{bmatrix} \qquad (III-9)$$

The partials of range, azimuth, and elevation with respect to the state vector $\underline{X}_o$ given in Eqs (III-6) - (III-8) are

38

evaluated using the current estimate, $\hat{\underline{X}}_o$ and are defined by the following matrix equation

$$\frac{\partial \underline{b}_i}{\partial \underline{X}_o} = \begin{bmatrix} \frac{\partial R}{\partial \underline{X}_o} \\[6pt] \frac{\partial A_z}{\partial \underline{X}_o} \\[6pt] \frac{\partial E}{\partial \underline{X}_o} \end{bmatrix}_i = \begin{bmatrix} \frac{\partial R}{\partial X_o} & \frac{\partial R}{\partial Y_o} & \frac{\partial R}{\partial Z_o} & \frac{\partial R}{\partial \dot{X}_o} & \frac{\partial R}{\partial \dot{Y}_o} & \frac{\partial R}{\partial \dot{Z}_o} \\[6pt] \frac{\partial A_z}{\partial X_o} & \frac{\partial A_z}{\partial Y_o} & \frac{\partial A_z}{\partial Z_o} & \frac{\partial A_z}{\partial \dot{X}_o} & \frac{\partial A_z}{\partial \dot{Y}_o} & \frac{\partial A_z}{\partial \dot{Z}_o} \\[6pt] \frac{\partial E}{\partial X_o} & \frac{\partial E}{\partial Y_o} & \frac{\partial E}{\partial Z_o} & \frac{\partial E}{\partial \dot{X}_o} & \frac{\partial E}{\partial \dot{Y}_o} & \frac{\partial E}{\partial \dot{Z}_o} \end{bmatrix}_i \qquad \text{(III-10)}$$

The set of equations given by Eqs (III-6) - (III-8) when the higher order terms are neglected is a set of linear equations in the unknowns $\Delta\underline{X}$. It is to this set of equations that we apply the principle of least-squares. First we make the notationally simplifying definitions

$$\underline{\mathcal{E}} = \left(\epsilon_{R_1}, \epsilon_{A_1}, \epsilon_{E_1}, \epsilon_{R_2}, \epsilon_{A_2}, \epsilon_{E_2}, \cdots, \epsilon_{R_m}, \epsilon_{A_m}, \epsilon_{E_m} \right)^T \qquad \text{(III-11)}$$

$$H = \begin{bmatrix} \dfrac{\partial \underline{b}_1}{\partial \underline{X}_o} \\[10pt] \dfrac{\partial \underline{b}_2}{\partial \underline{X}_o} \\[10pt] \dfrac{\partial \underline{b}_3}{\partial \underline{X}_o} \\[6pt] \cdot \\ \cdot \\ \cdot \\[6pt] \dfrac{\partial \underline{b}_m}{\partial \underline{X}_o} \end{bmatrix}_{3m \times 6} \qquad \text{(III-12)}$$

$$
\underline{V} = \begin{bmatrix} R_{o_1} - R_1(\hat{\underline{X}}_o, t_1) \\ A_{z_{o_1}} - A_{z_1}(\hat{\underline{X}}_o, t_1) \\ E_{o_1} - E_1(\hat{\underline{X}}_o, t_1) \\ \vdots \\ R_{o_m} - R_m(\hat{\underline{X}}_o, t_o) \\ A_{z_{o_m}} - A_{z_m}(\hat{\underline{X}}_o, t_o) \\ E_{o_m} - E_m(\hat{\underline{X}}_o, t_o) \end{bmatrix}_{3m \times 1}
\tag{III-13}
$$

With the above definitions, the linearized observation equations can be rewritten as

$$
\underline{\varepsilon} = \underline{V} - H \underline{\Delta x}
\tag{III-14}
$$

Some of the residuals of Eq (III-14) are in terms of range units and some are in terms of angle units; and even though the range measurements are more accurate than the angle measurements, the numerical values of the range residuals (in meters) will most certainly be larger than the angle residuals (in degrees). This forces us to apply weights to the observations to normalize the residuals so that all are given equal consideration. Or we might want to apply weights even if all the observations were of one type (say range) to give more accurate observations greater influence and less accurate observations less influence. Assuming we may want to assign a distinct weight to each observation we define

W_{Ri} = weight applied to the ith range observation

W_{Ai} = weight applied to the ith azimuth observation

W_{Ei} = weight applied to the ith elevation observation

and

$W^{\frac{1}{2}}$ = the 3n-by-3n diagonal weighting matrix whose

diagonal elements are W_{Ri}, W_{Ai}, W_{Ei}, $i = 1, 2, \ldots n$.

With the above definitions, the weighted observation equations are given by premultiplying Eq (III-14) by $W^{\frac{1}{2}}$.

$$\underline{\mathcal{E}}_w = W^{\frac{1}{2}}\underline{Y} - W^{\frac{1}{2}}H\underline{\Delta X} \qquad \text{(III-15)}$$

where the subscript W on $\underline{\mathcal{E}}$ is to indicate that this is the weighted error function.

Applying the principle of least squares to Eq (III-15) we obtain the sum of the squared residuals to be

$$\underline{\mathcal{E}}_w^T \underline{\mathcal{E}}_w = (W^{\frac{1}{2}}\underline{Y} - W^{\frac{1}{2}}H\underline{\Delta X})^T (W^{\frac{1}{2}}\underline{Y} - W^{\frac{1}{2}}H\underline{\Delta X}) \qquad \text{(III-16)}$$

Taking the partials of the above scalar function with respect to $\underline{\Delta X}$ gives

$$\frac{\partial(\mathcal{E}^T\mathcal{E})}{\partial \underline{X}_0} = -2(W^{\frac{1}{2}}\underline{Y} - W^{\frac{1}{2}}H\underline{\Delta X})^T W^{\frac{1}{2}}H \qquad \text{(III-17)}$$

Setting Eq (III-17) to zero, transposing and solving for $\underline{\Delta X}$ results in the standard weighted-least-squares estimate

$$\underline{\Delta X} = (H^T W H)^{-1} H^T W \underline{Y} \qquad \text{(III-18)}$$

41

where

$$W = W^{\frac{1}{2}} W^{\frac{1}{2}}$$

(III-19)

Had the Eq (III-2) - (III-4) been linear, the optimal least-squares estimate of X_o would be given by adding the ΔX determined from Eq (III-18) to the initial estimate, $\hat{X}_o$. As it is, however, since the observation equations are not linear, the optimal estimate must be determined in stages by adding the differential, ΔX determined from Eq (III-18) at each stage to the current estimate, $\hat{X}_o$ and iterating the above equation until the process converges to the optimal weighted-least-squares estimate.

In algorithm form the weighted-least-squares-differential-correction method may be summarized by the following steps:

1. Somehow determine initial estimates, $\hat{X}_o$ for all of the unknown parameters (e.g. see page 54).

2. Using the estimate, $\hat{X}_o$, propogate $\hat{X}_o$ in time (integrate $\hat{X}_o$) to the time of each observation and evaluate $\underline{V}$ and H.

3. Determine ΔX from Eq (III-18).

4. Add ΔX to $\hat{X}_o$ to form a better estimate

$$\hat{X}_o \Longleftarrow \hat{X}_o + \Delta X$$

5. Return to Step 2, and repeat Setps 2-4 checking for convergence[*] after Step 4 of each iteration.

---

[*]As given on page 38.

42

6. At convergence the optimal least-squares estimate is $\hat{X}_o$. (Note: no notation distinction is made between the converged estimate and the initial estimate, $\hat{X}_o$)

In step 4 the⟸denotes replacement or writing over.

The above procedure converges quite rapidly (< 4 iterations) for good initial estimates. With poor initial estimates, the above procedure may not converge at all. In fact, it will most likely diverge. A technique for determining good initial estimates is given later in this chapter.

Minimum Variance and Maximum Likelihood Estimation

The weighted-least-squares estimator developed in the previous section was done so from purely "reasonableness" arguments. No knowledge of the underlying probability distributions of the observation errors (ϵ_R, ϵ_A, ϵ_E) was required and none was used. Weights were assigned in a somewhat arbitrary manner where it seems reasonable that more accurate measurements should receive more weight than less accurate measurements. As a result nothing can be said about the accuracy of the WLS estimate. Clearly from Eq (III-18), the least squares estimate is a function of W. Therefore, it appears that there may be an "optimal" W to use in the least-squares estimator. Junkins (Ref 18) shows that if the optimality criterion is to determine the estimate $\hat{X}_o$ with minimum covariance matrix, then W should be the inverse of the covariance matrix of the observation errors. When the weighting matrix is so defined, the least-squares estimator,

43

in the _linear_ case, is called the minimum variance (MV) estimator. Defining Q as the covariance of the observation errors and P ? the covariance of $\hat{X}_O$, the first order approximation to a MV estimator for our nonlinear problem is given as

$$\Delta \underline{X}_o = (H^T Q^{-1} H)^{-1} H^T Q^{-1} \underline{Y} \qquad \text{(III-20)}$$

$$P = (H^T Q^{-1} H)^{-1} \qquad \text{(III-21)}$$

where $\hat{X}_O$ is determined exactly as in Steps 1-6 of the previous section with W now replaced by Q^{-1} and P is determined using the converged $\hat{X}_O$. Since P of Eq (III-?) is only a first-order approximation of the covariance matrix, it may, for very nonlinear problems, be a poor estimate of the errors in $\hat{X}$. Therefore, Monte Carlo simulations are usually required to validate the covariance matrix. This is discussed more fully in Chapter IV.

Since the diagonal elements of the covariance matrix, P are the mean squared errors of the individual state variables, the MV estimator given by Eqs (III-20) and (III-21) is sometimes referred to as the minimum mean square (MMSE) estimator. See Liebelt (Ref 23). It is also (Ref 32) called the Markov estimator.

Another assumption, which is almost always made in actual application, is that the observation errors are Gaussian distributed with zero mean. Using this assumption,

Wiesel (Ref 36) develops the maximum likelihood (ML) esti-
mator which is identical to Eqs (III-20) and (III-21) where
Q is now the covariance of the normal distribution of the
observation errors. For ML estimation, see also (Ref 16,18,24).

Another assumption which was made in developing the
estimator for this application is that the observational
errors are not correlated in time nor spatially. This is
not strictly true spatially since the radar doesn't make
its measurements in range, azimuth, and elevation but in-
stead transforms "raw" measurements into range, azimuth, and
elevation. In addition, if the measurements are from a
moving sensor which has been transformed to a fixed location,
then the errors are correlated in time. The effect of this
approximation is to make Q a diagonal matrix with the error
variances on the diagonal. Considerable storage and calcula-
tions can be saved if the error variances are identical
from time to time, i.e.,

$$\sigma_{R_i}^2 = \sigma_{R_j}^2 \qquad \text{(III-22)}$$

$$\sigma_{A_i}^2 = \sigma_{A_j}^2 \qquad \text{(III-23)}$$

$$\sigma_{E_i}^2 = \sigma_{E_j}^2 \qquad \text{(III-24)}$$

for any two times, t_i and t_j where σ_{Ri}^2, σ_{Ai}^2, and σ_{Ei}^2 are the
variances in range, azimuth and elevation at t_i. This being
the case, the 3n-by-3n covariance matrix, Q can be represented

45

by three scalars, σ_R, σ_A and σ_E. The σ_R, σ_A, and σ_E used in the numerical examples to validate the estimator equations and the programming are given in Table I-1 of Chapter I.

A Priori Statistics

It was mentioned earlier that good initial estimates of the unknown state parameters are required for the differential correction process to converge. If in addition, statistics for the initial estimates are also known the estimator is modified to reflect these a priori statistics (Ref 2) as

$$\Delta \underline{X} = (P_o^{-1} + H^T Q' H)^{-1} H^T Q' \underline{V} \qquad \text{(III-25)}$$

$$P = (P_o^{-1} + H^T Q' H)^{-1} \qquad \text{(III-26)}$$

where P_o is the covariance of the initial estimate, $\hat{\underline{X}}_o$.

The Sequential Estimator

The weighted-least-squares estimator developed in the preceding sections assumed a deterministic system model where the system model is given as

$$\ddot{\underline{X}} = f(X, Y, Z, \dot{X}, \dot{Y}, \dot{Z}, \phi, C_T, C_c, t) \qquad \text{(III-27)}$$

Another way of saying this is, if the unknown state variables were known, we could propagate the state forward in time perfectly. That would imply the models for gravity, drag,

46

and lift given in Chapter II are exact. Whereas no model
is ever perfect, some are very nearly so such that determin-
istic least squares works exceptionally well. A case in
point is the missile in free-flight where the only force
acting is gravity. Gravity can be modeled with sufficient
accuracy, and is in this algorithm, that all of the free-
flight data can be processed simultaneously in a single batch
using the six-state estimator given previously. On the other
hand, the drag model for an RV is not so well known, and the
lift model is even less well known. This motivates us to
seek an estimator for the reentry flight regime to process
the data sequentially, a small batch at a time. The size of
the batch, specified by the number of time points, should, as
a general rule, be the largest over which the model may be
considered perfect (sufficiently accurate). This number
varies with altitude, accuracy of the observation data, etc.
and no attempt was made in this research to determine the
optimum batch size. Instead the user of the program is al-
lowed to specify the batch size anywhere from one point to
all the data. Examples will be given in Chapter IV.

The sequential estimator which was developed for this
problem is based on Eqs (III-25) and (III-26) and an addi-
tional equation for propagating the covariance in time (Ref 15).

$$P(t_{i+1}) = \Phi(t_{i+1}, t_i) P(t_i) \Phi(t_{i+1}, t_i)^T \qquad \text{(III-28)}$$

The sequential estimator which was implemented is similar to that suggested by Barker (Ref 4) and is outlined in the following steps:

1. The number of points in batch one (NPB1[*]) is specified, and the initial estimates, $\hat{X}_{o1}$ and P_{o1} are determined. (The subscript, 1 refers to the batch number).

2. The WLS differential correction algorithm (steps 2-5) given previously is iterated until convergence is achieved using Eq (III-25) instead of (III-18), i.e.,

$$\Delta \underline{X}_1 = (P_{o_1}^{-1} + H^T Q^{-1} H)^{-1} H^T Q^{-1} \underline{V} \qquad (III-29)$$

3. After step 2 has converged, update the covariance using Eq (III-26)

$$P_1 = (P_{o_1}^{-1} + H^T Q^{-1} H)^{-1} \qquad (III-30)$$

4. Propagate the optimal estimate, determined for batch one, $\hat{X}_{o1}$ and the covariance P_1 to the time of the next epoch. (Generally speaking the epoch is advanced one time interval but this is selected by the user by specifying the number of points

---

[*]Program input

48

between epochs one and two, NPBE12[*])

$$\hat{X}_{o_2} = \hat{X}_{o_1} + \int_{t_1}^{t_2} \dot{X}_{o_1} dt \qquad (\text{III-31})$$

$$P_{o_2} = \Phi(t_2, t_1) P_1 \Phi(t_2, t_1)^T \qquad (\text{III-32})$$

(The number of points in batch two and succeeding batches is specified separately as NPBA1[*] so that batch one may incorporate all of the free flight data if desired)

5. Again the WLS differential correction algorithm is iterated until the optimal estimate of X_{o2} is converged upon.

6. After step 5 has converged, the covariance of $\hat{X}_{o2}$ is updated by

$$P_2 = (P_{o_2}^{-1} + H^T Q^{-1} H)^{-1} \qquad (\text{III-33})$$

7. Propagate the optimal state estimate, $\hat{X}_{o2}$ and co-variance P_2 to the time of the next epoch where the time of the next epoch is specified by the number of points between epochs, NPBE[*]. (NPBE and NPBE12 are specified separately again so that batch one may be treated separately).

---

[*]Program input, NPBE12 $\leq$ NPB1 and NPBE $\leq$ NPBA1

49

8. Repeat steps 5 and 6 for batch 3.

9. This propogate-update cycle is repeated for subsequent batches until the final data point is included in a batch.

10. Once the final point is included in a batch, the batch size is gradually collapsed to a single data point.

Thus, the sequential, weighted-least-squares estimator is controlled by four inputs NPB1, NPBE12, NPBA1 and NPBE where

NPB1 = number of points in batch one

NPB12 = number of time intervals between epochs one and two

NPBA1 = number of points in all batches after one

NPBE = number of time intervals between succeeding batches

When NPB1 is set to 3n or greater, all of the data are processed simulcaneously in a single batch. When NPB1 and NPBA1 are both set to one and the differential correction algorithm is not iterated (MAXIT = 0), the equations make up one form of the Kalman filter (see Ref 24).

Finite Memory Estimator

Experience gained in developing the estimator, indicates that for data simulated as indicated in Table I if the batch sizes are 50 points or greater, then no a priori statistics are needed (i.e., $P_{oi}^{-1} = 0$, all i). On the other hand, when

50

the batch size is sufficiently small that the normal matrix, $(H^T Q^{-1} H)$ is ill-conditioned or singular, a priori statistics are required. In this small batch size applications, it has been found that with the infinite memory estimator given above which includes Eq (III-26), that the covariance matrix

$$P = (P_0^{-1} + H^T Q^{-1} H)^{-1} \qquad \text{(III-33)}$$

becomes indefinite as the batch number, i becomes larger. To prevent this from happening, a technique described by others[*] was implemented to deweight the a priori covariance. This results in modifying Eq III-33 as

$$P = (C P_0^{-1} + H^T Q^{-1} H)^{-1} \qquad \text{(III-34)}$$

where C is a diagonal matrix (Barker used a scalar) whose diagonal elements C_{ii} are between zero and one. Many simulations were run to determine a C to keep P_i positive definite. No conclusions can be drawn but it seems that the larger the batch size, the smaller C must be. Small batch sizes required $C_{ii} \geq .8$. One way to avoid this problem would be to use large batch size (NPBA1 $\geq$ 50) and set $C_{ii} = 0$ and this appears to work fine for ballistic flight; however, if the MaRV undergoes some high-g maneuvers, small batch sizes would be necessary as the coefficients of turn, C_T and climb, C_C are modeled as constant over the batch time interval. The case of high-g maneuvering was not investigated in this study.

---

[*]This deweighting accomplished in various ways. See (Ref 4,16,14).

Adaptively Increasing the Estimator Order

As has been mentioned previously, during free-flight, the estimator is a six-state estimator corresponding to the six elements of the free-flight state vector, $(X,Y,Z,\dot{X},\dot{Y},\dot{Z})^T$. In the sequential mode, as the estimator is stepping through the data, there is a point after which the free-flight estimator is no longer adequate. This is a result of the slow-down of the RV due to drag making the free-flight equations no longer adequate for modeling the RV's motion. At this time, we want to switch to the seven-state BRV estimator defined by the BRV state vector $(X,Y,Z,\dot{X},\dot{Y},\dot{Z},\beta)^T$. However, this point is not well defined a priori. If we switch to the seven-state estimator too soon (i.e., before the ballistic coefficient becomes observable), then the normal matrix, $(H^T Q^{-1} H)$ will be singular, and therefore not invertible. This condition will lead to the estimator failing. The penalty for switching late is not so great. It will just mean that for a period of time, the RV motion is modeled inaccurately. This inaccurate modeling of the RV motion will lead to larger than expected residuals. This divergence of the residuals is what is used to determine when to switch to the higher order estimator. This is accomplished by keeping track of what is called the total root mean square, (RMST) error of the range residuals[*]

---

[*]Originally azimuth and elevation RMS's were also used but too many false switches occurred. See Example 2 Chapter IV.

$$RMST = \sqrt{\sum_{i=1}^{N} \frac{(R_{oi} - R_{ci})^2}{N-1}} \qquad\qquad \text{(III-35)}$$

where

$R_{oi} - R_{ci}$ = the ith range residual

N = the total number of range observations which

have been processed at any given time

For N greater than 30, the RMST should be very nearly equal to the standard deviation of the normal distribution of the range errors, which for the simulated data is five meters. A long free-flight track is useful in determining a good value of the RMST.

The RMST is used to detect divergence by comparing it to the range RMS for any batch. Call the range RMS calculated from a single given batch the BRMS. In the limit, $BRMS_K - RMST_K$ should be less than $2RSTD_K$ with a probability of about .95, so if

$$BRMS_K - RMST_K \geqslant 2RSTD_K \qquad\qquad \text{(III-36)}$$

then divergence has occurred and the switch is made, where RSTD is a measure of the dispersion of the BRMS's defined as

$$RSTD_K = \sqrt{\sum_{i=1}^{K} \frac{(BRMS_i - RMST_i)^2}{K}} \qquad\qquad \text{(III-37)}$$

where K is the number of batches processed thus far. The check is not made until K is greater than four to allow time for "settling" of RSTD. The value four is arbitrary.

Once the switch from the six-state estimator to the seven-state estimator has been made, the last batch is re-processed with the higher order estimator, and then the same logic is used to detect the onset of maneuvering. If a man-euver is detected, the program switches to the nine-state estimator given by the MaRV state vector, $(X, Y, Z, \dot{X}, \dot{Y}, \dot{Z}, \beta, c_T c_c)^T$.

Initial Conditions

Good initial conditions for the state variables are required for the differential correction process to converge. The state variables, β, c_T, and c_c are not so critical and a rough guess is sufficient, e.g., $\beta = 7000$ kg/m^2, $c_T = 0$ and $c_c = 0$. On the other hand, the position and velocity initial conditions are very critical and there is no way to guess them. Thus a routine was written to determine initial estimates as follows

1. The range, azimuth, and elevation measurements are transformed into ECI X, Y, and Z.

2. The ECI coordinates are fit in a least-squares sense to a special 4th order polynomial in time (given here only the X coordinate)

$$X_i = a_1 + a_2 (t_i - t_i) + a_3 (t_i - t_i)^2 + a_4 (t_i - t_i)^3 + a_5 (t_i - t_i)^4, \qquad \text{(III-38)}$$
$$i = 1, 2, \cdots, m$$

where a_3, a_4 and a_5 are first determined from

$$\ddot{X}_{qi} = 2 a_3 + 6 a_4 (t_i - t_i) + 12 a_5 (t_i - t_i)^2, \quad i = 1, 2, \cdots, m \qquad \text{(III-39)}$$

54

where $\ddot{X}_{gi}$ is determined from the gravity subroutine using the raw X,Y,Z coordinates.

3. Once the a's have been determined, the fourth order polynomial is differentiated to determine velocity.

If all the data are free-flight,[*] the above procedure works exceptionally well resulting in convergence of the differential correction algorithm in one or two iterations. It also works very well with data which includes reentry provided a substantial portion is free flight. If all the data are reentry, better initial conditions are provided by ignoring the second-order polynomial constraint on a_3, a_4 and a_5 given in step 2 i.e., Eq (III-39).

---

[*]This technique for determining initial position and velocity was developed by the author originally for program TEAP, a program used at FTD for fitting free-flight data.

IV Numerical Examples

Many numerical simulations were run to validate the estimator equations and the programming of them. The program was designed in stages with each stage being checked for accuracy before proceeding to the next stage. The first stage consisted of the free-flight equations of motion with the batch WLS estimator equations. Numerical partials were generated to check the accuracy of the analytic partials used in the estimator equations. Subsequent stages included the BRV equations of motion, the sequential estimator equations, and finally the MaRV equations of motion with the required partials. Numerical partials were simulated for each stage to test the accuracy of the analytic partials. These tests verified the fact that the simplified equations of motions used for the partials calculations were of sufficient accuracy.

Once the program was completed, many more simulations were run, and refinements and modifications were made where necessary. The results of several of these have been alluded to in previous chapters. It was found, for instance, that the a priori covariance matrix had to be deweighted to maintain positive variances as output of the estimator equations. Simulations showed that the deweighting had to be increased as the batch size increased. Because of the time involved in tuning the estimator equations for various batch

sizes, no conclusion can be reached as to how best to use the a priori covariance information. It was determined, however, that for batch sizes of 10 or more points no a priori covariance was necessary to keep $H^T Q^{-1} H$ positive definite. As a result, the numerical simulations discussed in the remainder of this chapter were run with no a priori covariance.

Two numerical examples are presented in detail in the remainder of this chapter. The first discusses the operation of the estimator in the batch WLS mode where all data are fit simultaneously. The second example discusses the results of running the estimator in the sequential mode. A ten run Monte Carlo simulation was performed for each of the two examples.

Example One - The Batch Estimator

The purpose of this example was twofold, (1) to verify the accuracy of the models used in the program and (2) to look at the accuracy that could be attained when using the estimator in the batch WLS mode where all the data are fit simultaneously. This mode represents the ultimate in the accuracy which can be attained from radar data of a given accuracy and is applicable to the RV in free-flight and to the RV for ballistic reentry. In order to accomplish the first goal, the data used in this example were simulated using the Foreign Technology Division's MRVRAP program - a program which has been tested and proven to be accurate for

57

simulating the flight of a ballistic RV. Ten sets of simu-
lated radar tracking data were generated. Each set of data
was corrupted by random noise from normal distributions having
zero means and standard deviations of 5 m, 0.015 deg, and
0.020 deg for range, azimuth, and elevation, respectively.
The errors in the data were determined from a random number
generator by specifying the "SEED".[*] The SEED was specified
to be different for each data set, so that, even though the
errors for each set were from the same three normal distribu-
tions, the samples were different for each.

Data for this first example were simulated for a
ballistic RV having a hypersonic ballistic coefficient of
3300 kg/sq m. The ballistic coefficient was modeled to vary
with Mach number as discussed in Chapter II. Figure IV-1 is
a plot of normalized ballistic coefficient, drag acceleration,
air relative velocity and altitude plotted versus time from
120 km to impact to show how these parameters are related to
one another through out reentry. Epoch was defined to be at
reentry (120 km altitude) and only the data from reentry to
impact were considered. Figure IV-2 is a plot of one sample
of the tracking data used. The parameters have been normal-
ized so as to be able to display them on a single graph.
Ten points per second were simulated for a total of 500 data
points.

All of the data in each set were fit simultaneously
solving for the nine elements of the MaRV state vector. The
initial conditions for the position and velocity states were

---

[*]The SEED is just a starting value for the random
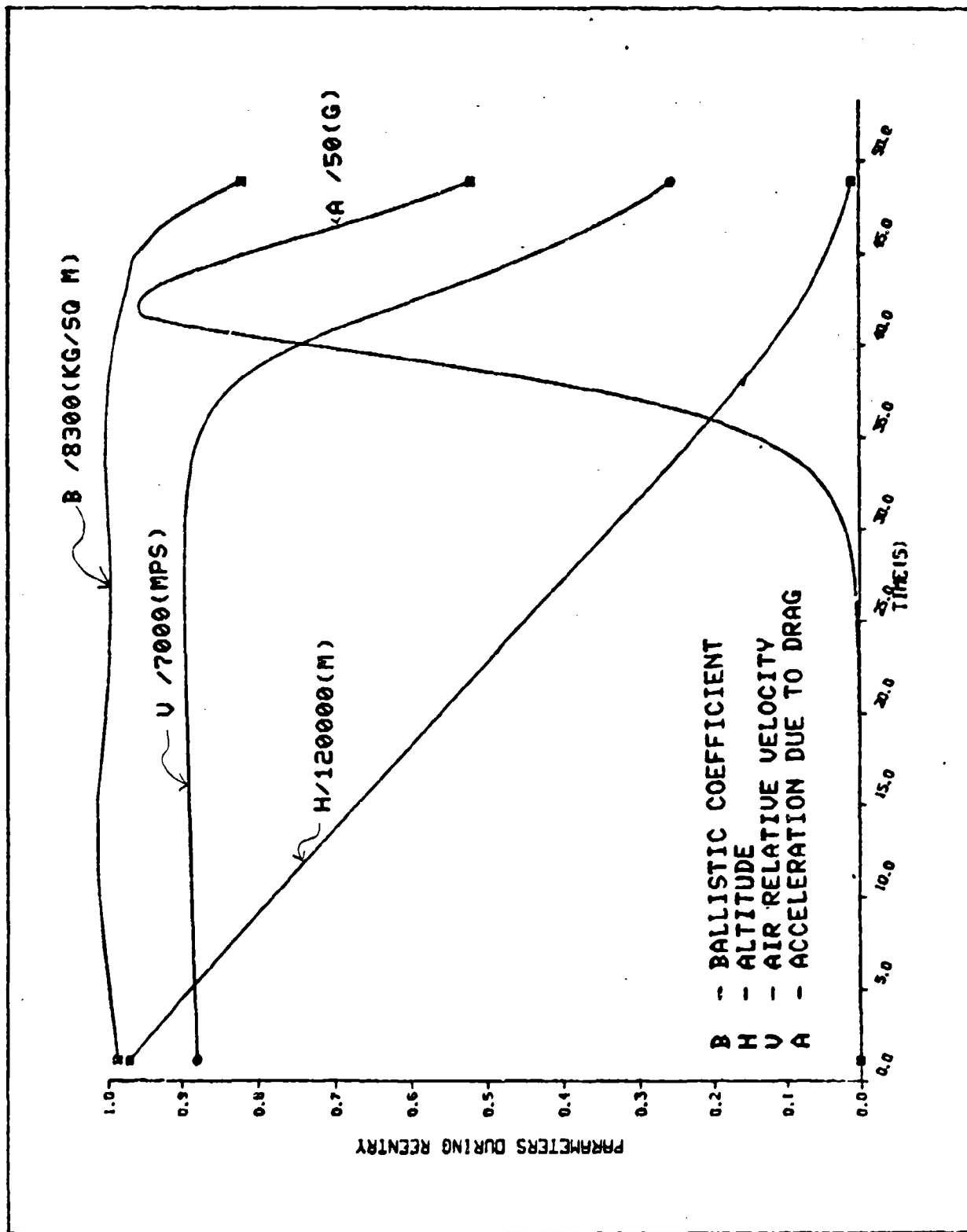number generator.

58

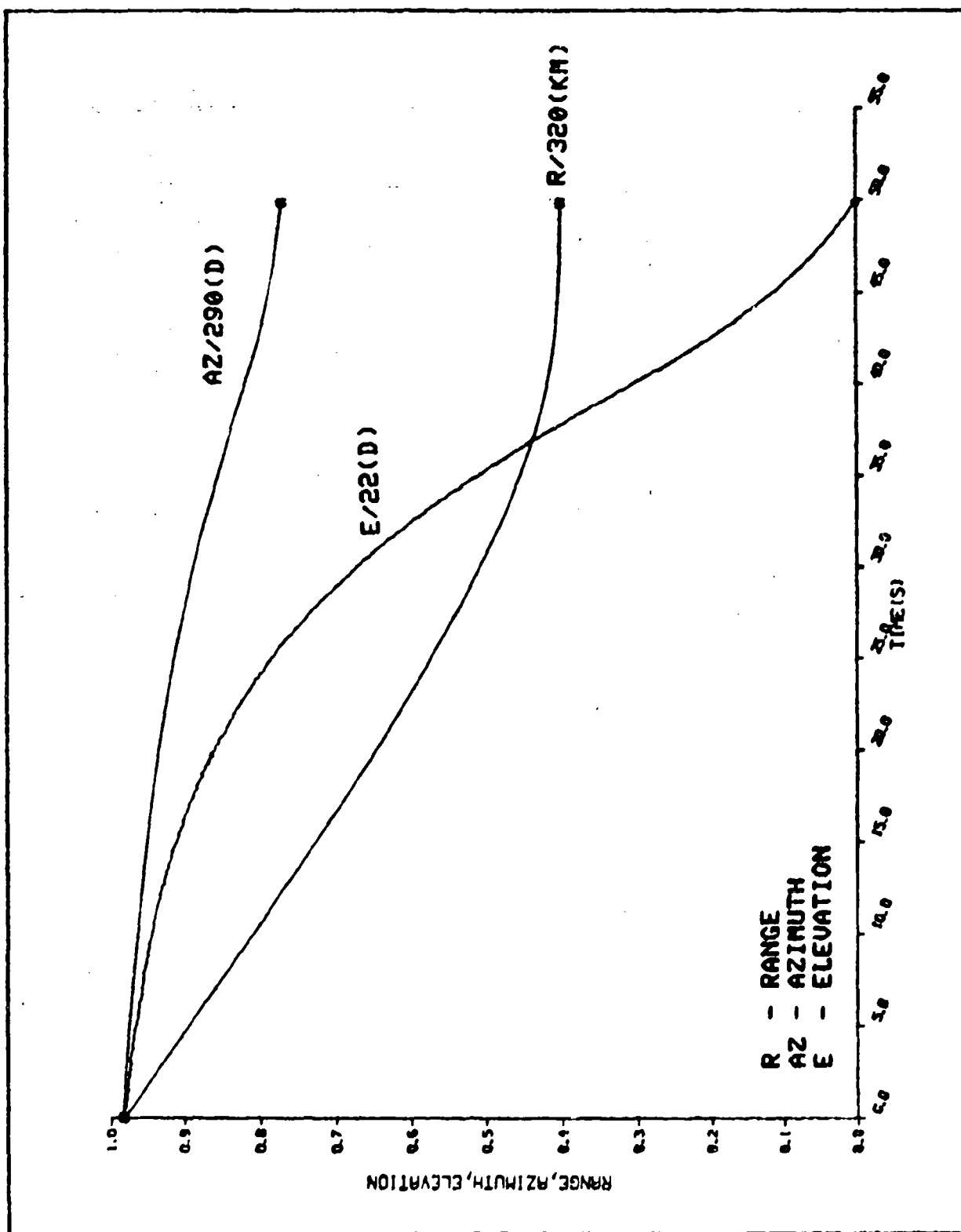FIG IV-1 THE VARIATION OF KEY PARAMETERS WITH TIME
FOR EXAMPLE ONE

FIG IV-2   DATA USED IN EXAMPLE ONE

determined automatically by the program as described in Chapter III; β_O was initialized at 500 kg/sq m and both C_T and C_C were initialized at 0.0.

Since the data for this example were generated from known conditions, the performance of the estimator can be judged by how well the estimated parameters match the true state parameters. Table IV-1 is a list of the results from the ten simulations. In the upper left block of Table IV-1 are given the true errors in the state estimates $(\hat{X}_O - X)$ for the ten runs. The last rows of Table IV-1 give the means and standard deviations for the ten run sample. The last three rows of the table, give the standard deviations of the range residuals, σ_E. All runs converged in three iterations. Table IV-2 contains the standard deviation-correlation coefficient matrix from one of the single sample runs. Since this matrix is symmetric, only the lower triangular form is given. This matrix is determined from the estimator covariance matrix, $(H^T Q^{-1} H)^{-1}$. The diagonal elements are the standard deviations. Comparing the standard deviations from Table IV-2 with the last column of Table IV-1 shows a very good agreement.

Another indication as to how well the model agrees with the data is given by plotting the residuals. Figure IV-3 is a plot of the range, azimuth, and elevation residuals from one of the single sample runs. The absence of trend in the residuals indicates that the data have been modeled correctly and accurately.

61

Table IV-1

Results of 10-Run Monte Carlo Simulation: Example One

RUN NO:	1	2	3	4	5	6	7	8	9	10	MEAN	σ
$(X-\hat{X})$m	6	14	5	7	3	5	15	4	18	15	9.2	5.6
$(Y-\hat{Y})$m	-2	0	2	0	-4	-4	-1	0	3	-1	-0.9	2.3
$(Z-\hat{Z})$m	1	-10	-10	-6	5	5	-8	-5	-15	-6	4.9	6.6
$(\dot{X}-\hat{\dot{X}})$mps	-.04	.25	-.02	.08	-.06	-.15	.36	-.13	.33	.22	.08	0.19
$(\dot{Y}-\hat{\dot{Y}})$mps	-.09	-.02	.04	-.05	-.13	-.16	-.02	-.05	.05	-.05	-.04	0.07
$(\dot{Z}-\hat{\dot{Z}})$mps	.14	-.23	-.11	.02	-.20	-.31	-.26	-.01	-.39	-.02	0.10	0.20
$(B-\hat{B})$xsm	-7	2	-2	-2	-5	5	-9	5	-2	3	-1.8	4.7
$(C_f-\hat{C_f})$xsm	.0000	.0000	.0000	.0000	.0000	.0000	.0000	.000	.0000	.0000	.0000	.0000
$(C_c-\hat{C_c})$xsm	.0000	.0000	.0000	.0000	.0000	.0000	.0000	.000	.0000	.0000	.0000	.0000
σ_p(m)	5.4	5.2	5.3	5.4	5.3	5.3	5.4	5.3	5.3	5.4		
σ_A(deg)	.015	.016	.015	.015	.016	0.015	.016	.015	.015	.015		
σ_B(deg)	.021	.020	.020	.020	.021	.020	.020	.020	.021	.020		

σ = standard deviation

Table IV-2

Lower Triangular Form of the Standard Deviation - Correlation Coefficient Matrix for Example One

X	Y	Z	$\dot{X}$	$\dot{Y}$	$\dot{Z}$	β	C_T	C_C
.618+001								
-.226-001	.239+001							
-.547+000	-.792+000	.578+001						
-.917+000	-.799-001	.575+000	.208+000					
.120-001	-.980+000	.770+000	.139+000	.777-001				
.656+000	.563+000	-.893+000	-.759+000	-.585+000	.180+000			
-.236-008	.308-008	-.376-008	-.528-008	-.456-008	.628-008	.540+001		
.395-001	-.285+000	.280+000	-.619-001	.310+000	-.373+000	-.736-009	.567-008	
-.431+000	-.543-001	.296+000	.630+000	.121+000	-.523+000	-.197-008	.493-001	.332-007

The diagonal elements, standard deviations, are the square roots of the diagonal elements of the estimator covariance matrix. The off-diagonal elements are the correlation coefficients, ρ_{ij} defined as $\rho_{ij} = \dfrac{\sigma_{ij}}{\sqrt{\sigma_{ii}\sigma_{jj}}}$, where σ_{ij}'s are the elements of the estimator covariance matrix.
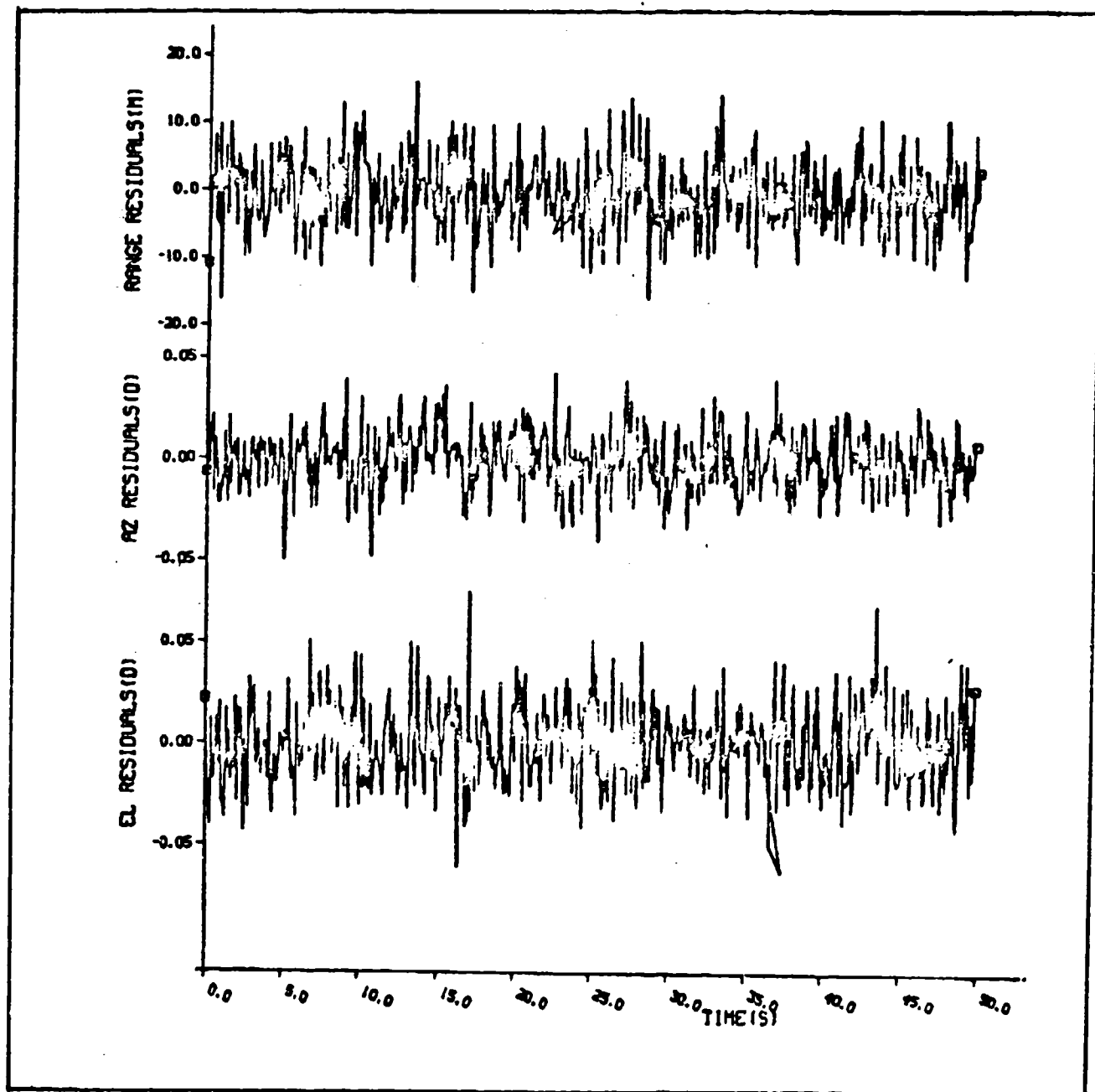
FIG IV-3. RANGE AZIMUTH AND ELEVATION RESIDUALS
FROM EXAMPLE ONE.

Example Two - The Sequential Estimator

This example was designed to show how the sequential mode of the estimator operated as the number of points per batch was varied. Three specific things were of interest:

(1) how the estimator switching algorithm operated as the number of points per batch was varied,

(2) how the accuracy in the estimated parameters varied with the number of points per batch, and

(3) how well the estimator covariance tracked the true errors in the estimated parameters.

For this example another ten sets of noisy data were generated. All ten samples were identical except for the random noise added to the data which was varied as was explained in Example One. The data were simulated this time starting at about 150 seconds prior to reentry and going to impact for a total of 206.5 seconds. The data were simulated as 1 pps prior to reentry and 10 pps thereafter. This amounted to a total of 698 time points, and as in the previous example, the errors in the data were simulated as zero mean, white Gaussian noises with standard deviations of 5 m, 0.015 deg, and 0.020 deg respectively for range, azimuth, and elevation. One of the data sets has been plotted in Figure IV-4 for reference. The data were simulated with a hypersonic ballistic coefficient of 10,000 kg/sq m and β varying with Mach number. A moderate maneuver was begun at approximately 10 seconds prior to impact ($\sim$ 25 km altitude) by setting C_T to 0.000001 and C_c to 0.00001 sq m/kg at this time. These values were
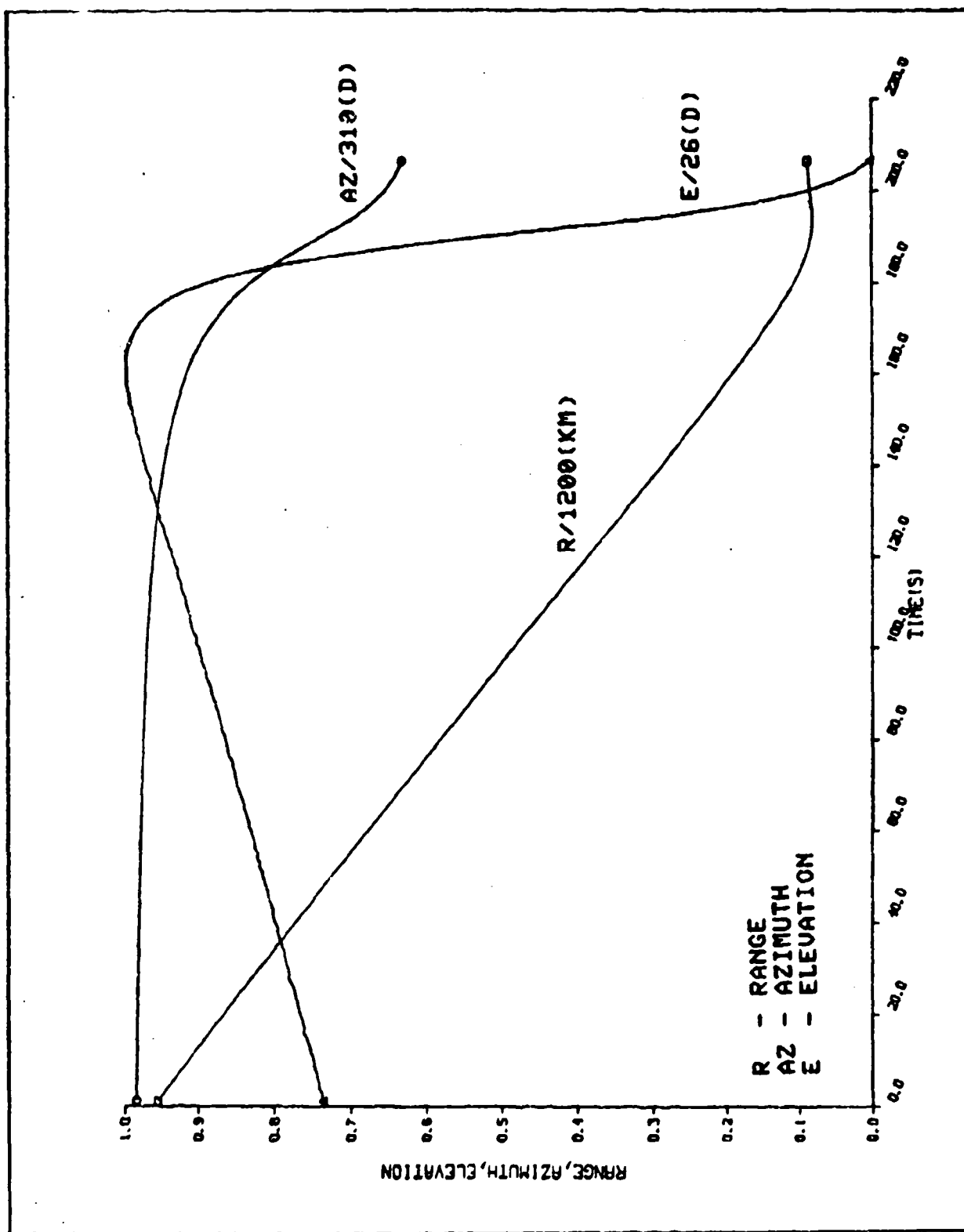
65

FIG IV-4 DATA USED IN EXAMPLE TWO

selected to extend the flight time by about five seconds. It was found that a value of C_c much larger than the one used, applied at this altitude, resulted in the RV skipping out. The plus sign on C_T implies a left turn and on C_c implies a climb up. The pertinent reentry parameters of this model are plotted in Figure IV-5.

Three separate cases were run. In each case all of the free flight data (first 152 seconds) were included in batch one. Then the epoch was propagated forward 150 seconds to the time of reentry. Thereafter each batch consisted of 50 points for case one, 30 points for case two and 10 points for case three with the epoch being advanced 2 points between batches. Initial estimates of position and velocity at the first epoch were determined automatically by the program and ballistic coefficient, C_T, and C_c were initialized at 5000 kg/sq m, 0.0, and 0.0 sq m/kg respectively. The propagated state estimates were used as initial estimates for subsequent batches. For each case, the estimator was initialized as the six state free-flight estimator consisting only of the position and velocity states with the program switching to the BRV and MaRV estimators when divergence of the range residuals was detected. This shows up vividly in Figure IV-6 where for case one, the total RMS (RMST) of the range residuals and the RMS of the range residuals for each individual batch (BRMS) are plotted as a function of time. The time on this figure is in seconds after the first data point. Recall that the estimator switches from six
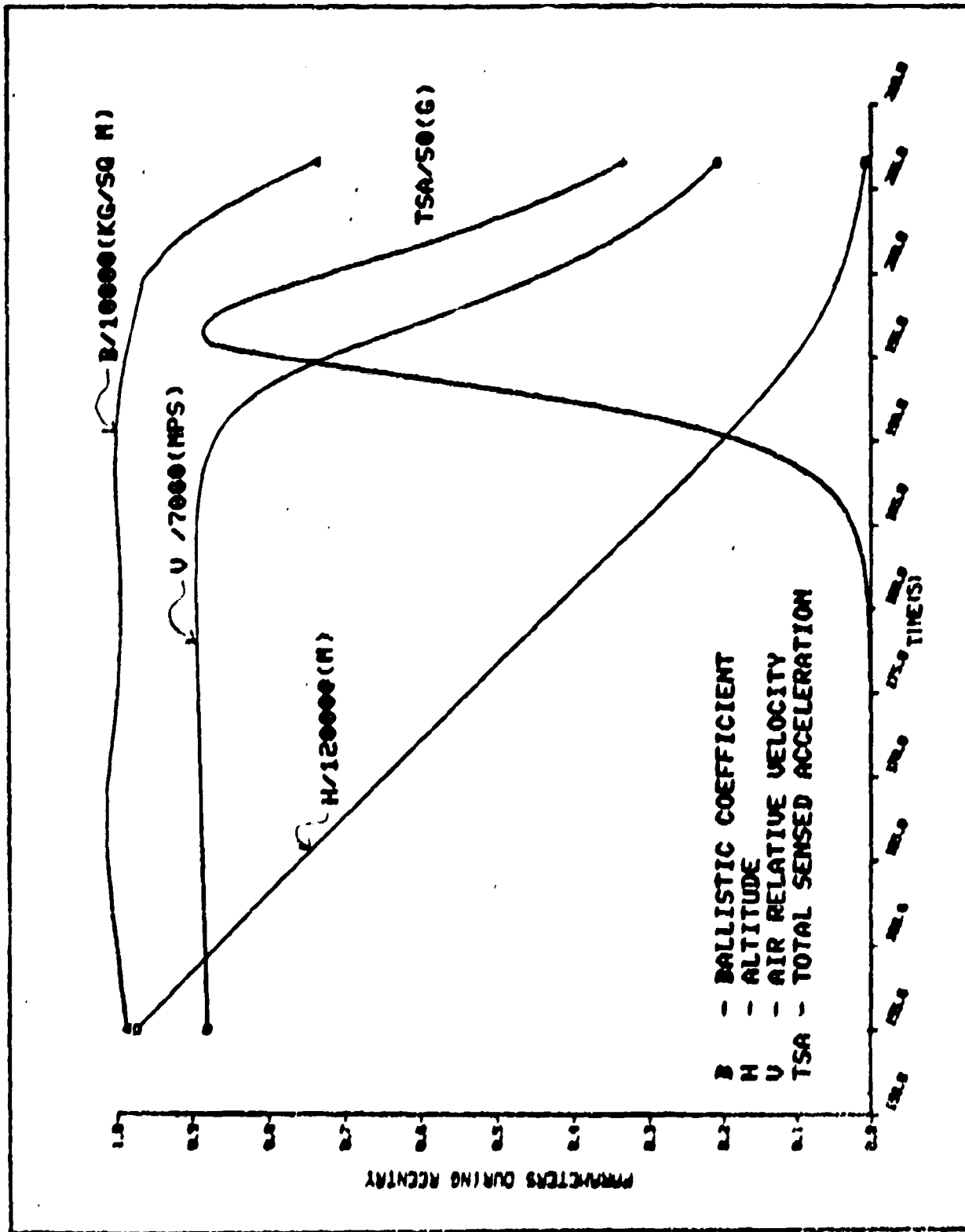
67

FIG IV-5 THE VARIATION OF KEY PARAMETERS WITH TIME
FOR EXAMPLE TWO

B   — BALLISTIC COEFFICIENT
H   — ALTITUDE
U   — AIR RELATIVE VELOCITY
TSA — TOTAL SENSED ACCELERATION

68

states to seven states when the magnitude of the BRMS be-
comes significantly larger, in a statistical sense, than
the RMST. This occurs at approximately 182 seconds in
Figure IV-6 when the difference, BRMS-RMST, becomes larger
than twice the standard deviation of the error in RMST. A
check is also made on the value of the dynamic pressure at
this time to prevent the filter from switching while aero-
dynamic parameters would still be unobservable. This pre-
vented the filter in this case from switching at 3 earlier
times when the BRMS went above the RMST + 2σ curve. The
estimator switches again at approximately 190 seconds when
the maneuver is detected, this time switching to the nine-
state MaRV estimator. The RMST goes straight line after
this switch because it is no longer updated once the switch
has been made to the MaRV estimator. No provision was made
to switch from a higher to lower order estimator, but then
it's not considered necessary since once the switch is made
C_T and C_C will be observable thereafter even though they may
be zero. Also plotted on Figure IV-6 is the mean of the
range residuals for each batch. Ideally this should be zero
for each batch. The same curves for the azimuth and eleva-
tion residuals are plotted as Figure IV-7 and IV-8 and as
can be seen for this case neither azimuth nor elevation de-
tected the divergence. This varied however with data sets.
In some the maneuver showed up dramatically in the elevation
residuals (see for example Figure IV-9). In every case-one
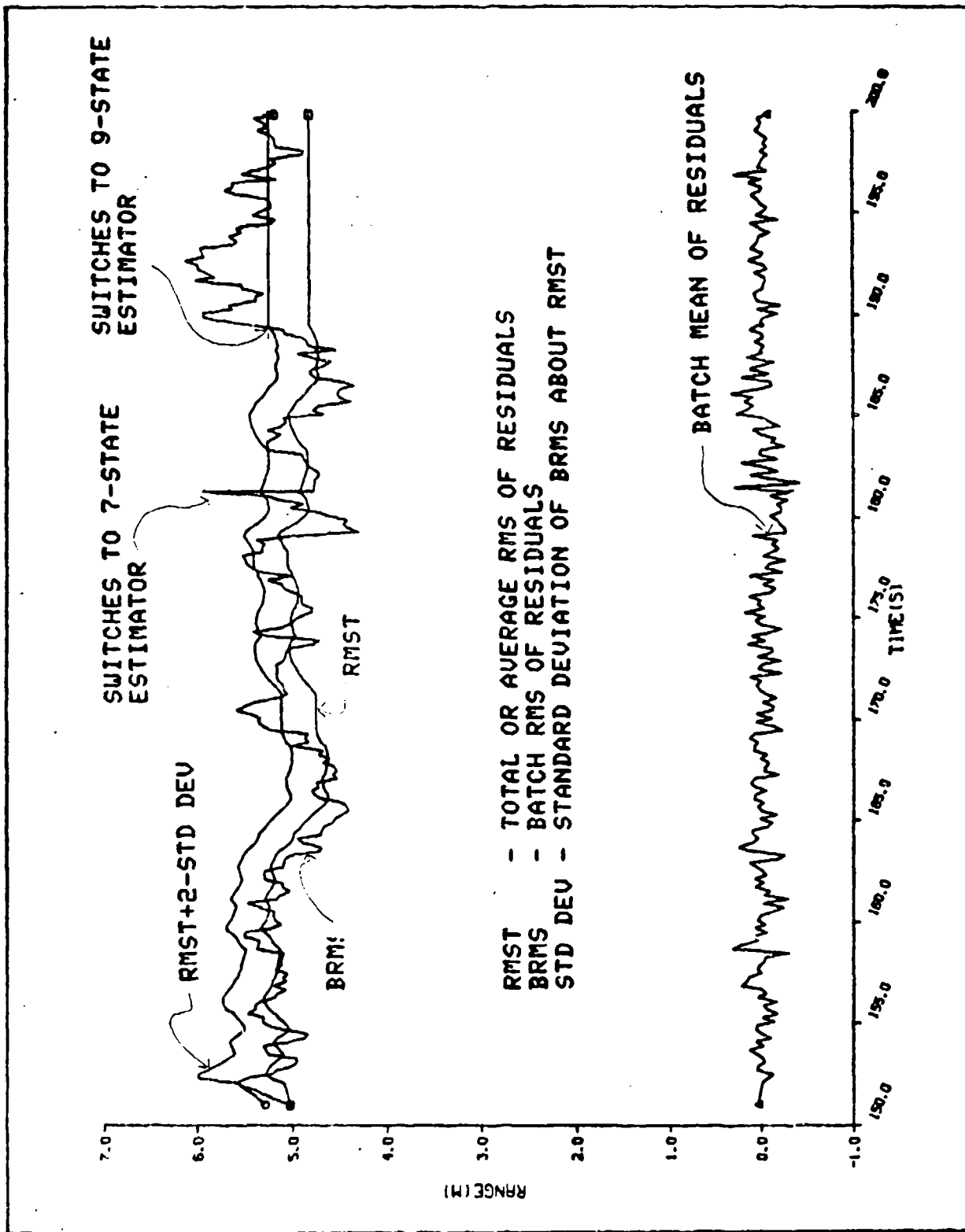run however, the divergences were detected in the range

69

FIG IV-6   RANGE STATISTICS FOR CASE ONE OF EXAMPLE TWO
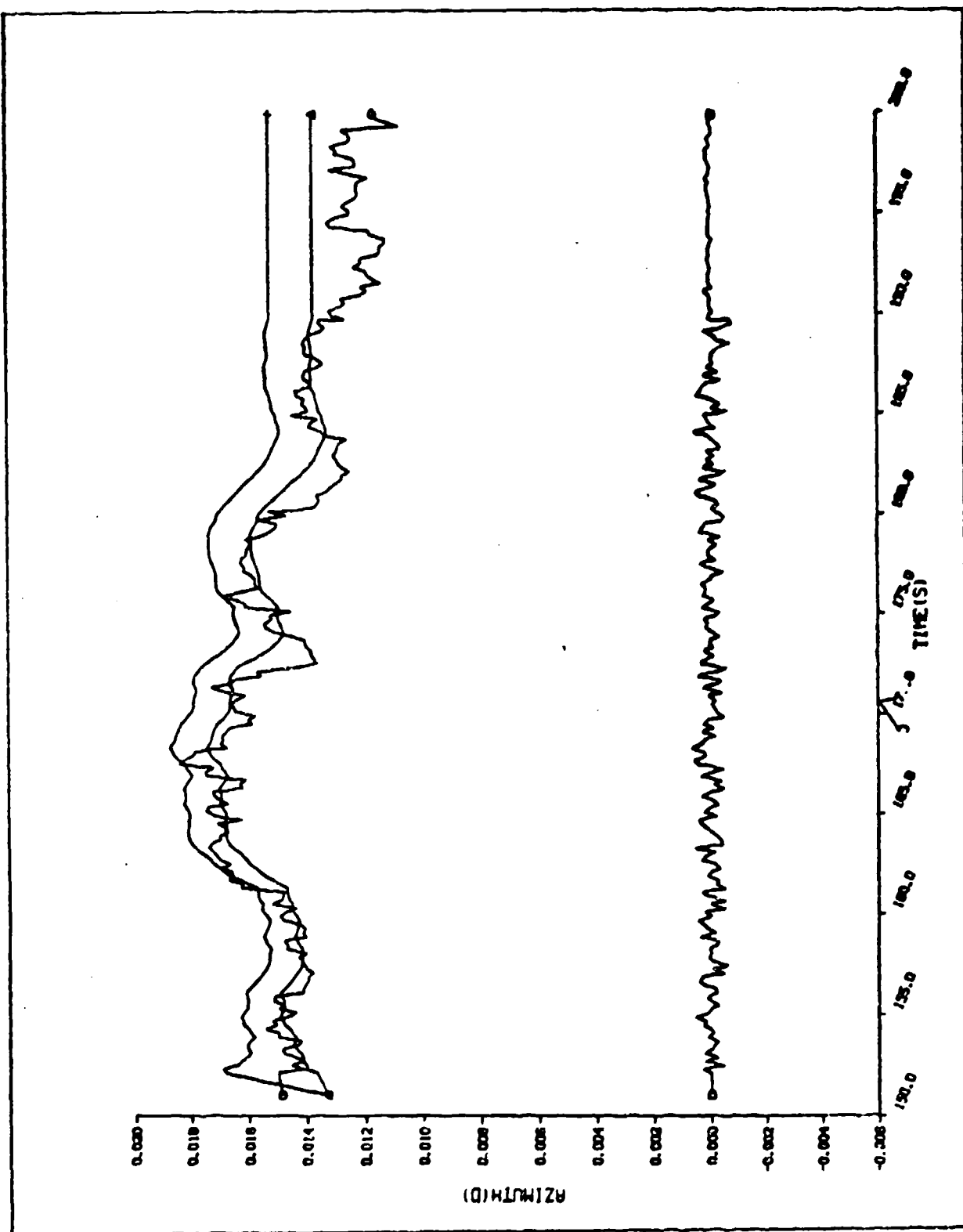   SHOWING THE ESTIMATOR SWITCHING

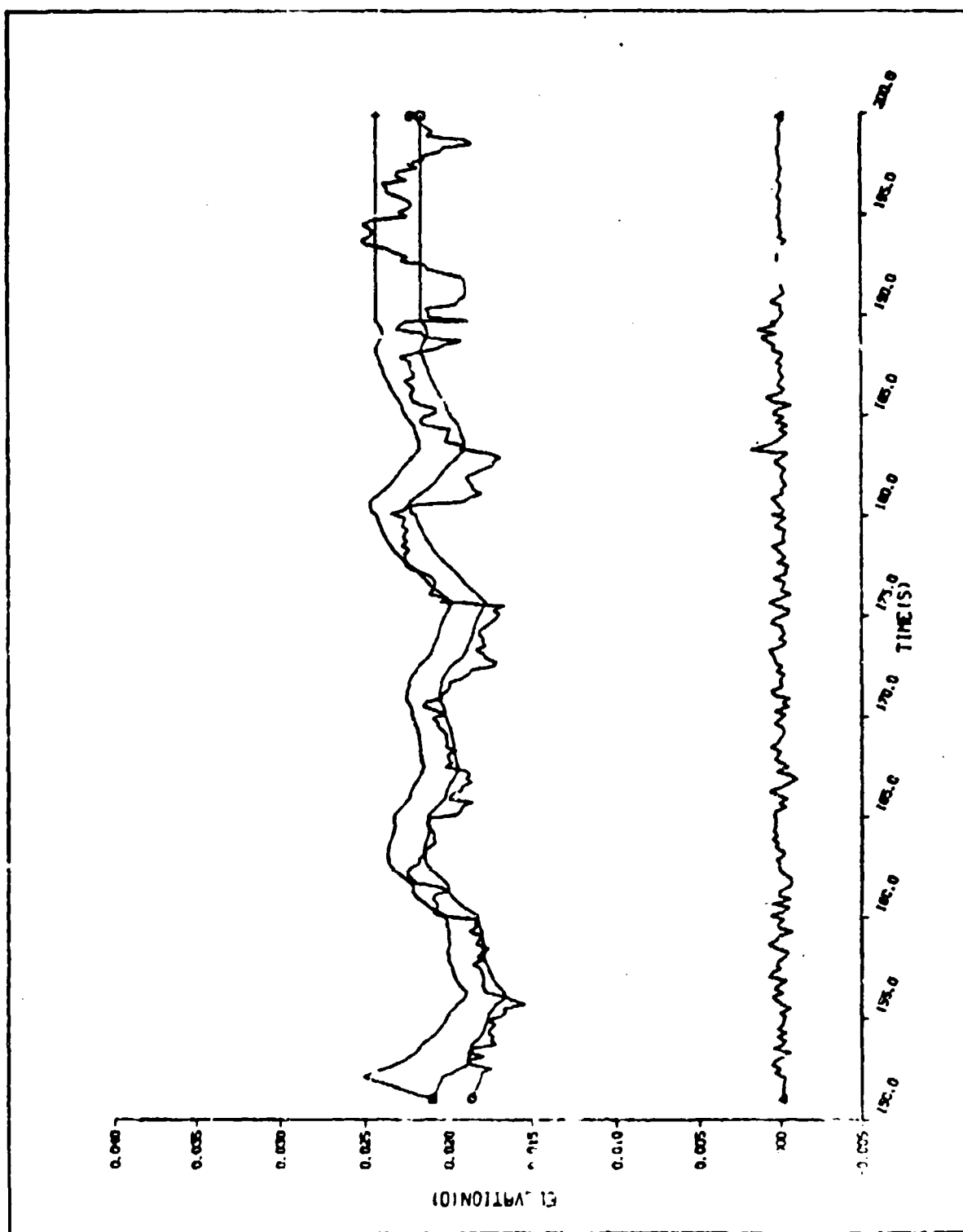FIG IV-7   AZIMUTH STATISTICS FOR CASE ONE OF EXAMPLE TWO

71

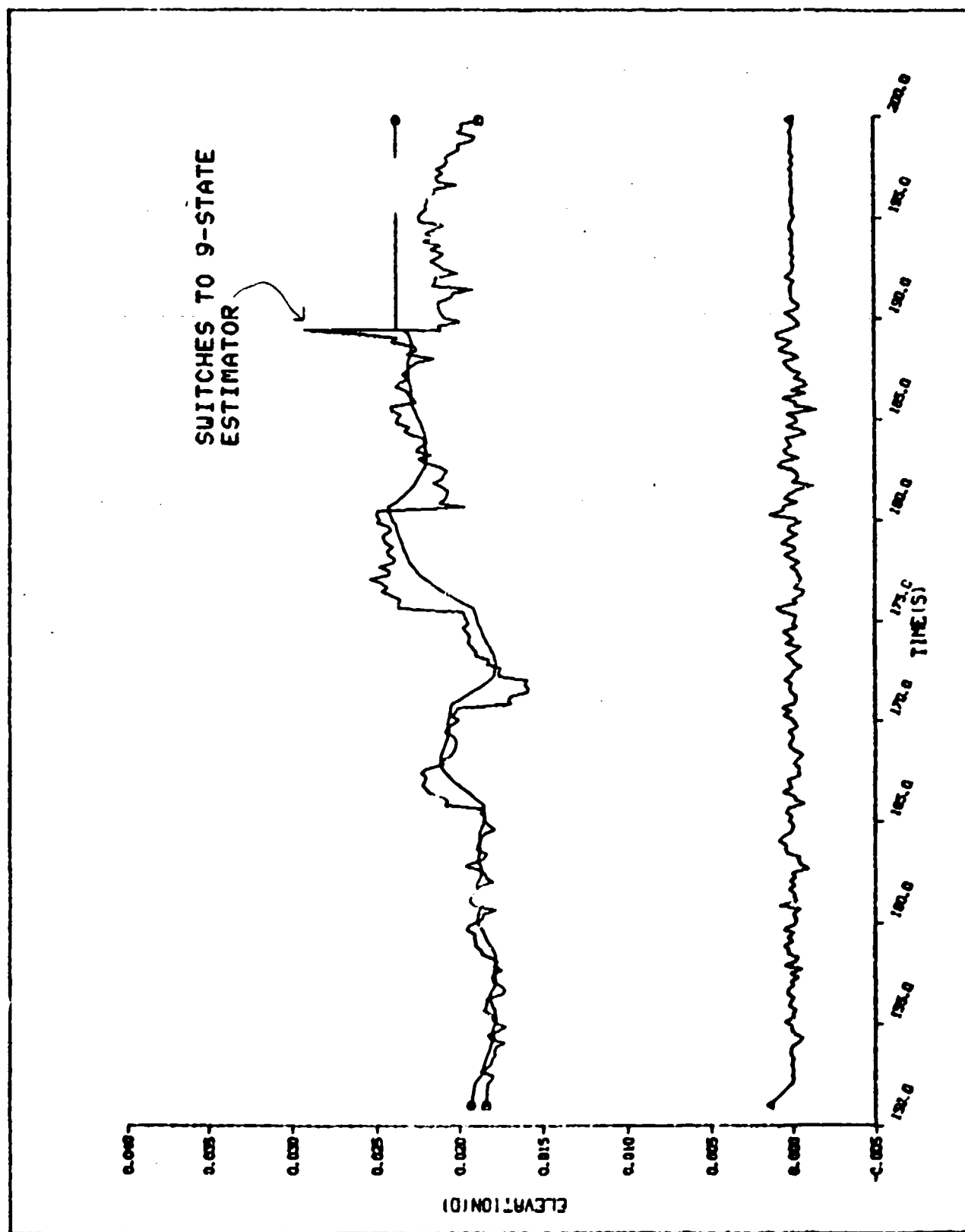FIG IU-8   ELEVATION STATISTICS FOR CASE ONE OF EXAMPLE TWO

72

FIG IV-9   CASE ONE EXAMPLE WHERE THE MANEUVER SHOWS UP IN
THE ELEVATION RESIDUALS

73

residuals. Originally the switching scheme included the
azimuth and elevation residuals but the final version uses
only the range residuals. For comparison purposes, similar
plots for case two and case three are given in Figures IV-10
through IV-15. The estimator switching algorithm didn't
work as well in either of these cases as it did in case one.
With 30 points per batch, the program switched from the six
state estimator to the BRV estimator at 185 seconds then im-
mediately switched to the MaRV estimator. With 10 points
per batch only one switch is made also this occurring at
192 seconds when the maneuver is detected. These comparisons
suggest the desirability of using the larger batch sizes.

Next a comparison of the accuracies of the estimated
parameters for the three cases was made. This was accom-
plished by comparing the differences between the estimated
parameters and their true values. In Figures IV-16 through
IV-21 the difference between the estimated position and veloc-
ity states and their true values from a single sample run
of case one are plotted. In Figures IV-22, IV-23, and IV-24
the estimated values of hypersonic ballistic coefficient, C_T
and C_c are plotted. Also in each of the Figures IV-16
through IV-24, plus and minus 3-σ curves from the estimator
covariances are plotted. In an effort to save space, when
the case two and case three comparisons are made only the X
component of position and velocity and the aerodynamic para-
meters are included. These are included as Figures IV-25
through IV-34. The comparisons may be summarized as follows:

(a) Except for position, the state estimates are significantly degraded as the number of points per batch is reduced from 50 to 30 to 10.

(b) The errors in the estimates of the aerodynamic parameters are most affected by the reduction in the number of points per batch.

(c) In all cases, except just before estimator switching, the true error is contained within the plus and minus 3σ curves.

Note, the apparent divergence of the estimator standard deviation on each of the Figures IV-16 through IV-34 is a result of the collapsing of the batch size once the last batch of data is encountered. For example, say the batch size is specified to be 50 points. Once the last 50 points of data are processed, then the batch size is reduced by the number of points the epoch is advanced until the epoch reaches the final point. An alternate way to mechanize this would be to just take the estimates from the last full batch and propagate them to the final time.

The results of the single sample runs indicate that the state parameters can be estimated exceptionally well for batch sizes of 50 points. In the region of peak deceleration, where the aerodynamic parameters are estimated most accurately, the standard deviations as determined from the estimator covariance matrix are well within a few percent of the true parameter values, about 2% for ballistic coefficient and 5% for the turn and climb parameters. In order to verify the
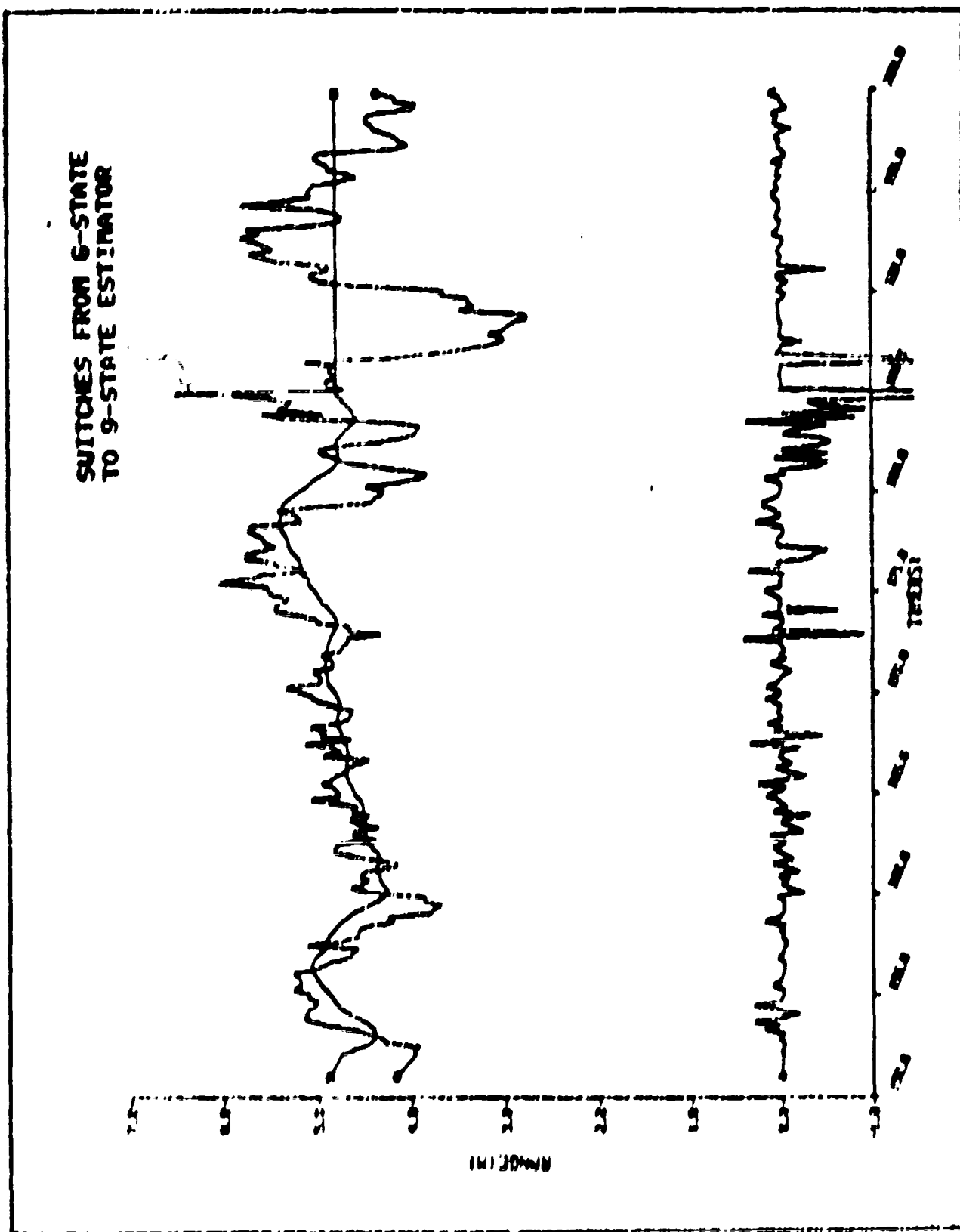
SWITCHES FROM 6-STATE
TO 9-STATE ESTIMATOR

THRESH

FIG IV-10 RANGE STATISTICS FOR CASE TWO OF EXAMPLE TWO
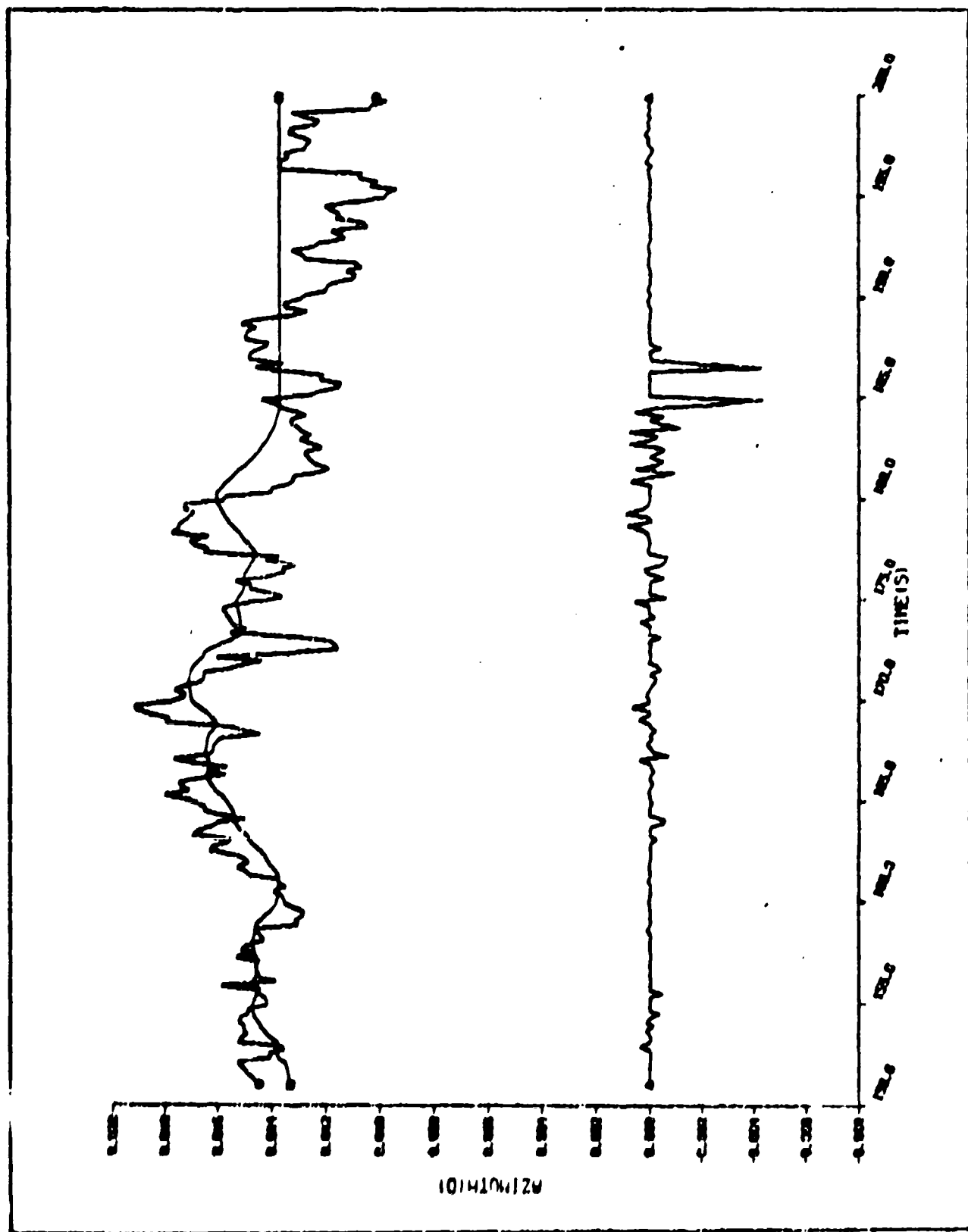SHOWING THE ESTIMATOR SWITCHING
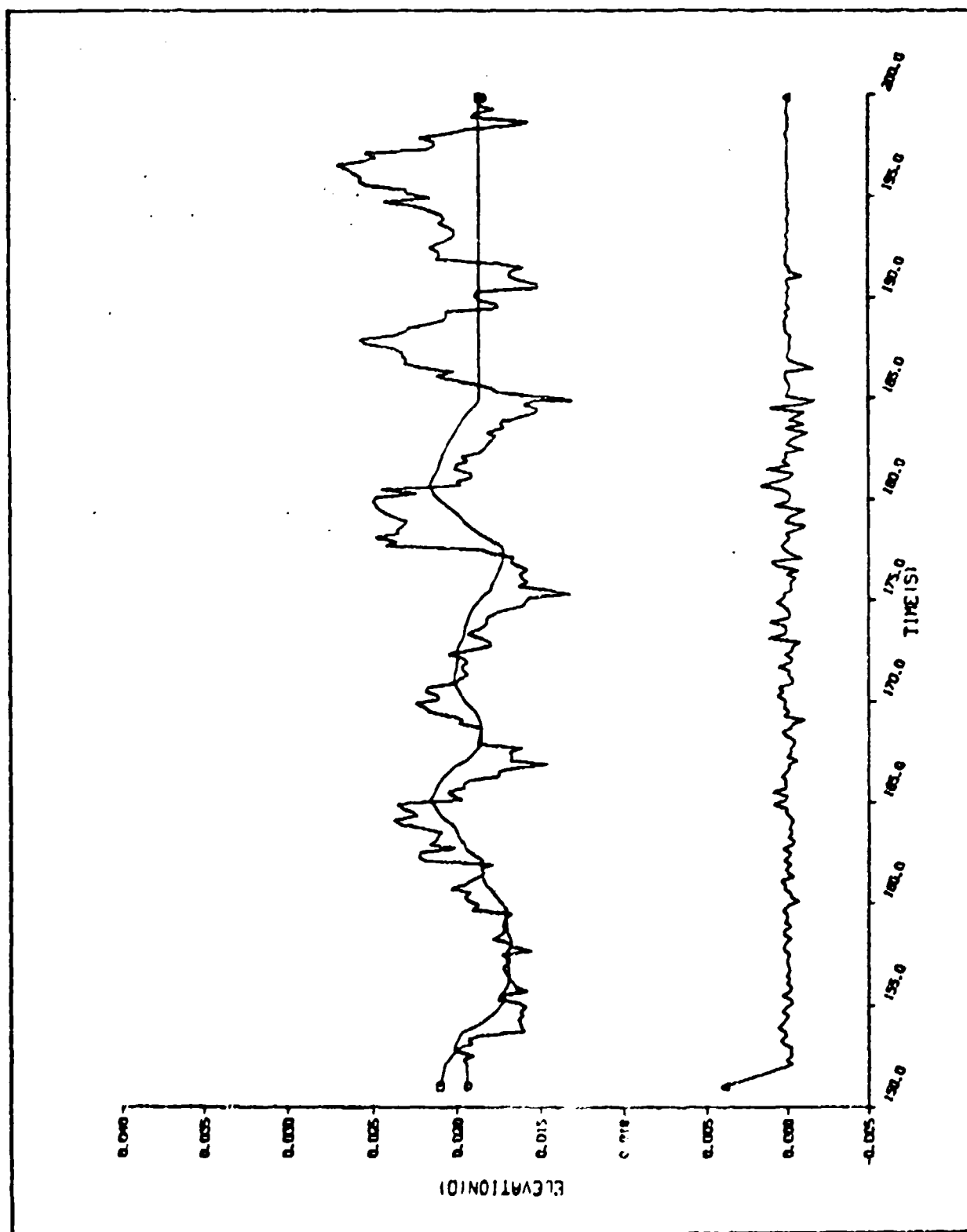
FIG IV-11 AZIMUTH STATISTICS FOR CASE TWO OF EXAMPLE TWO

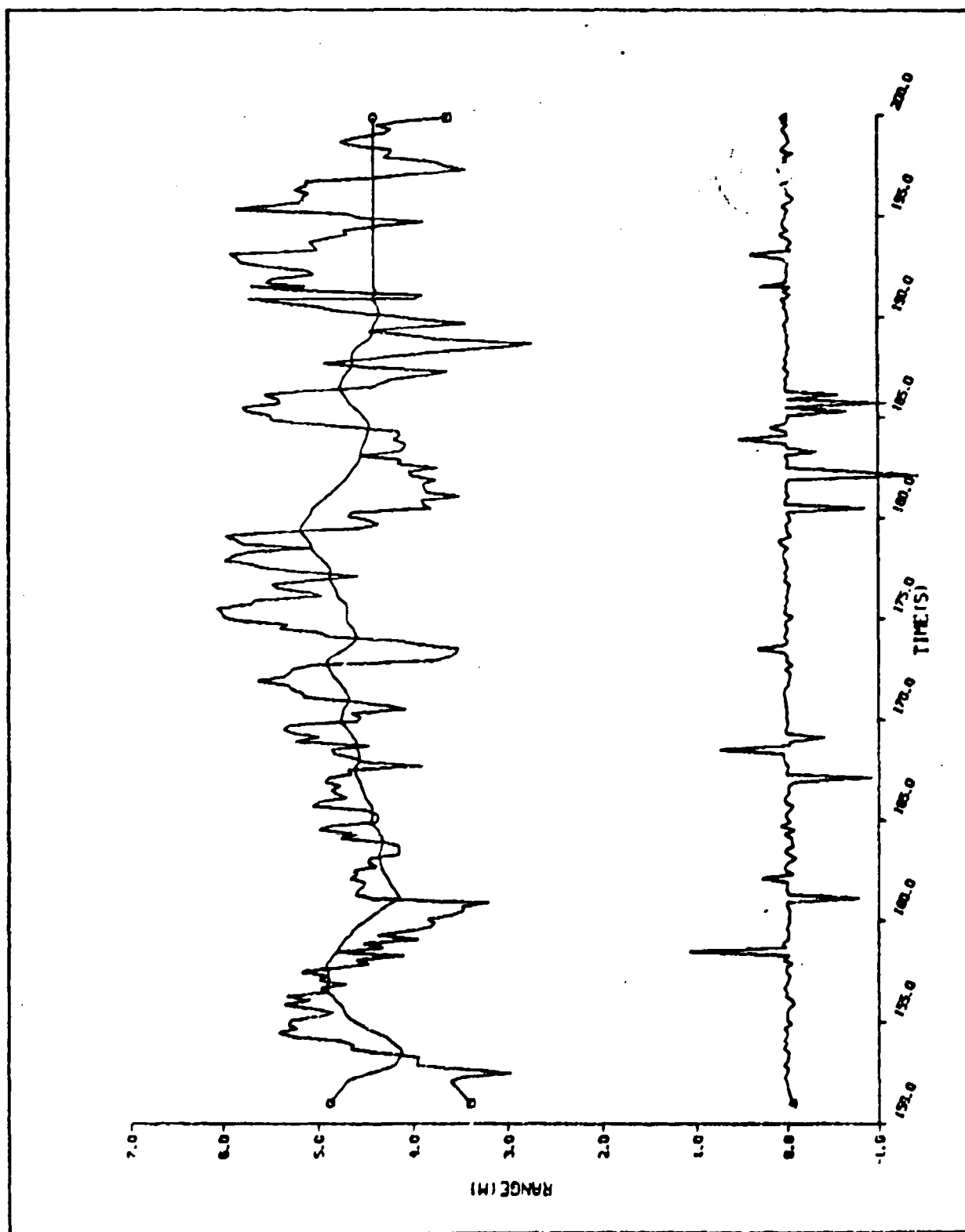FIG IU-12 ELEVATION STATISTICS FOR CASE TWO OF EXAMPLE TWO

78

FIG IV-13 RANGE STATISTICS FOR CASE THREE OF EXAMPLE TWO
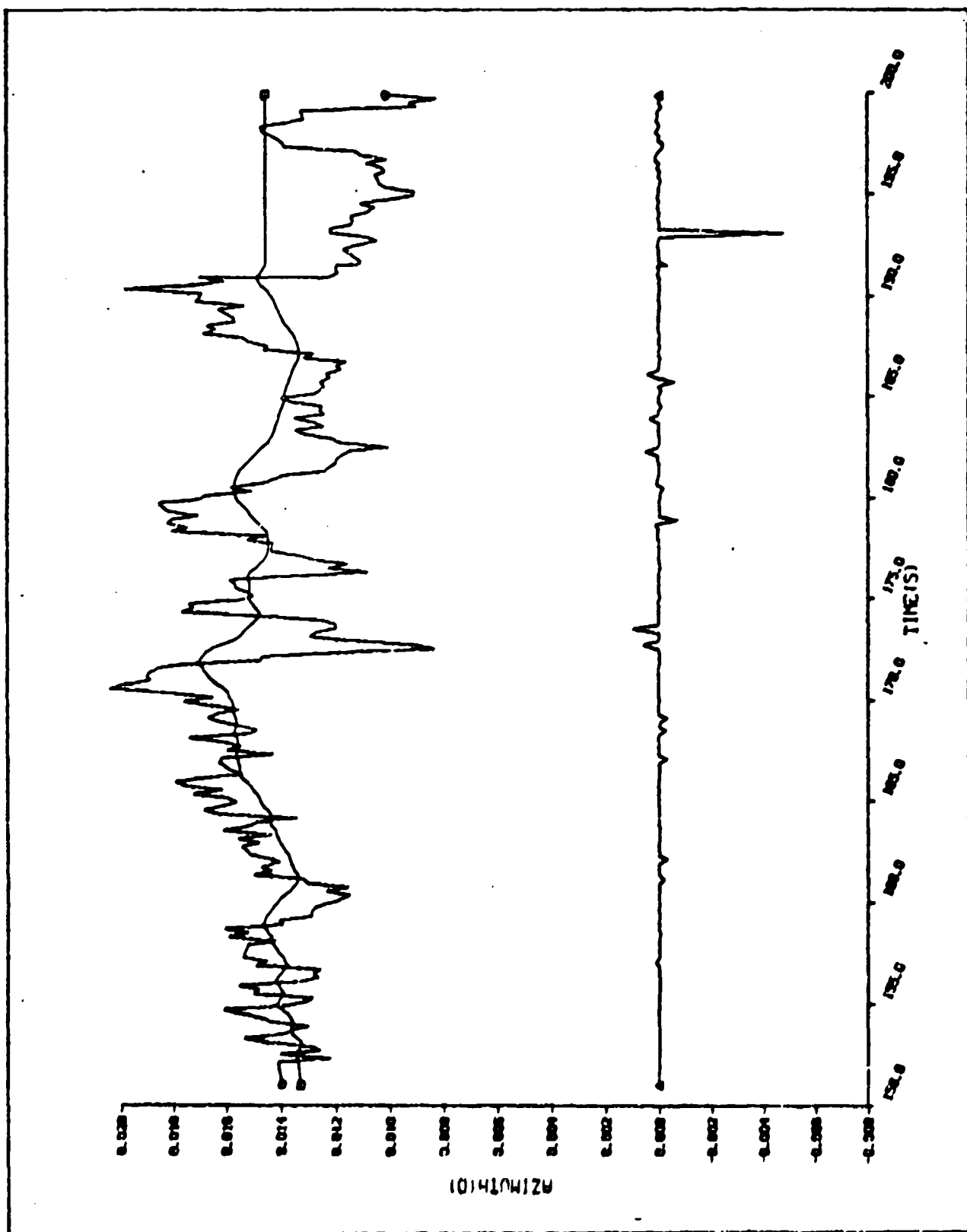SHOWING THE ESTIMATOR SWITCHING

79

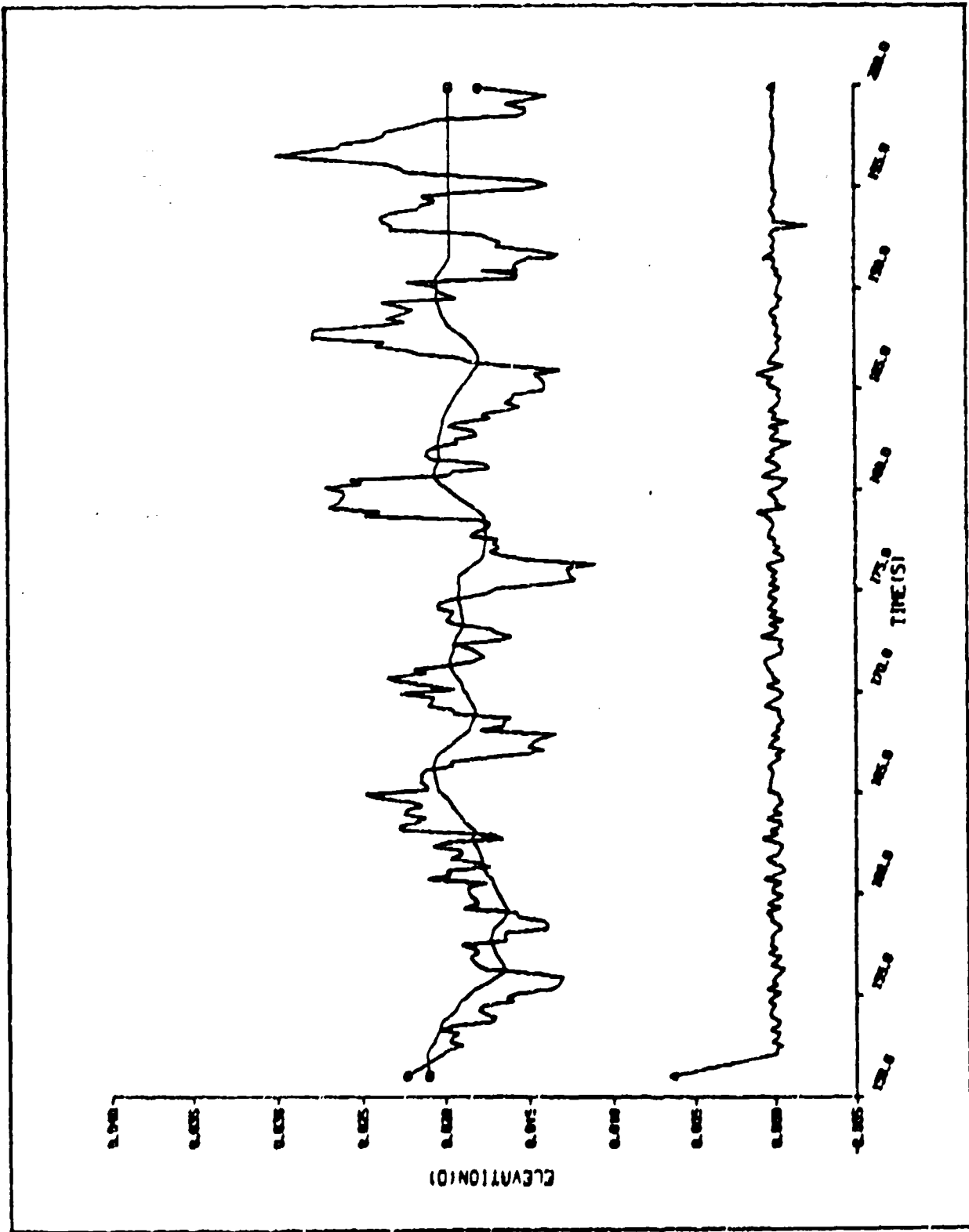FIG IV-14 AZIMUTH STATISTICS FOR CASE THREE OF EXAMPLE TWO

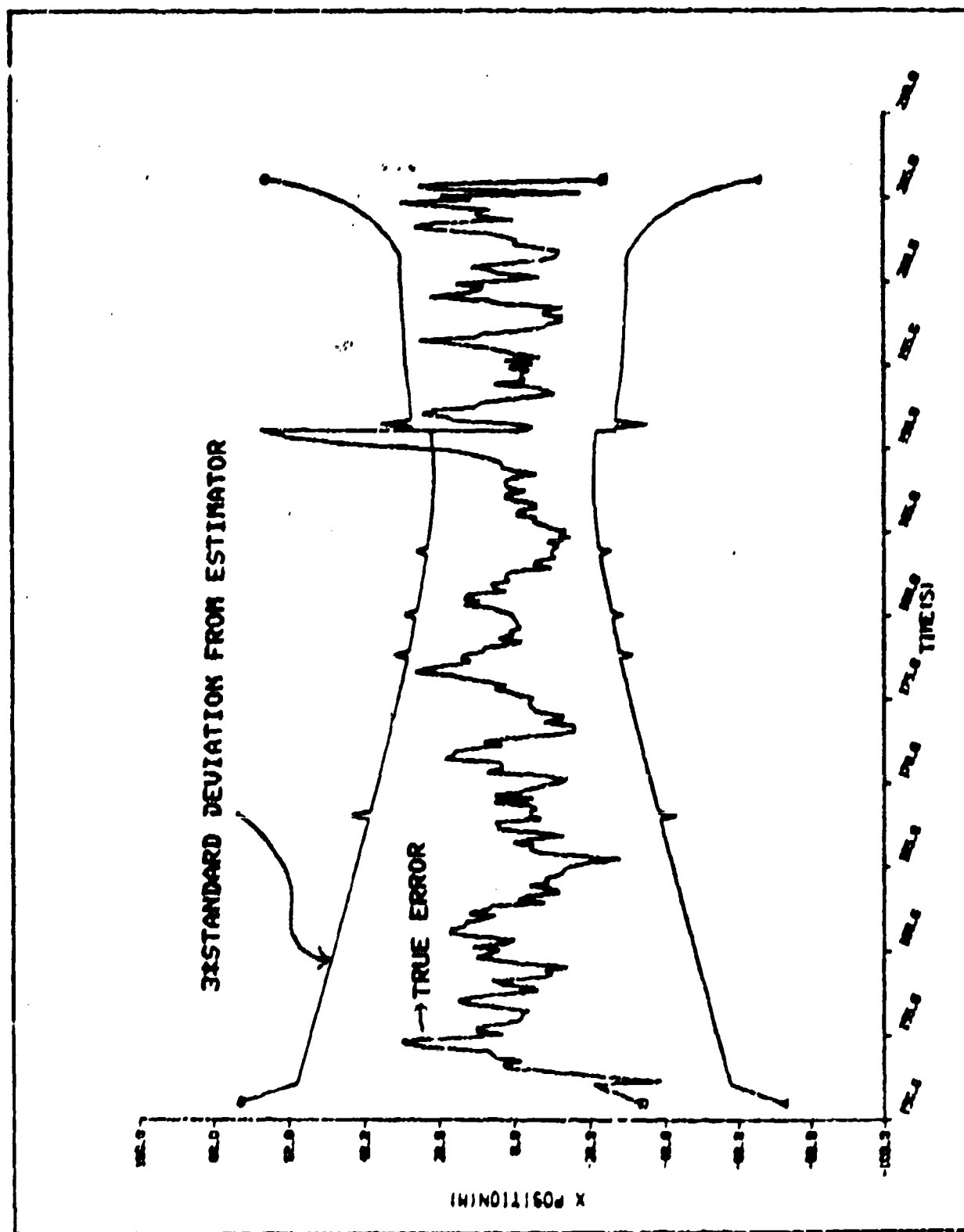FIG IV-15 ELEVATION STATISTICS FOR CASE THREE OF EXAMPLE TWO

FIG IU-16 X POSITION TRUE ERROR AND 3-SIGMA ERROR FOR A CASE-ONE,
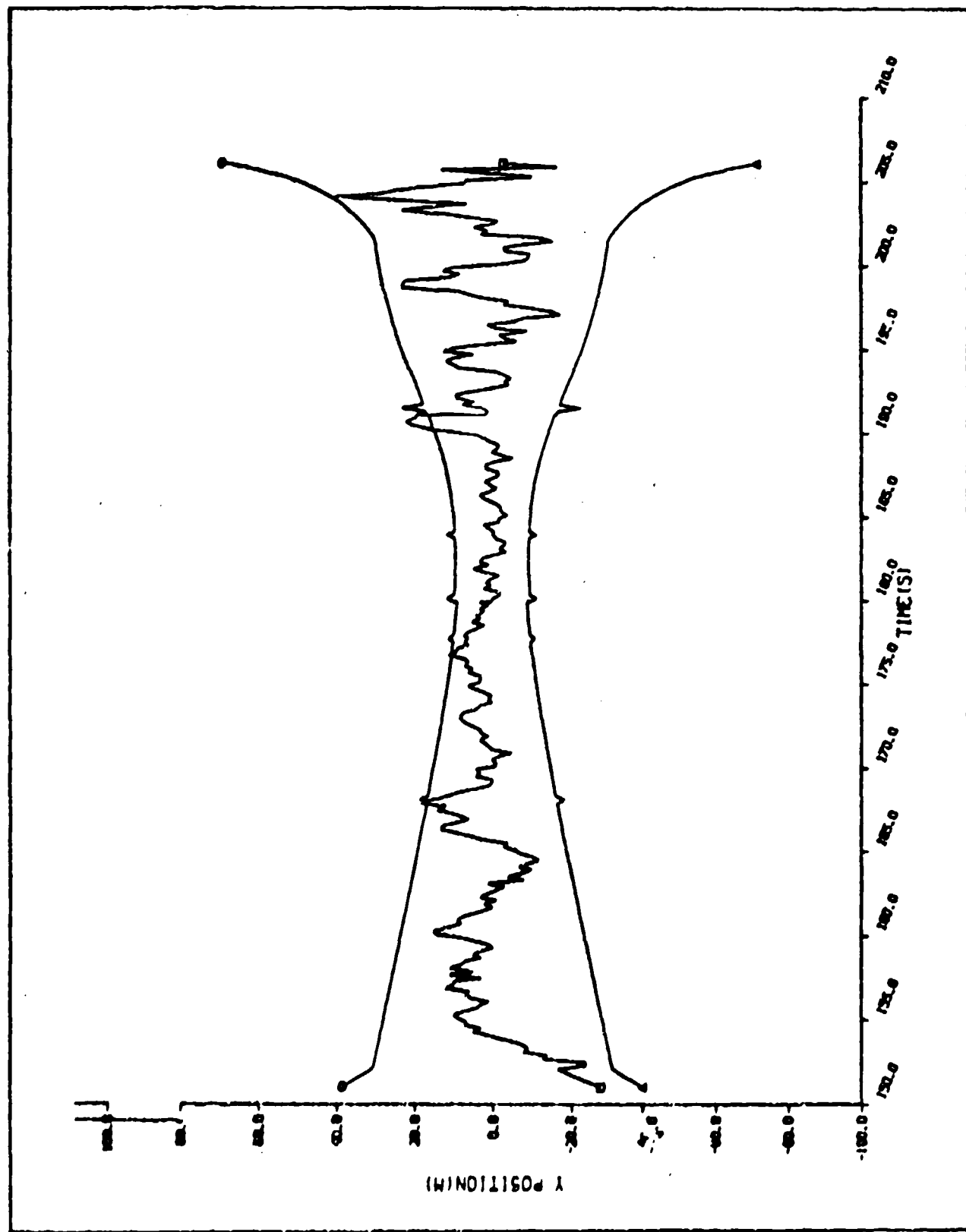EXAMPLE-TWO SINGLE SAMPLE RUN

FIG IV-17 Y POSITION TRUE ERROR AND 3-SIGMA ERROR FOR A CASE-ONE,
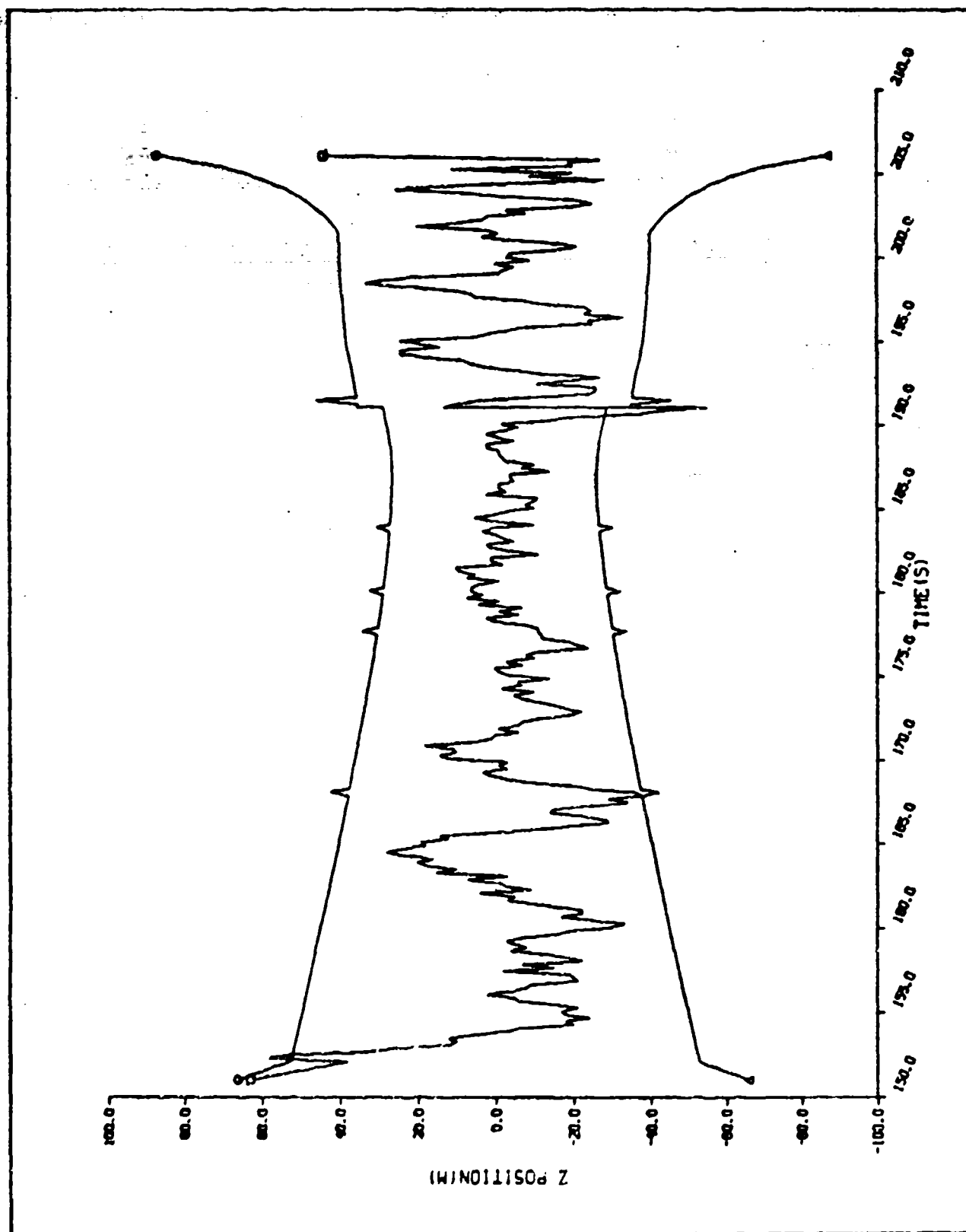EXAMPLE-TWO SINGLE SAMPLE RUN

FIG IU-18 Z POSITION TRUE ERROR AND 3-SIGMA ERROR FOR A CASE-ONE, EXAMPLE-TWO SINGLE SAMPLE RUN

FIG IU-19 X VELOCITY TRUE ERROR AND 3-SIGMA ERROR FOR A CASE-ONE,
EXAMPLE-TWO SINGLE SAMPLE RUN

FIG IU-20 Y VELOCITY TRUE ERROR AND 3-SIGMA ERROR FOR A CASE-ONE, EXAMPLE-TWO SINGLE SAMPLE RUN

86

FIG IV-21   Z VELOCITY TRUE ERROR AND 3-SIGMA ERROR FOR A CASE-ONE,
EXAMPLE-TWO SINGLE SAMPLE RUN

FIG IV-22   BALLISTIC COEFFICIENT TRUE ERROR AND 3-SIGMA ERROR FOR A
CASE-ONE, EXAMPLE-TWO SINGLE SAMPLE RUN

88

FIG IV-23 TURN PARAMETER TRUE ERROR AND 3-SIGMA ERROR FOR A
CASE-ONE, EXAMPLE-TWO SINGLE SAMPLE RUN

89

FIG IV-24 CLIMB PARAMETER TRUE ERROR AND 3-SIGMA ERROR FOR A
CASE-ONE, EXAMPLE-TWO SINGLE SAMPLE RUN

FIG IV-25 X POSITION TRUE ERROR AND 3-SIGMA ERROR FOR A CASE-TWO,
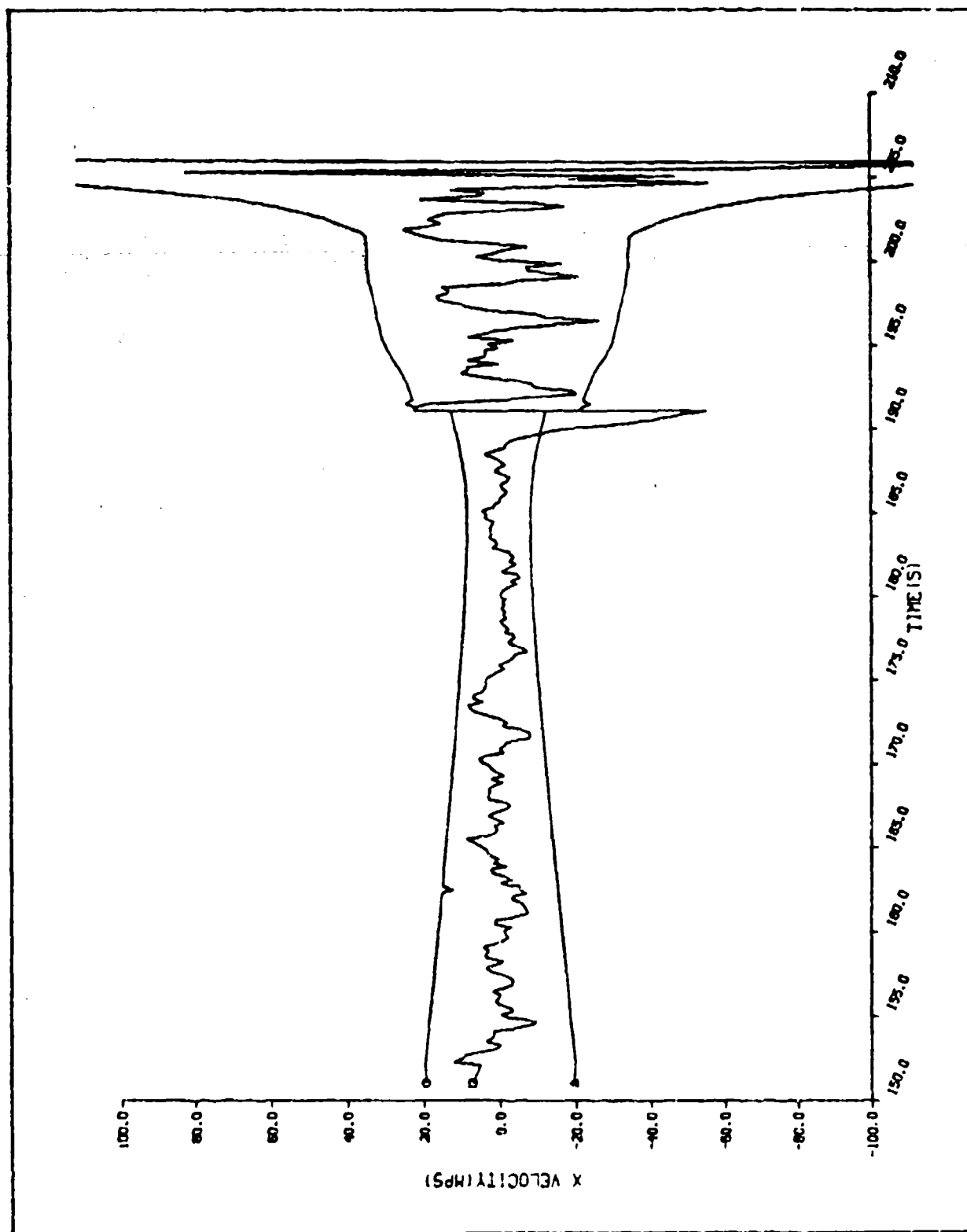EXAMPLE-TWO SINGLE SAMPLE RUN
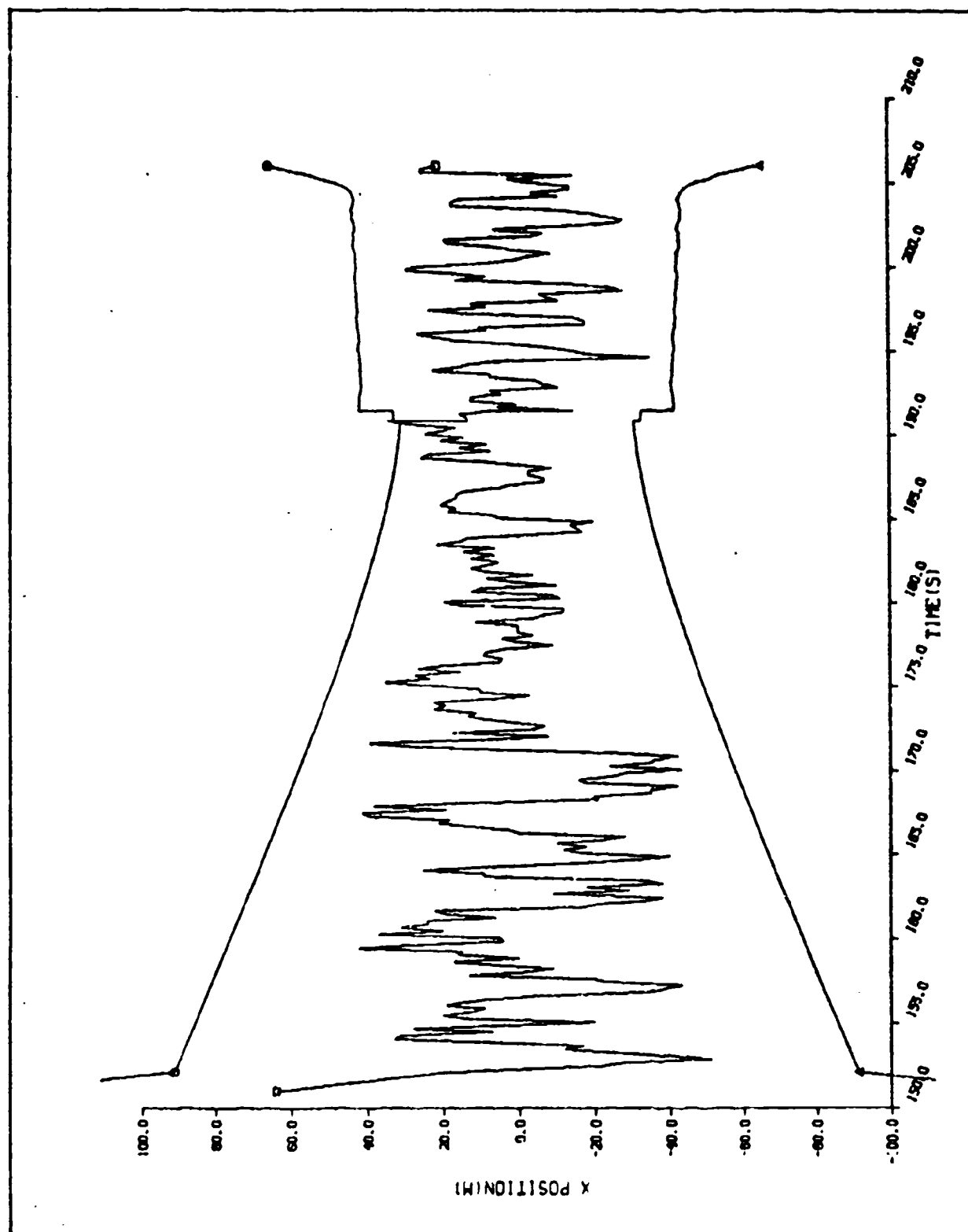
FIG IV-26 X POSITION TRUE ERROR AND 3-SIGMA ERROR FOR A CASE-THREE,
EXAMPLE-TWO SINGLE SAMPLE RUN
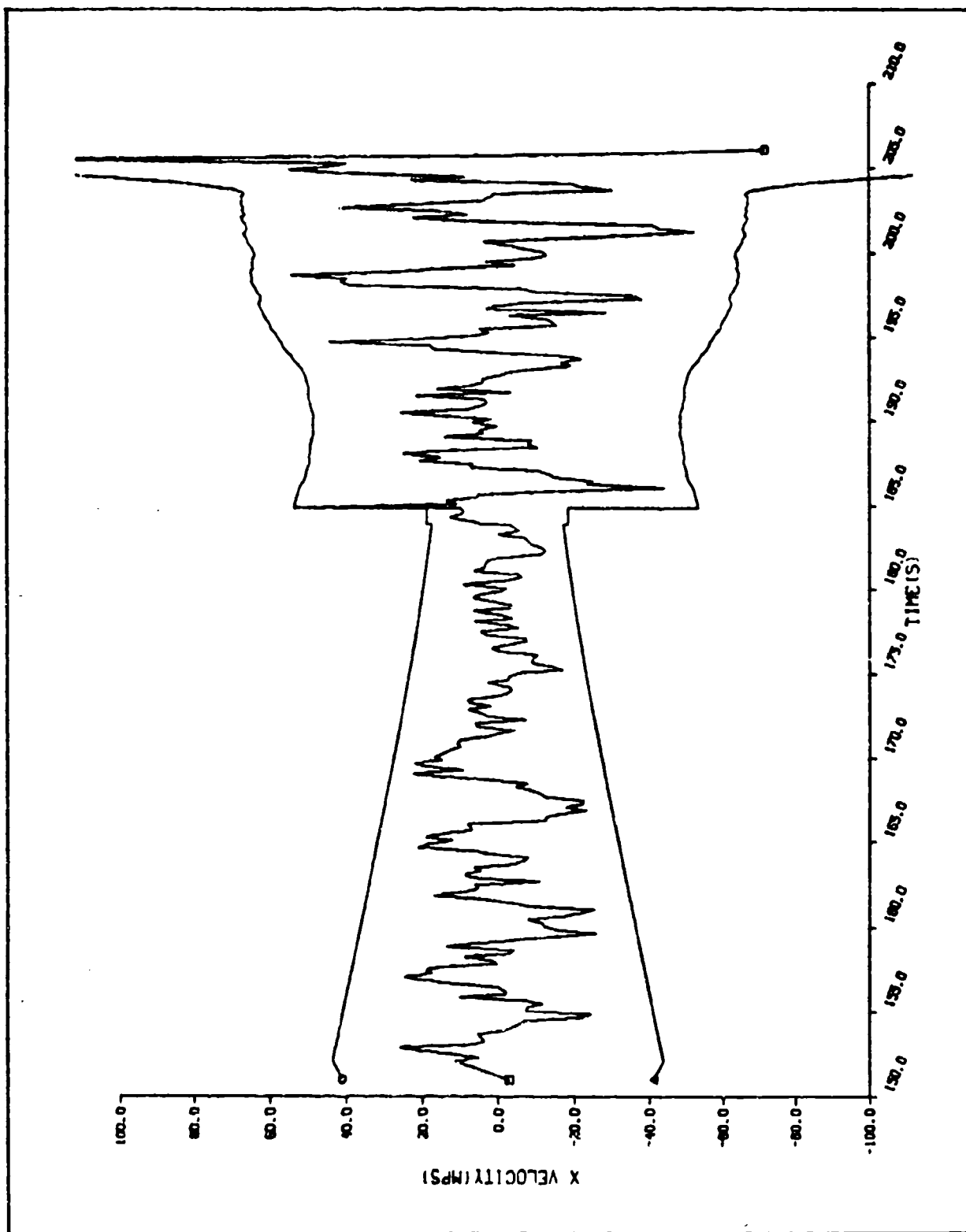
FIG IV-27 X VELOCITY TRUE ERROR AND 3-SIGMA ERROR FOR A CASE-TWO, EXAMPLE-TWO SINGLE SAMPLE RUN
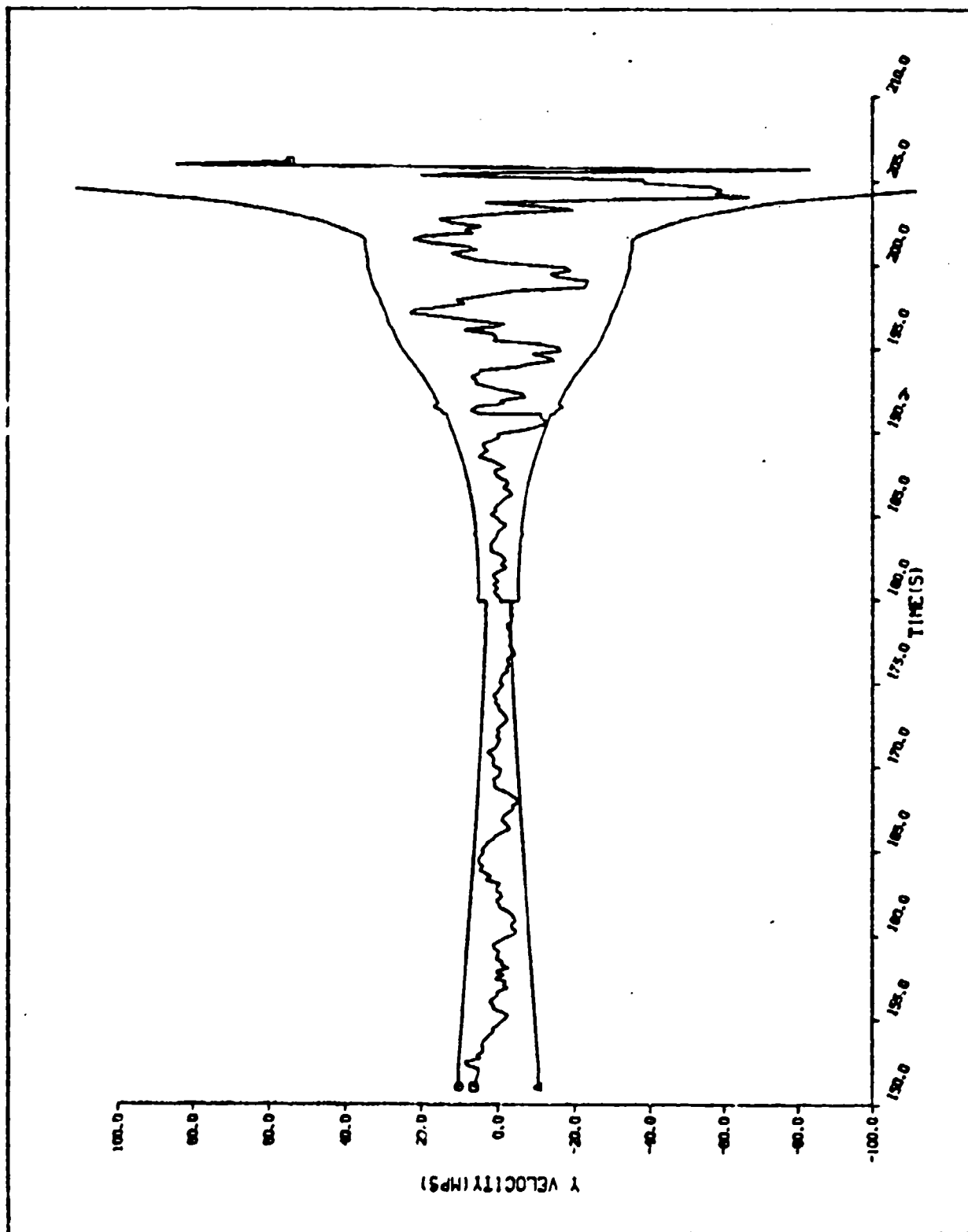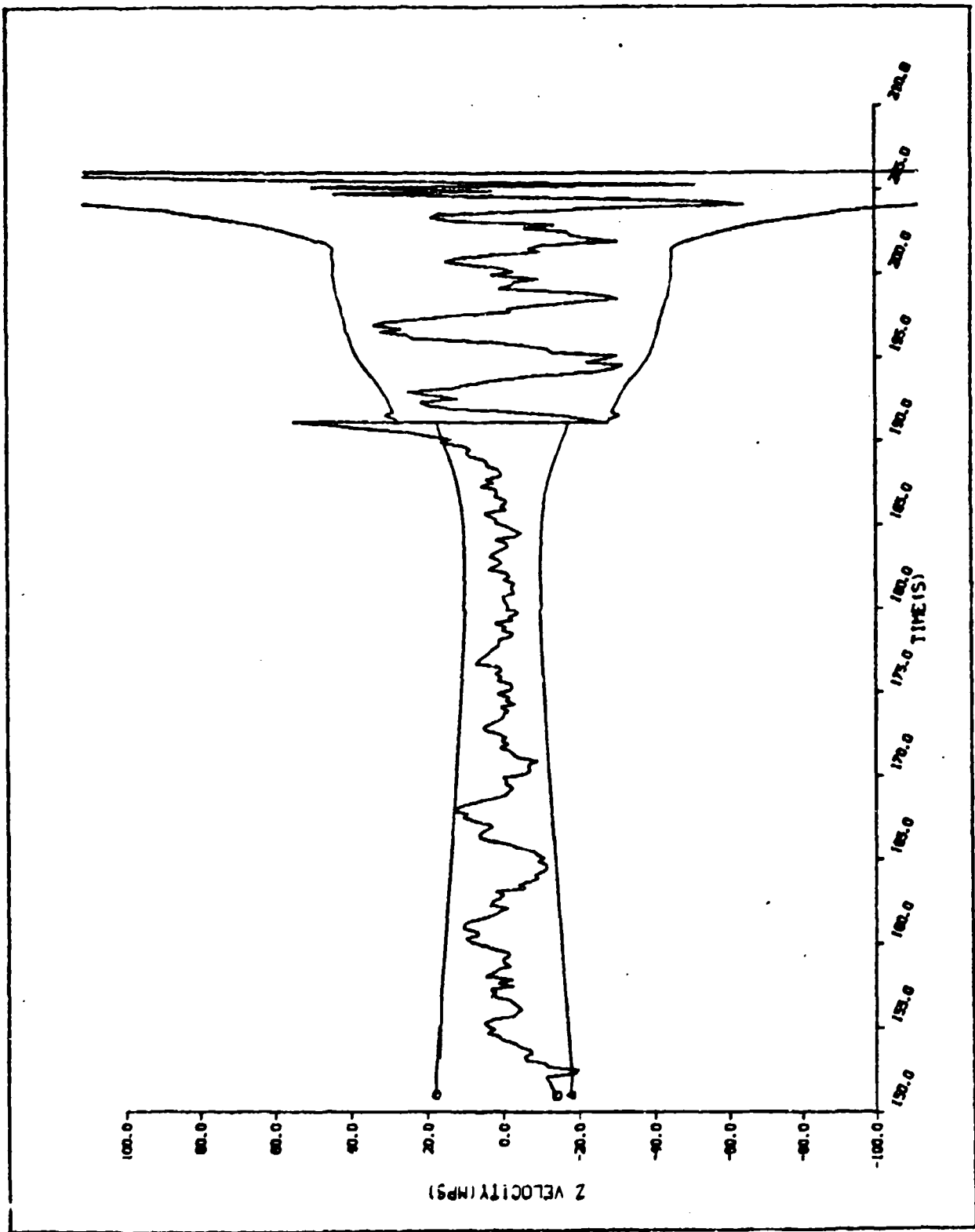
93
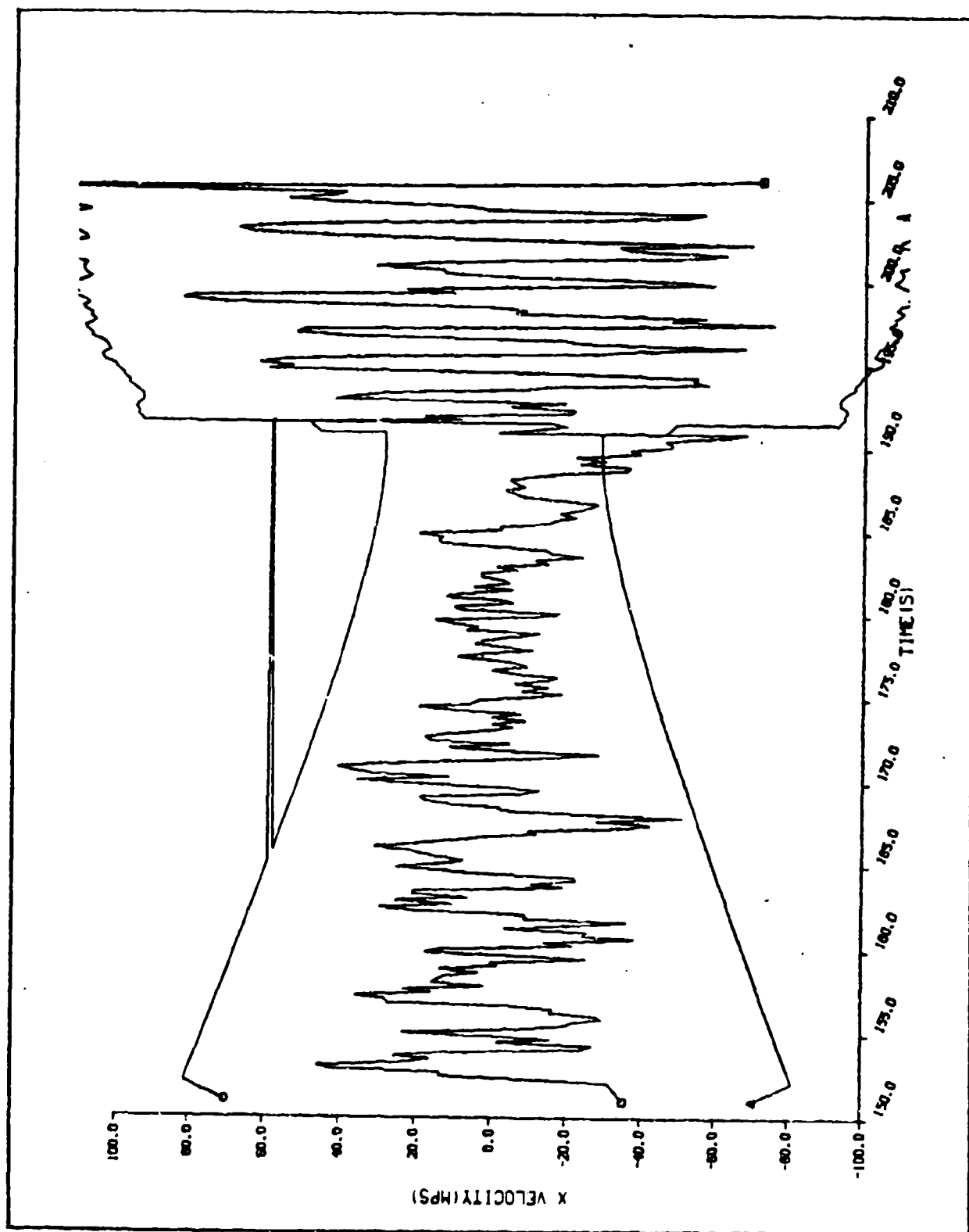
FIG IV-28 X VELOCITY TRUE ERROR AND 3-SIGMA ERROR FOR A CASE-THREE,
EXAMPLE-TWO SINGLE SAMPLE RUN

94
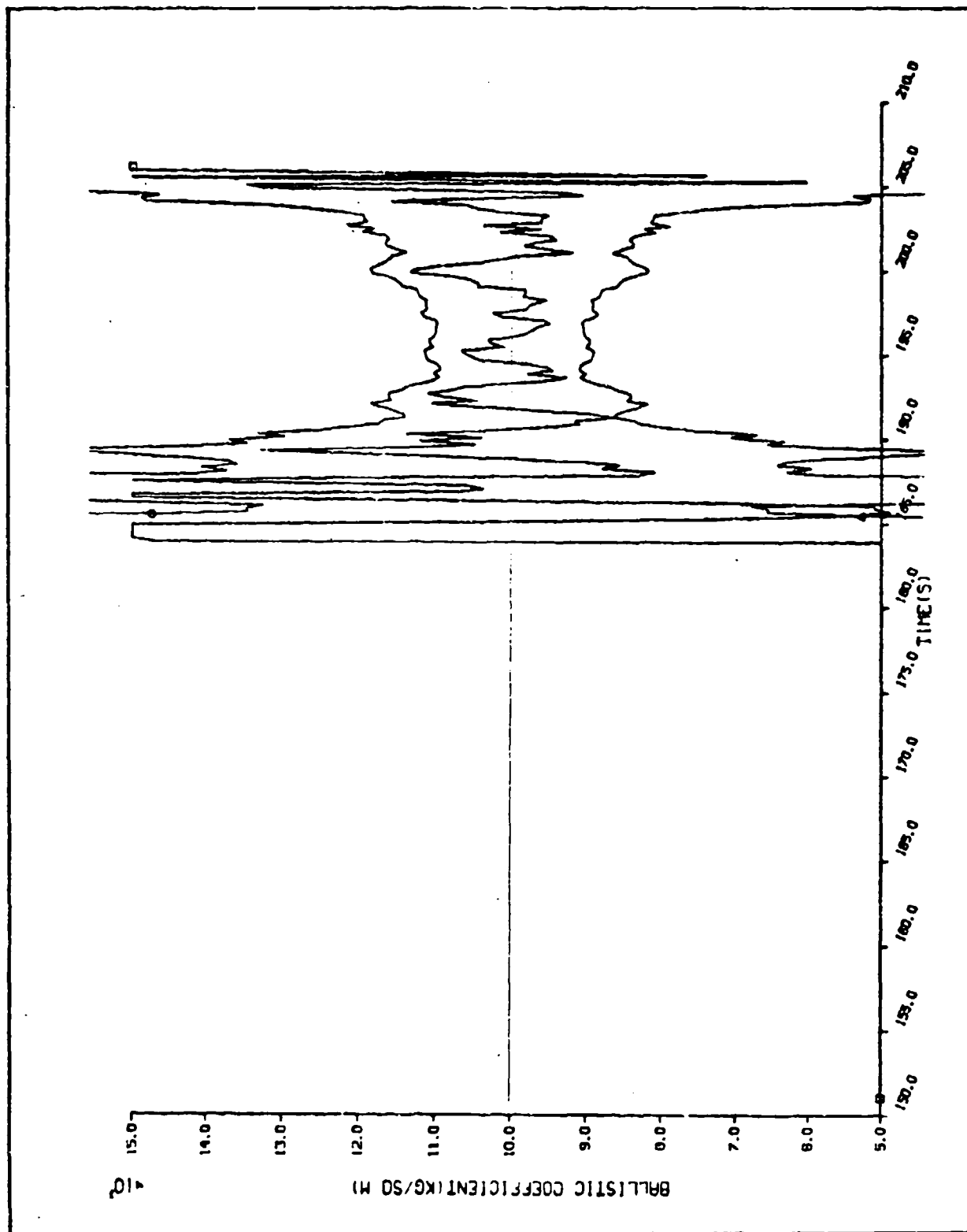
FIG IV-29 BALLISTIC COEFFICIENT TRUE ERROR AND 3-SIGMA ERROR FOR A CASE-TWO, EXAMPLE-TWO SINGLE SAMPLE RUN
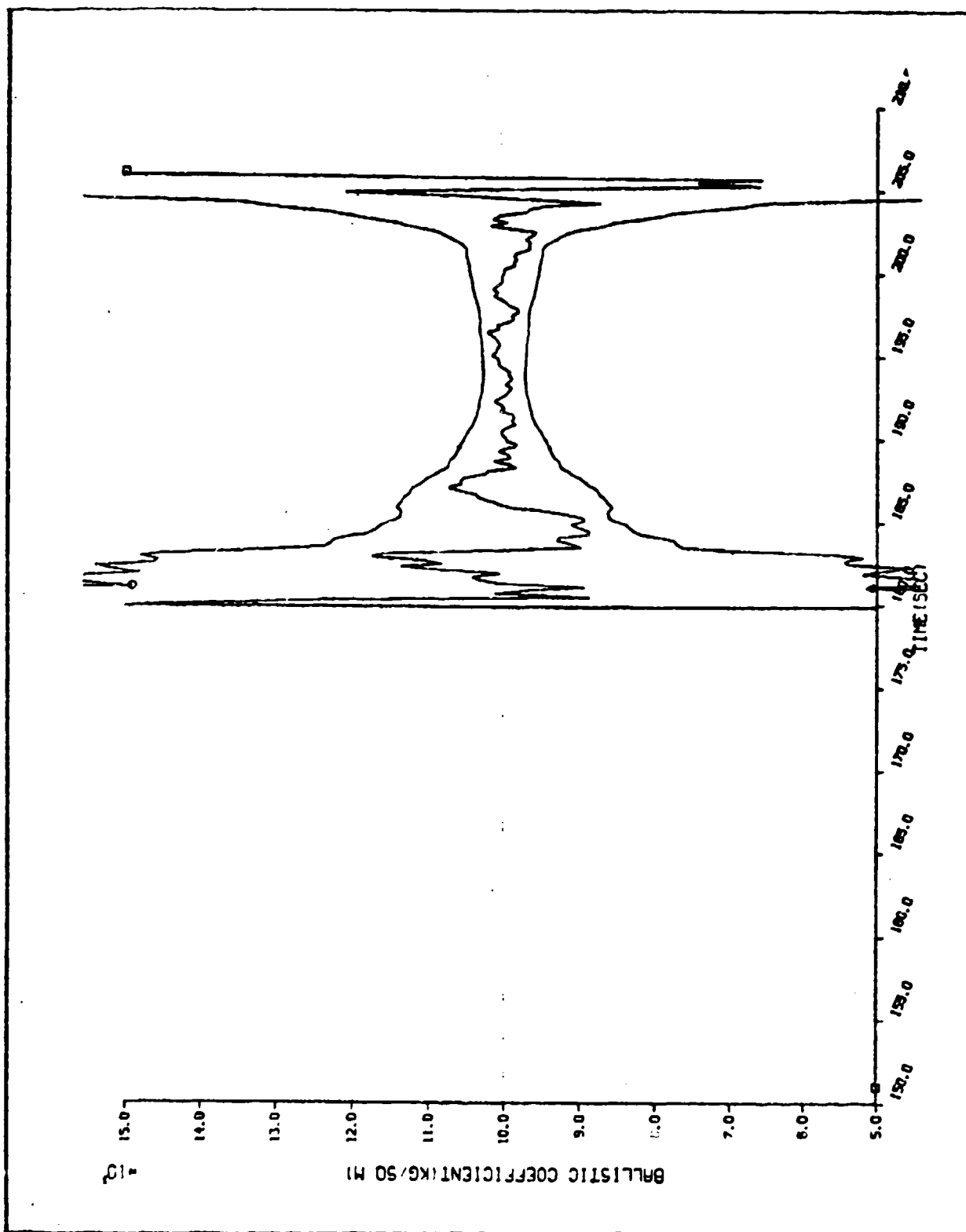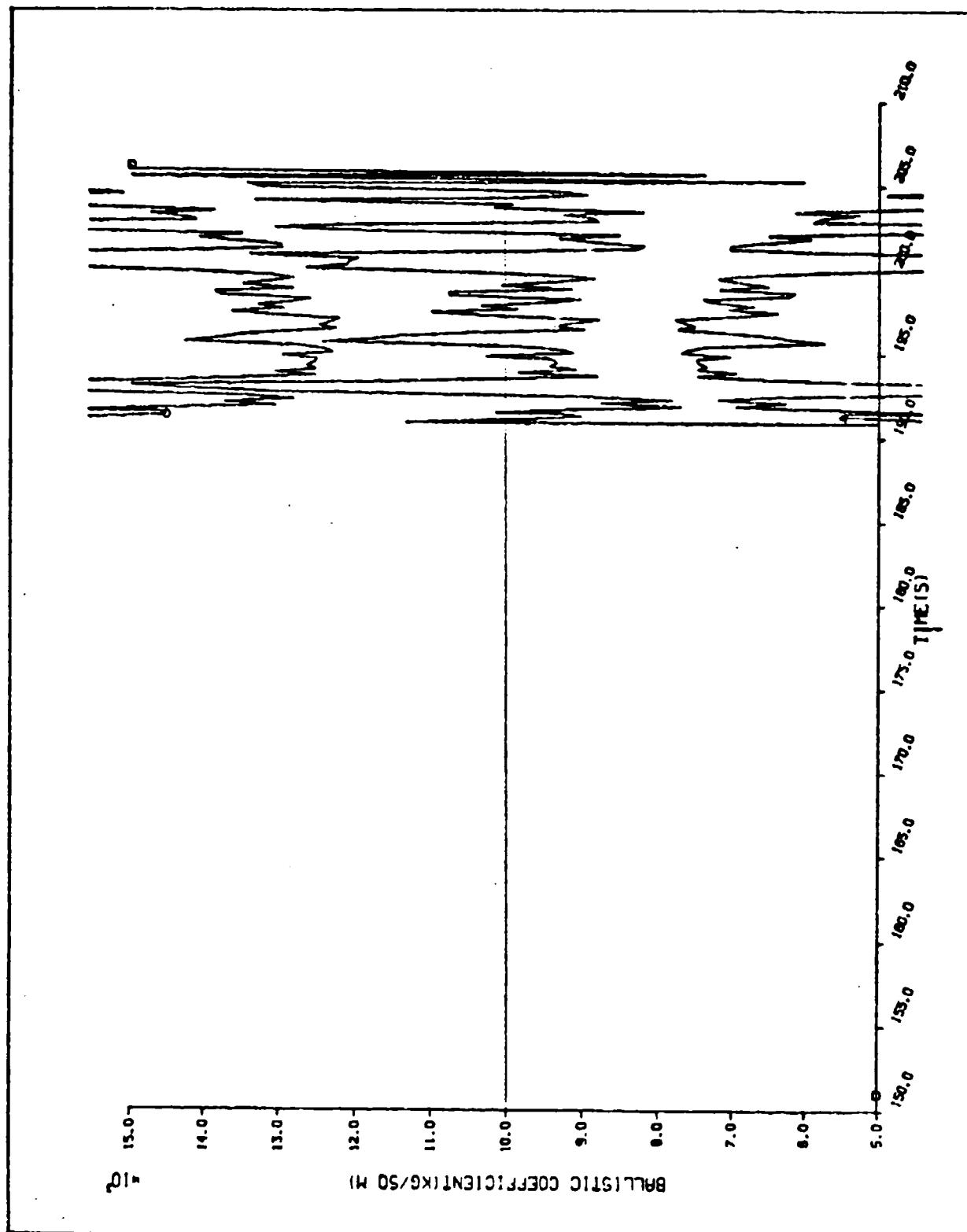
FIG IV-30 BALLISTIC COEFFICIENT TRUE ERROR AND 3-SIGMA ERROR FOR A
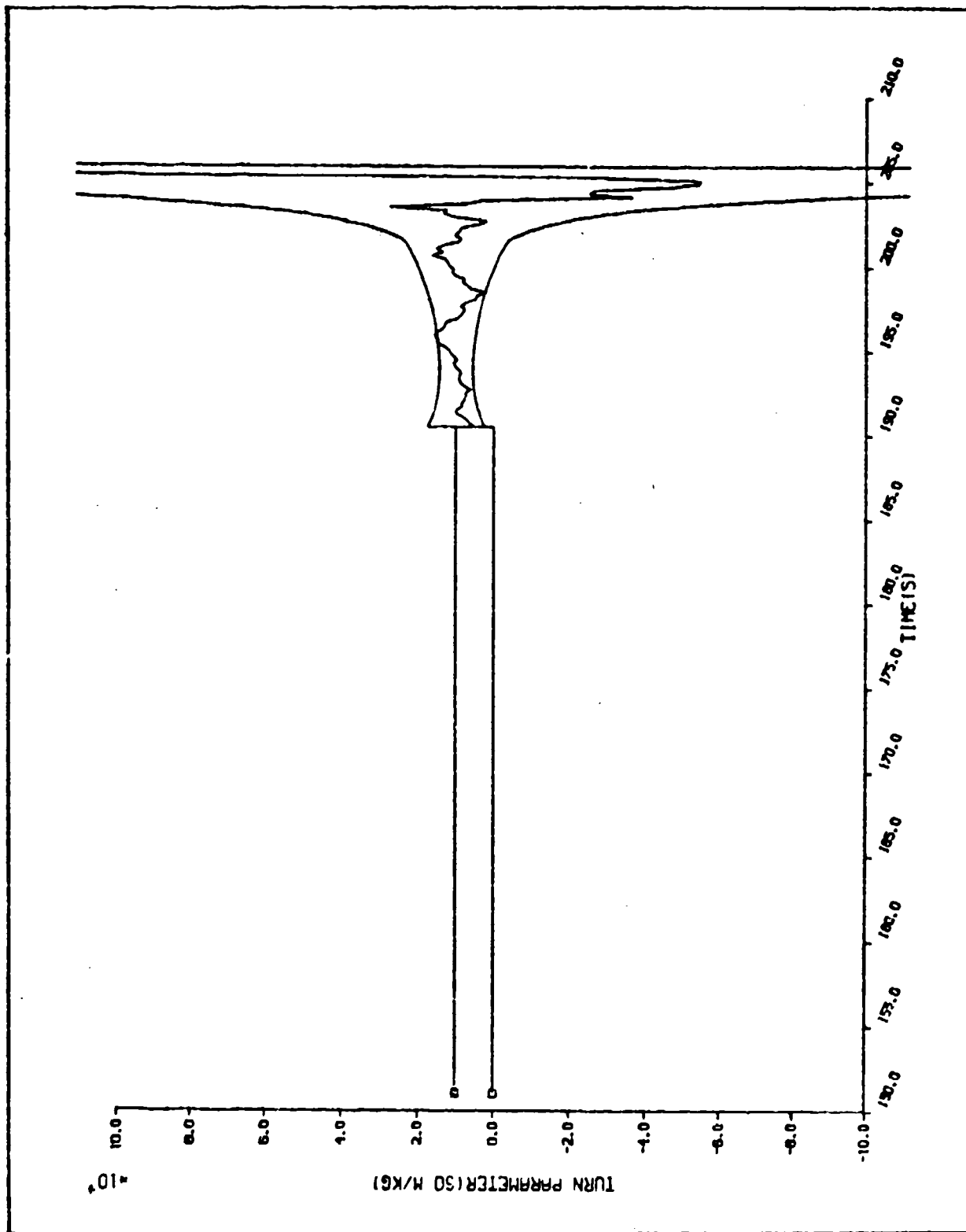CASE-THREE, EXAMPLE-TWO SINGLE SAMPLE RUN
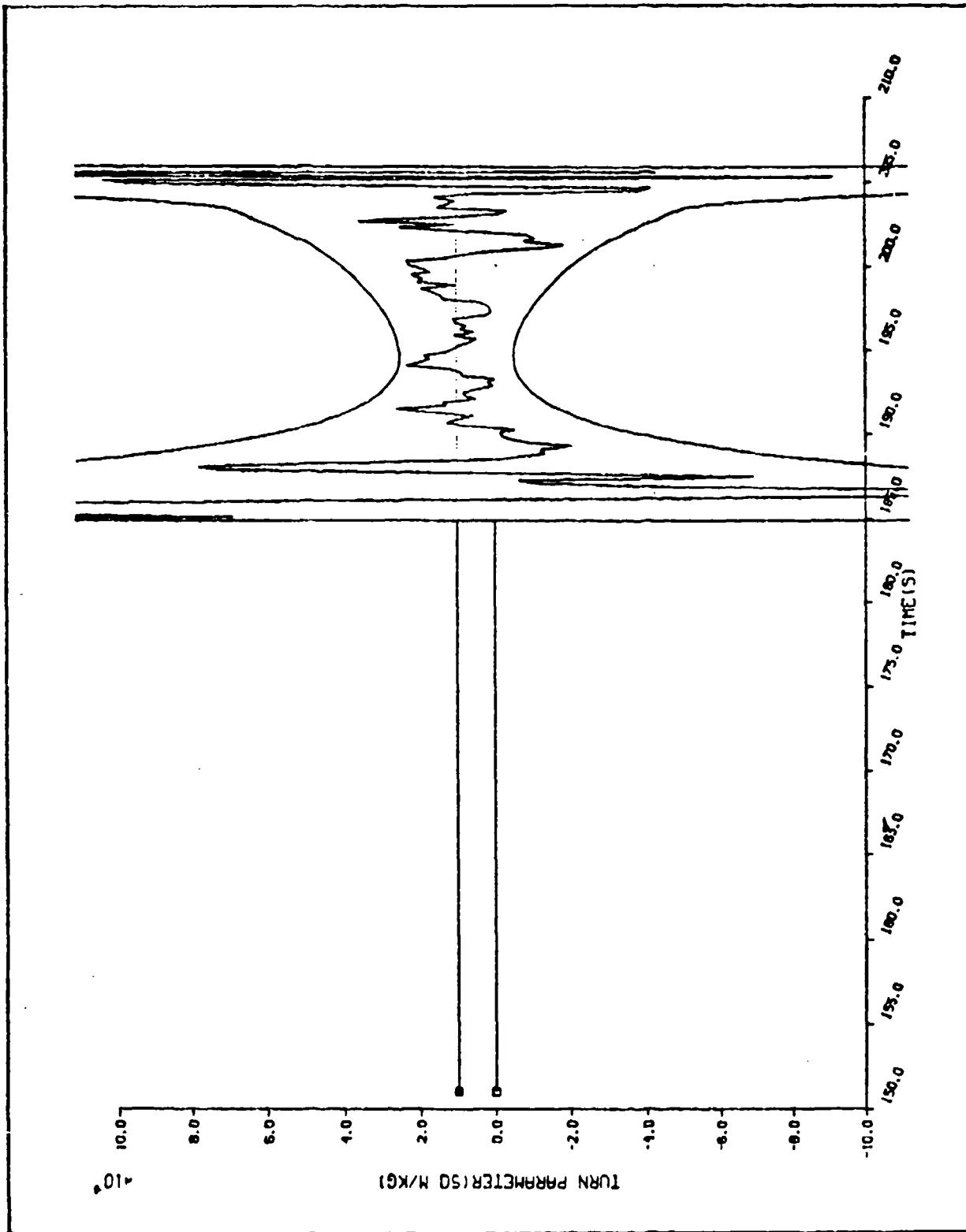
FIG IV-31 TURN PARAMETER TRUE ERROR AND 3-SIGMA ERROR FOR A CASE-TWO, EXAMPLE-TWO SINGLE SAMPLE RUN
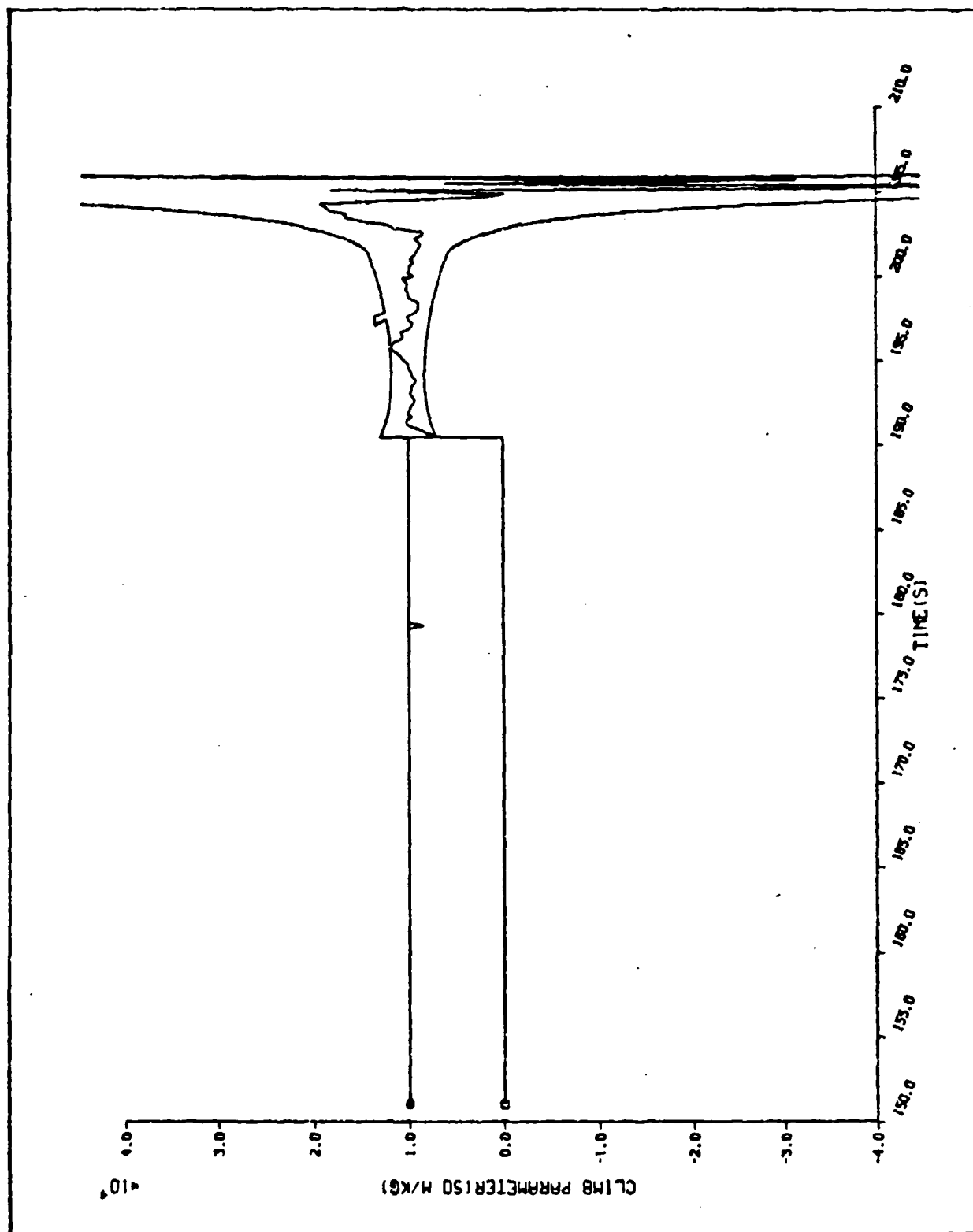
97
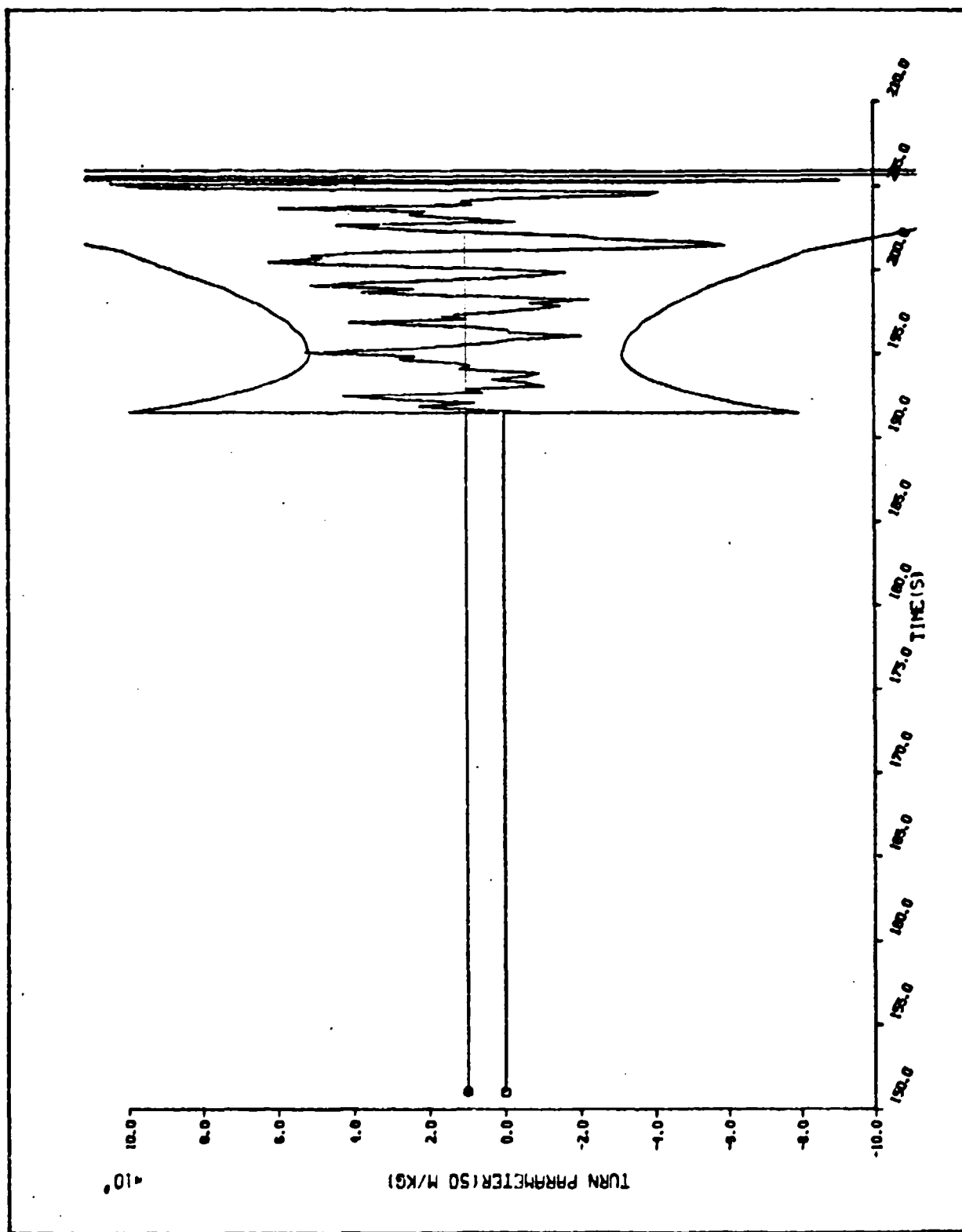
FIG IV-32 TURN PARAMETER TRUE ERROR AND 3-SIGMA ERROR FOR A
CASE-THREE, EXAMPLE-TWO SINGLE SAMPLE RUN

98
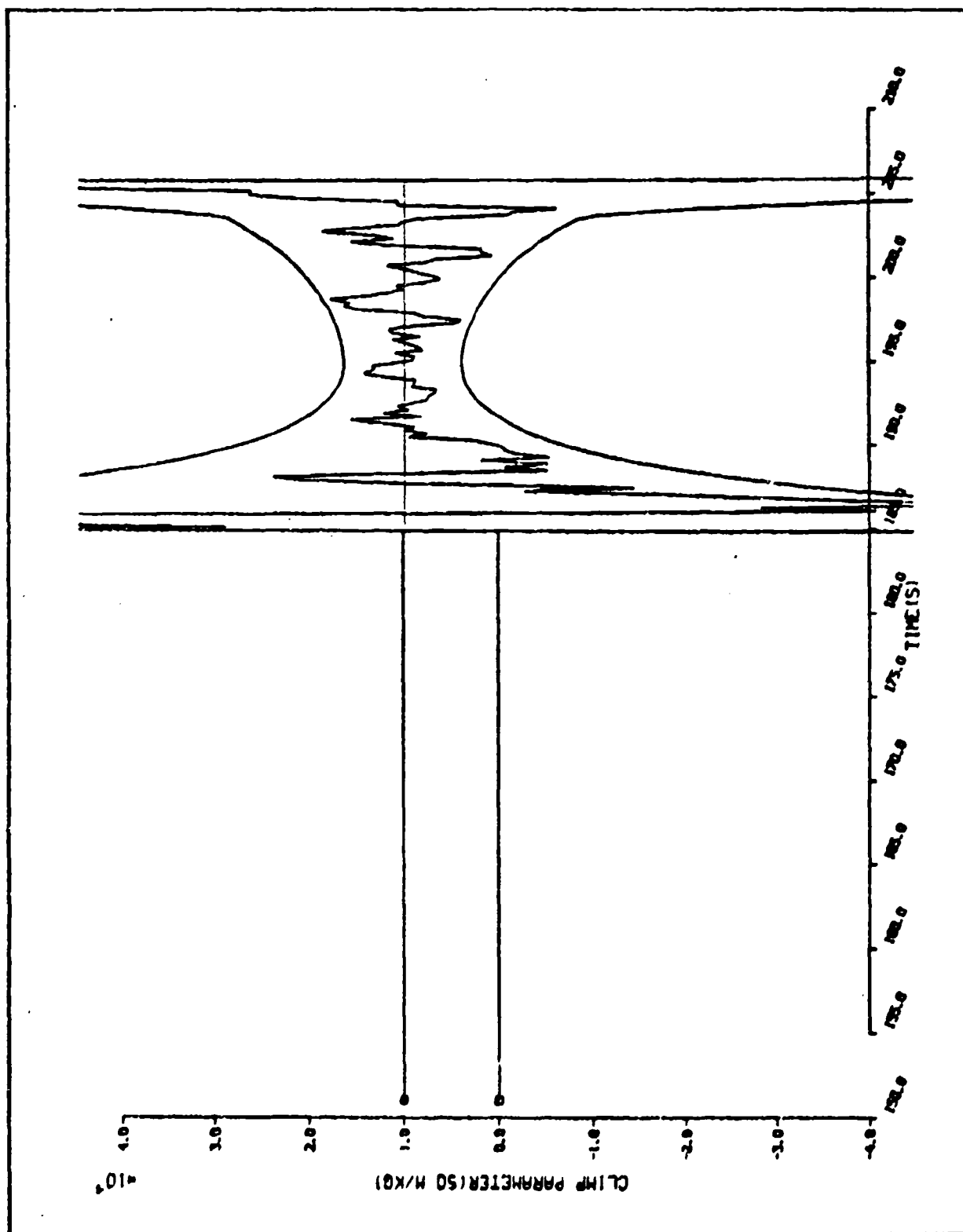
FIG IV-33   CLIMB PARAMETER TRUE ERROR AND 3-SIGMA ERROR FOR A
CASE-TWO, EXAMPLE-TWO SINGLE SAMPLE RUN

99
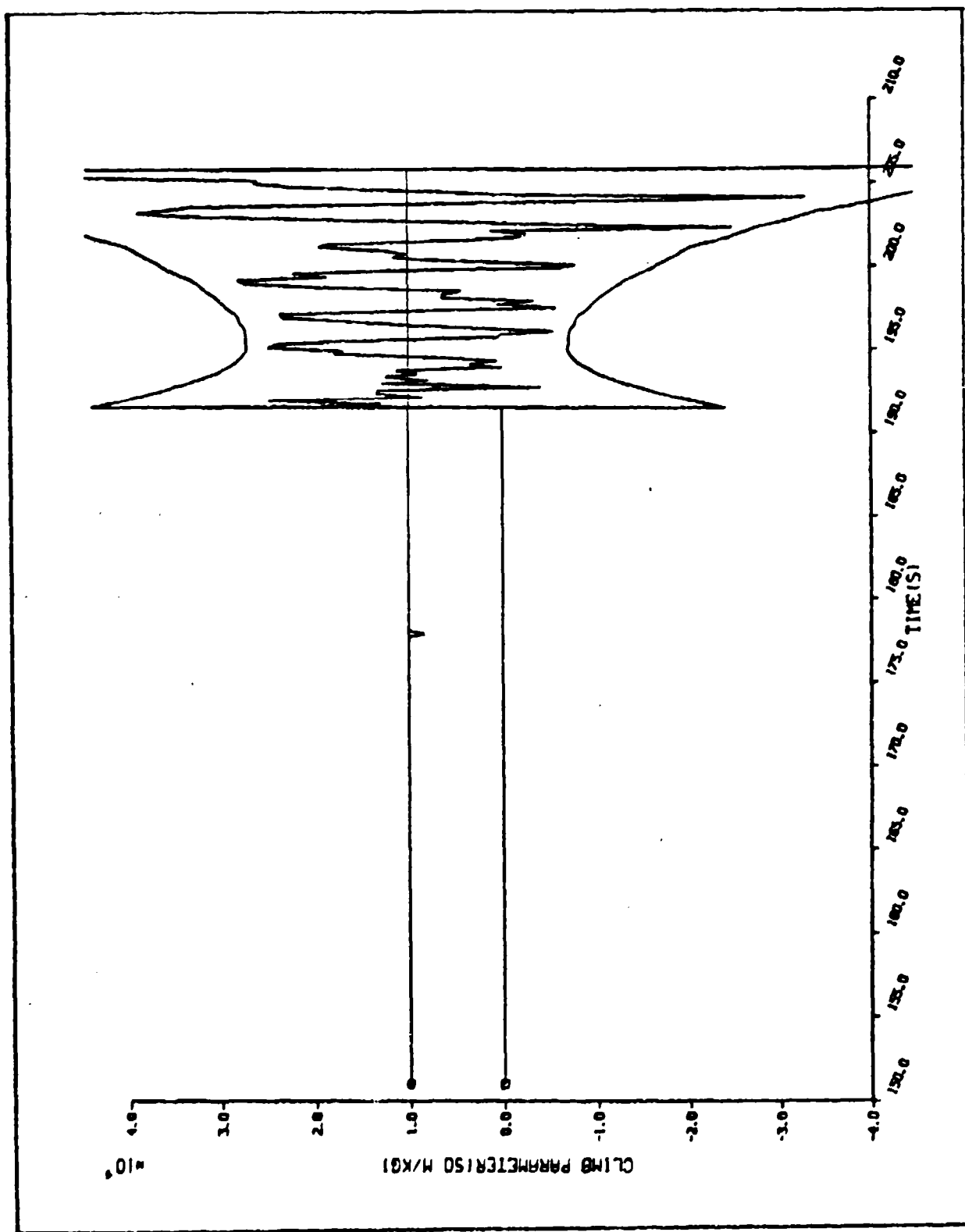
FIG IV-34   CLIMB PARAMETER TRUE ERROR AND 3-SIGMA ERROR FOR A
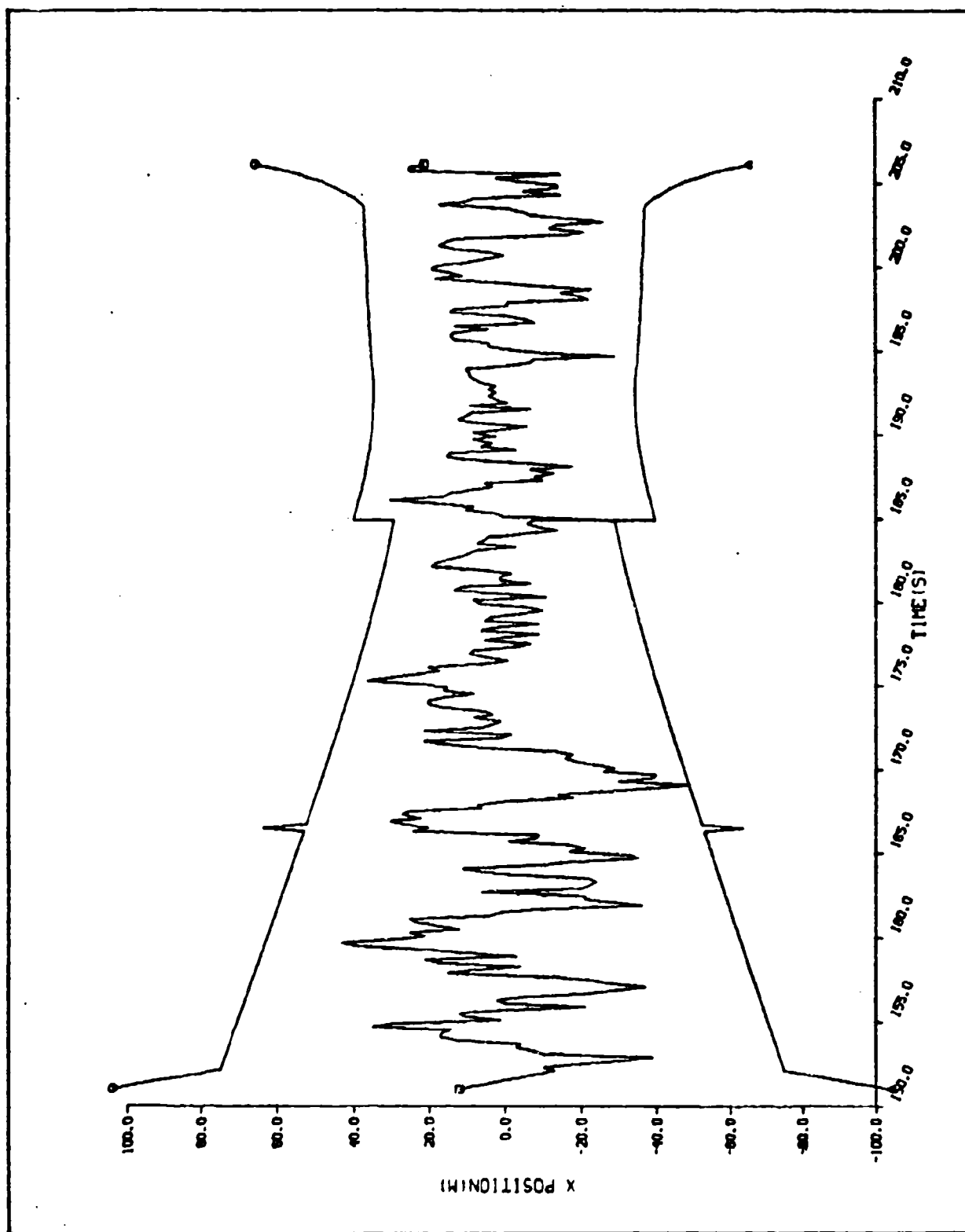CASE-THREE, EXAMPLE-TWO SINGLE SAMPLE RUN

100

results of the single sample covariance analysis, a ten run
Monte Carlo simulation was performed for the case one runs
(50 point batch sizes). The results of this Monte Carlo
simulation are plotted in Figures IV-35 through IV-43. In
each of these figures both the standard deviations from the
Monte Carlo simulation and from a single sample run are
plotted. Plus and minus values are plotted so as to locate
the zero line easily. The results of this Monte Carlo simula-
tion show that, in general the single sample standard devia-
tions are realistic, albeit conservative, estimates of the
errors in the estimated parameters.
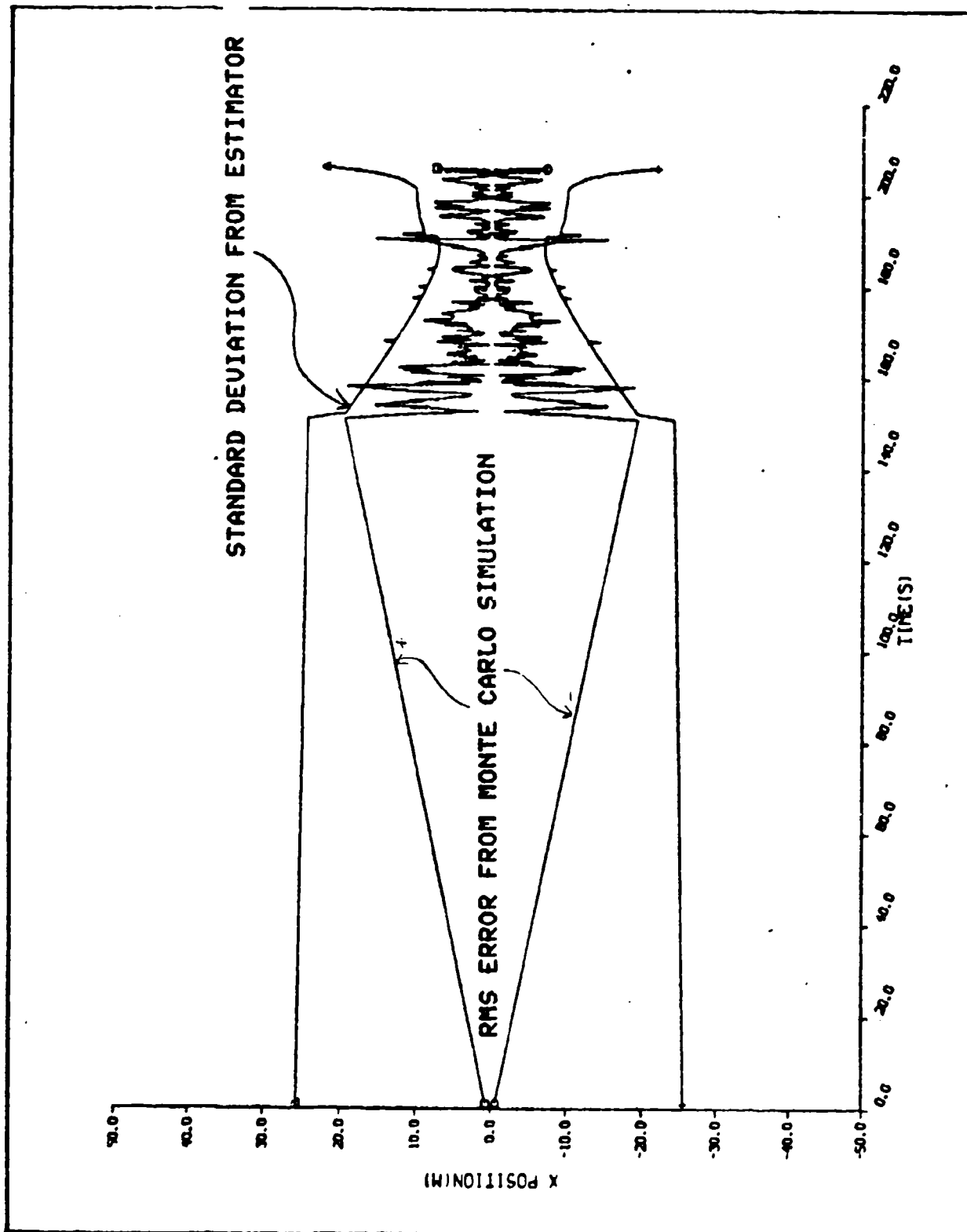
FIG IV-35 X POSITION COMPARISON OF THE SINGLE SAMPLE STANDARD
DEVIATION WITH THE RMS ERROR FROM A 10-RUN MONTE CARLO
SIMULATION. EXAMPLE TWO, CASE ONE TYPE
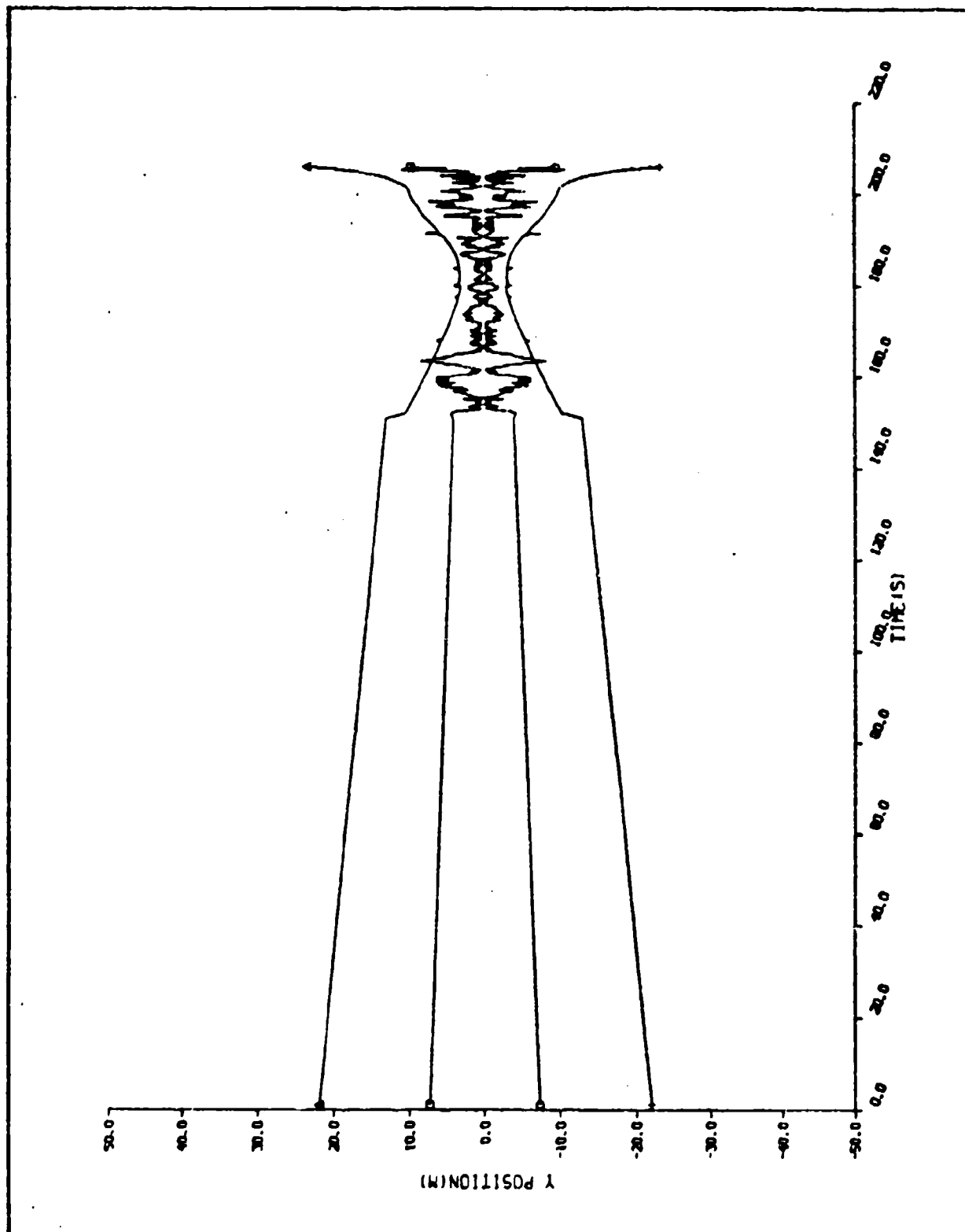
FIG IU-36   Y POSITION COMPARISON OF THE SINGLE SAMPLE STANDARD
DEVIATION WITH THE RMS ERROR FROM A 10-RUN MONTE CARLO
SIMULATION, EXAMPLE TWO, CASE ONE TYPE

103
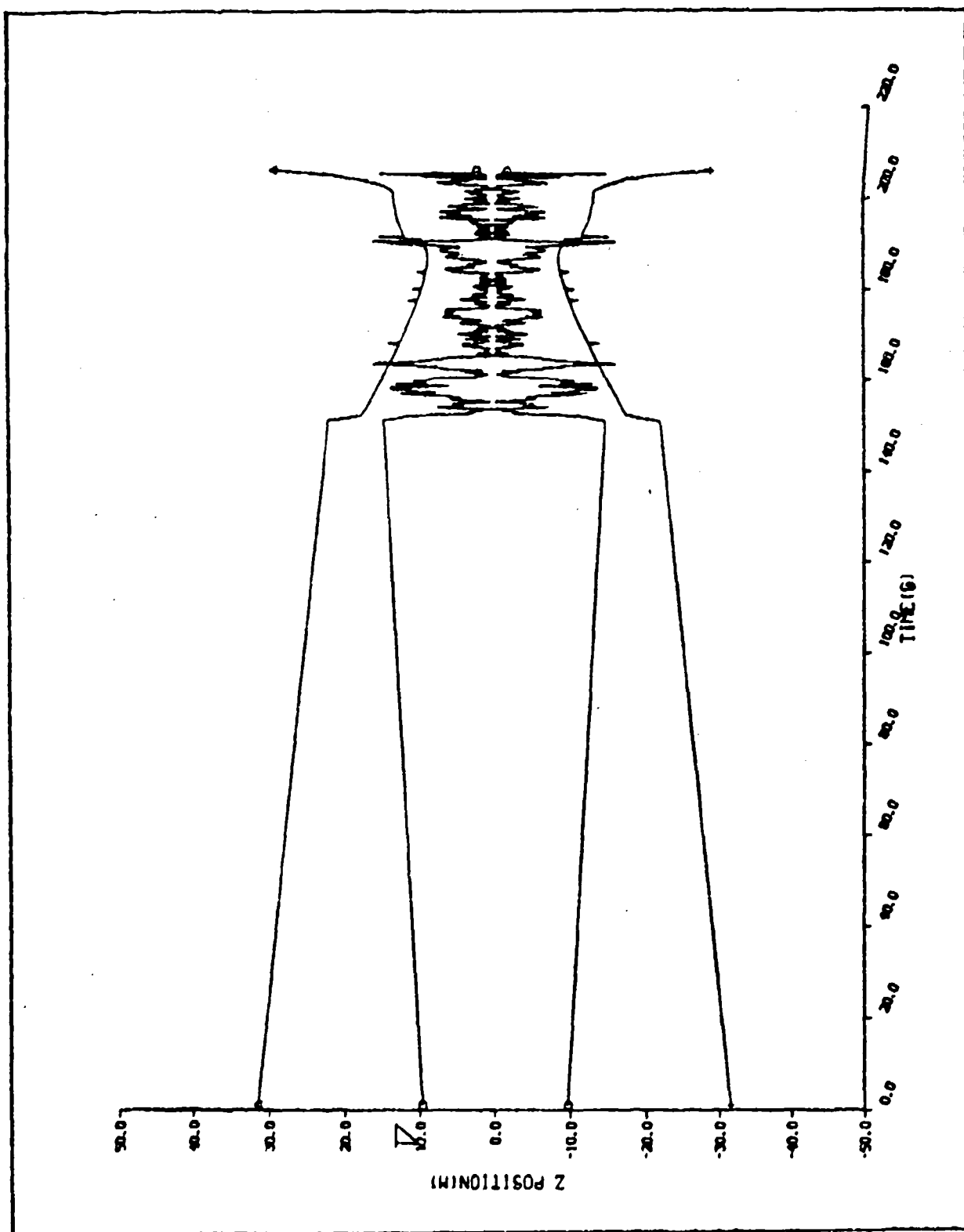
FIG IU-37 Z POSITION COMPARISON OF THE SINGLE SAMPLE STANDARD DEVIATION WITH THE RMS ERROR FROM A 10-RUN MONTE CARLO SIMULATION, EXAMPLE TWO, CASE ONE TYPE
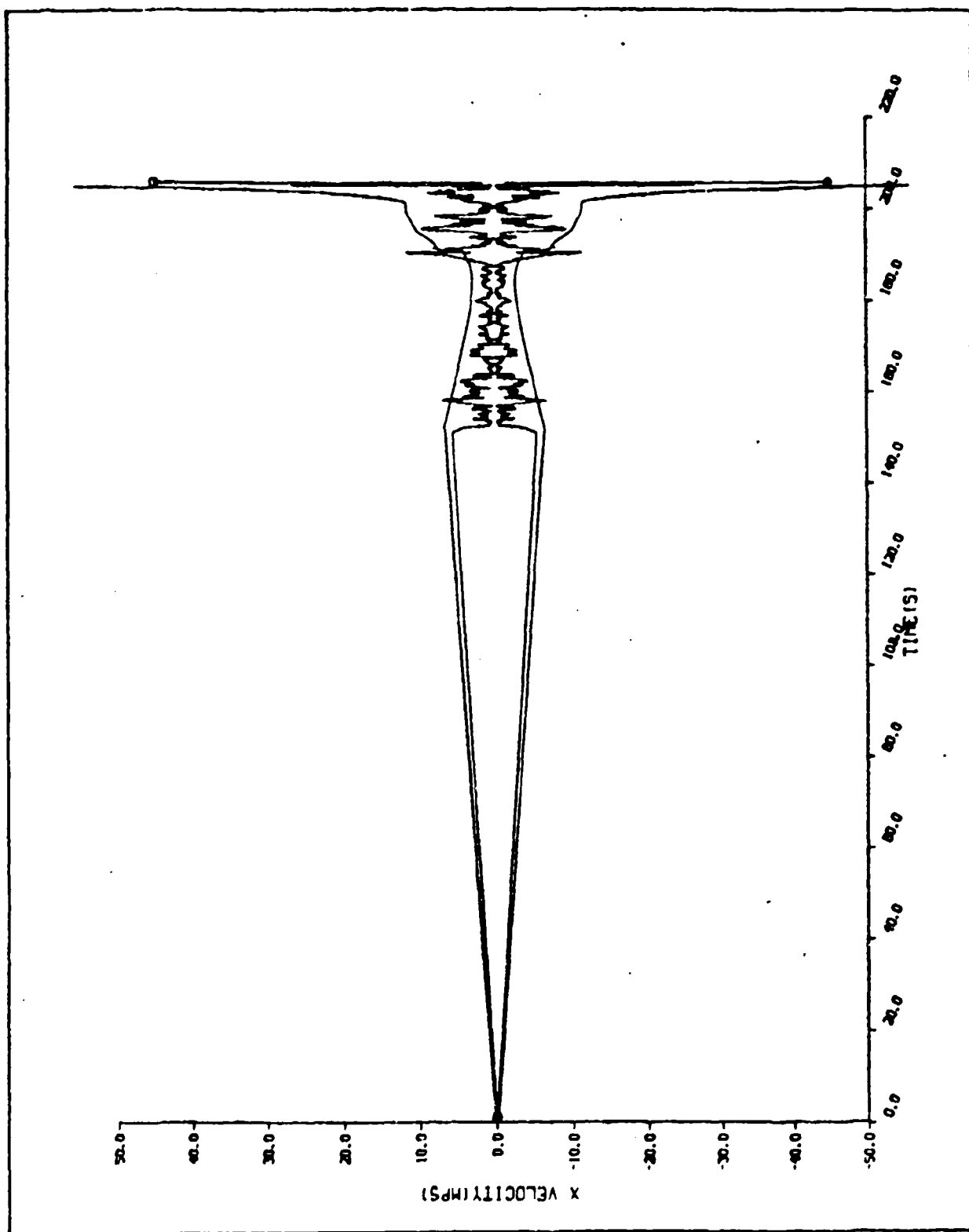
FIG IV-38 X VELOCITY COMPARISON OF THE SINGLE SAMPLE STANDARD
DEVIATION WITH THE RMS ERROR FROM A 10-RUN MONTE CARLO
SIMULATION, EXAMPLE TWO, CASE ONE TYPE
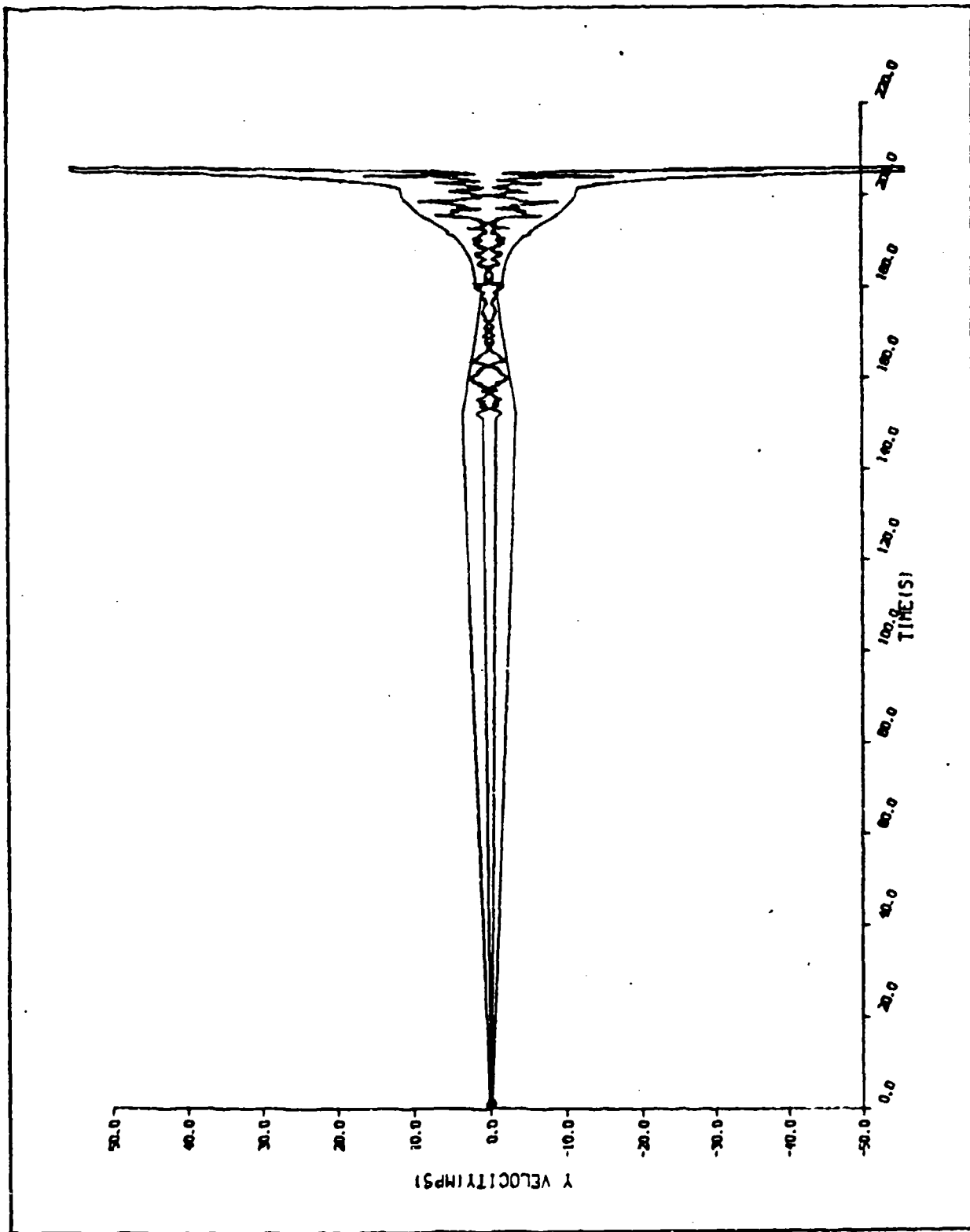
FIG IV-39 Y VELOCITY COMPARISON OF THE SINGLE SAMPLE STANDARD DEVIATION WITH THE RMS ERROR FROM A 10-RUN MONTE CARLO SIMULATION. EXAMPLE TWO, CASE ONE TYPE
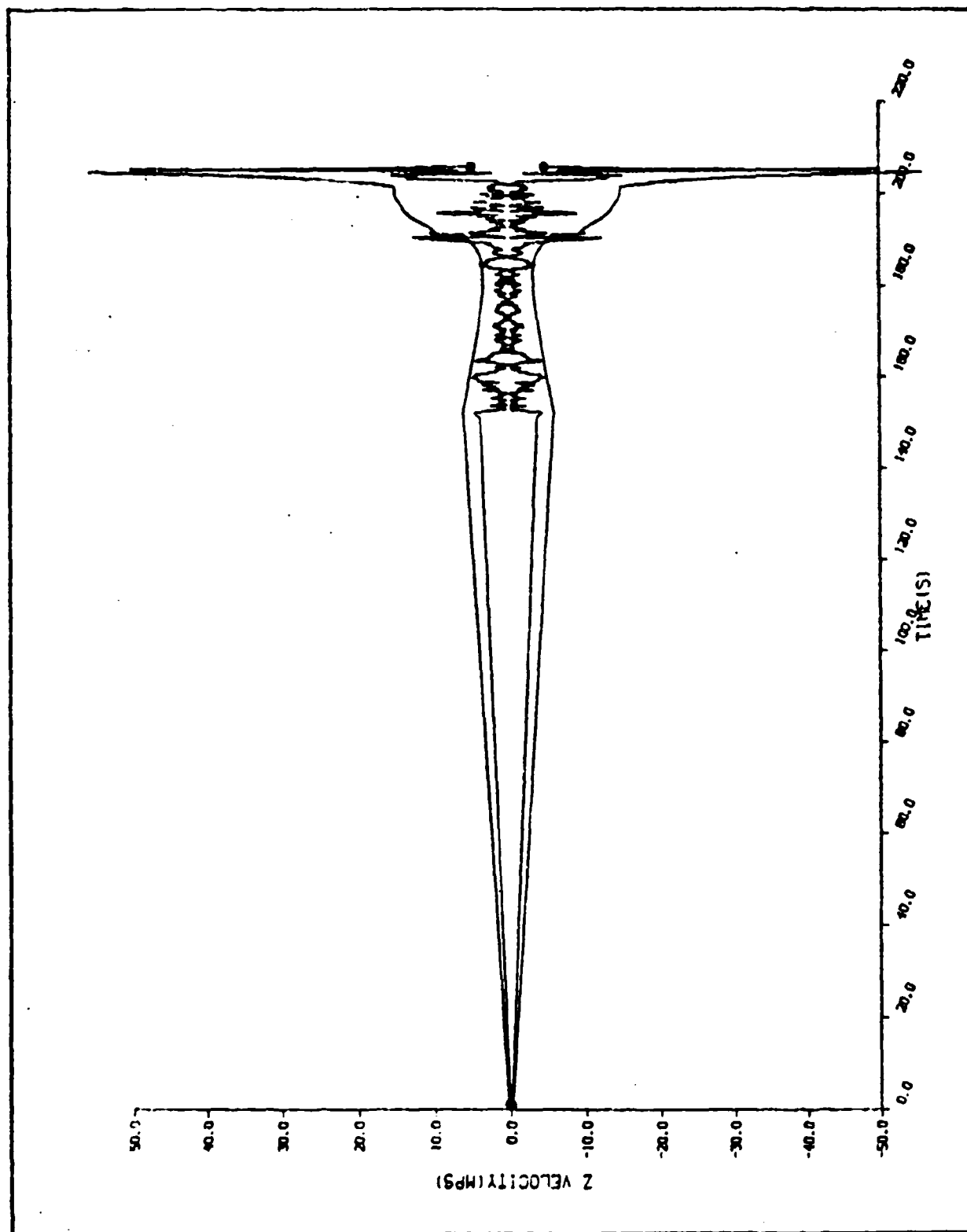
FIG IV-40 Z VELOCITY COMPARISON OF THE SINGLE SAMPLE STANDARD
DEVIATION WITH THE RMS ERROR FROM A 10-RUN MONTE CARLO
SIMULATION, EXAMPLE TWO, CASE ONE TYPE

107
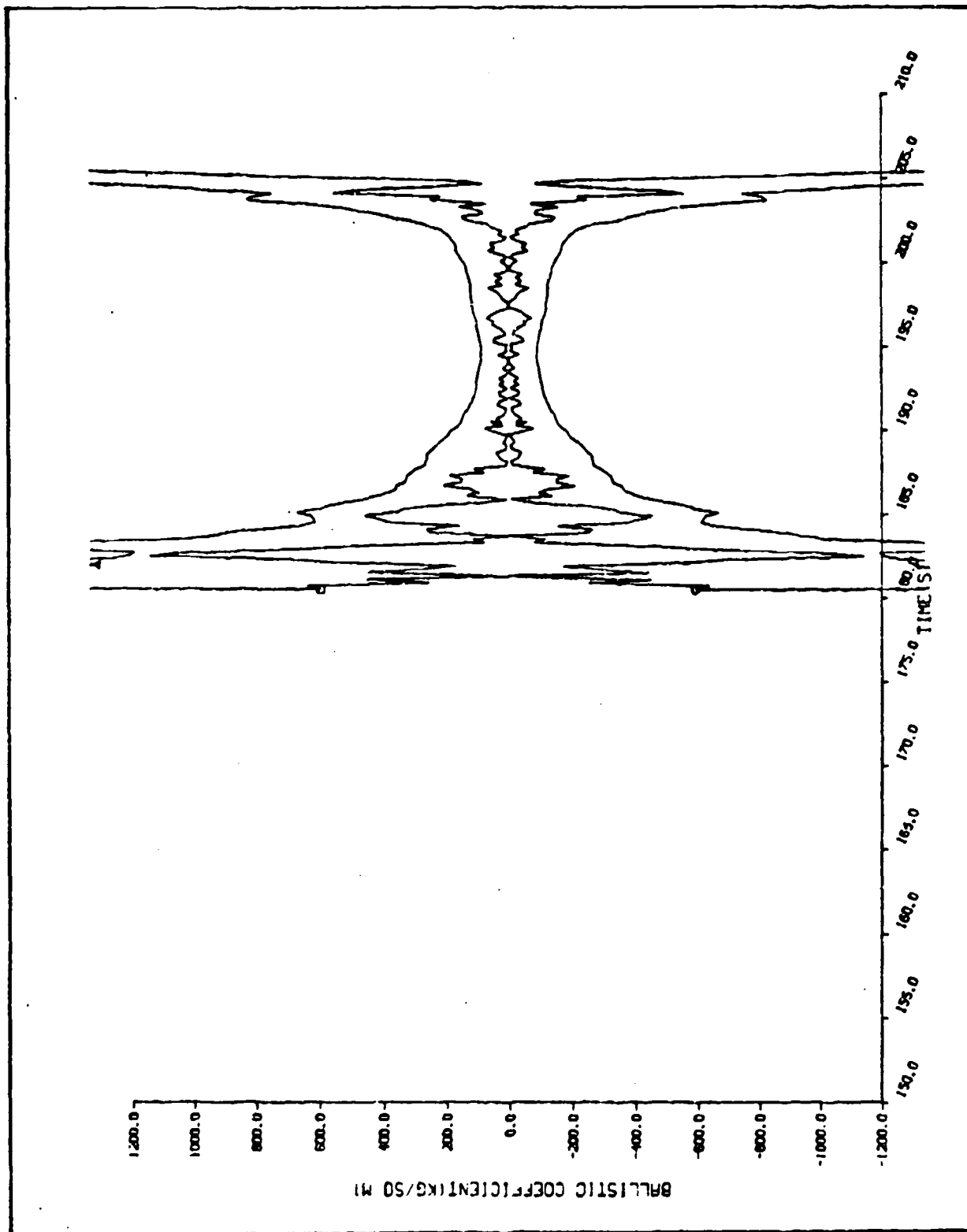
FIG IU-41 BALLISTIC COEFFICIENT COMPARISON OF THE SINGLE SAMPLE STANDARD
DEVIATION WITH THE RMS ERROR FROM A 10-RUN MONTE CARLO
SIMULATION, EXAMPLE TWO, CASE ONE TYPE

108
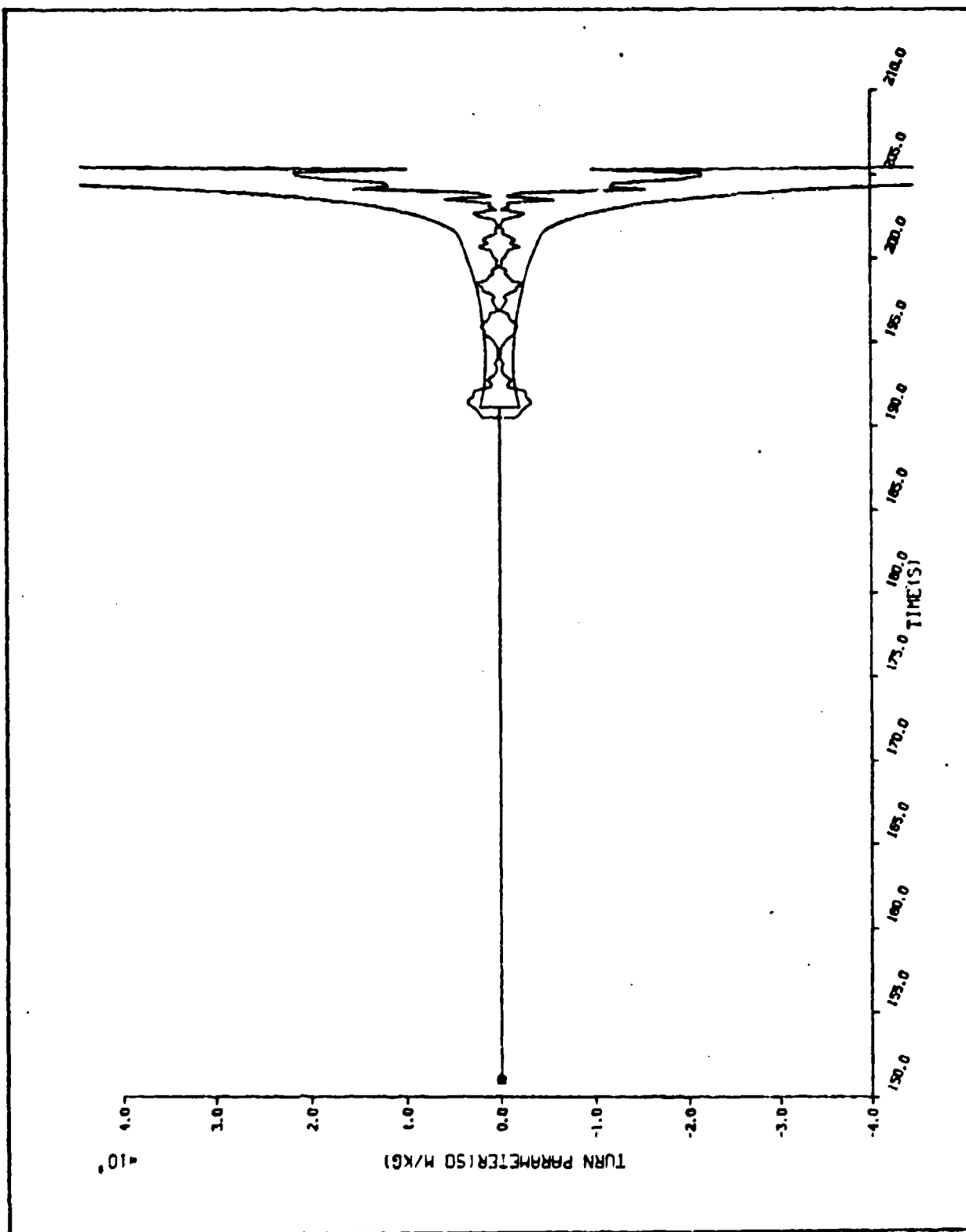
FIG IV-42 TURN PARAMETER COMPARISON OF THE SINGLE SAMPLE STANDARD DEVIATION WITH THE RMS ERROR FROM A 10-RUN MONTE CARLO SIMULATION, EXAMPLE TWO, CASE ONE TYPE
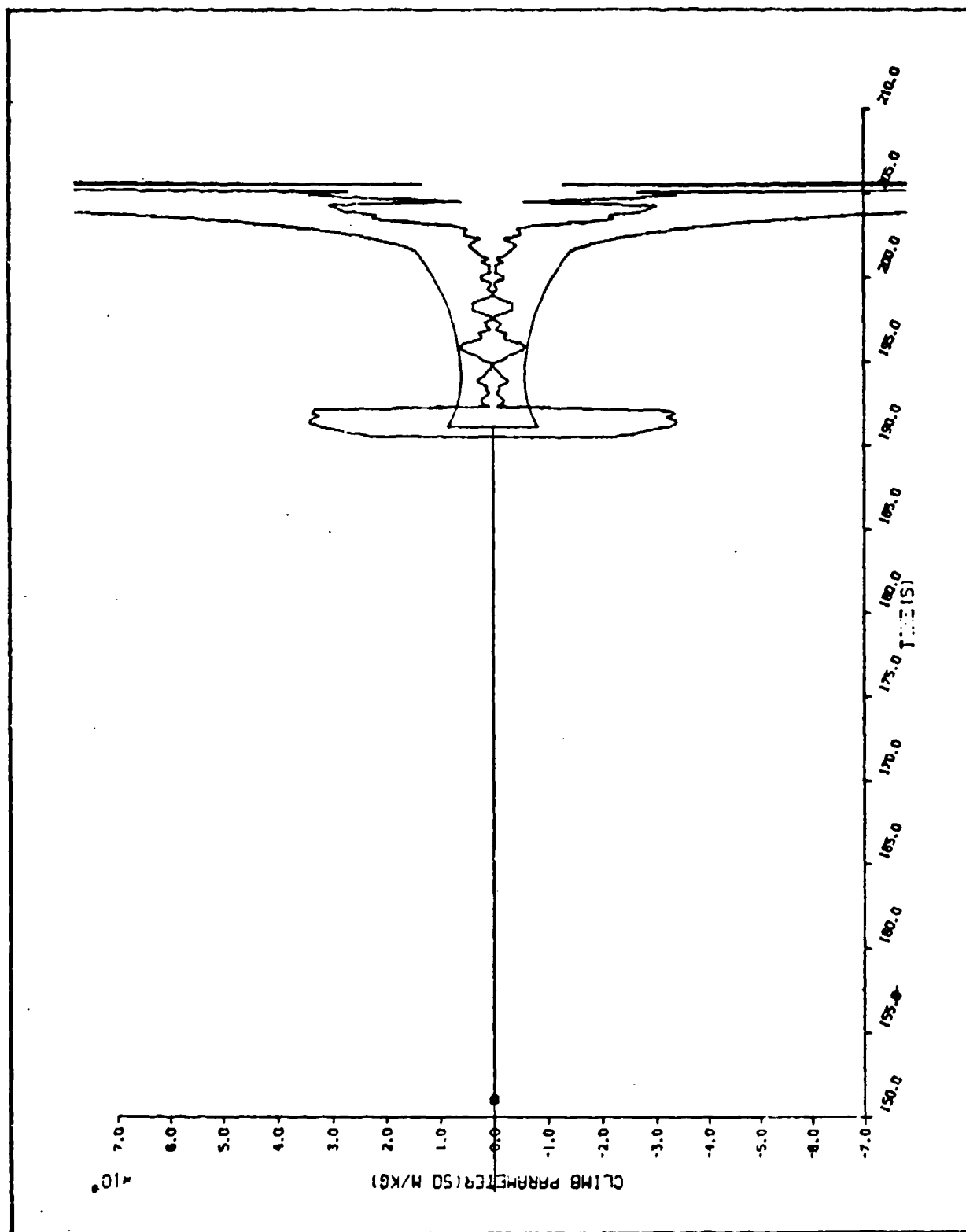
FIG IV-43 CLIMB PARAMETER COMPARISON OF THE SINGLE SAMPLE STANDARD DEVIATION WITH THE RMS ERROR FROM A 10-RUN MONTE CARLO SIMULATION. EXAMPLE TWO, CASE ONE TYPE

V   Summary, Conclusions and Recommendations

A very flexible algorithm for post-flight analysis of
radar tracking data collected on a ballistic missile has
been presented. It was shown that by specifying certain
values of input parameters, the algorithm would work in
either the batch weighted least squares mode or as a sequen-
tial estimator. Two numerical examples detailing the opera-
tion of the estimator in both modes were presented. For the
sequential estimator mode, a method was devised to allow the
program to switch automatically from a free-flight model to
a BRV model and then to a MaRV model. This means that the
algorithm can be used for free-flight or for reentry analyses,
and the reentry may be either BRV flight or MaRV flight. A
particular state vector of parameters to determine is selec-
ted by initializing the state transition matrix to the iden-
tity matrix. For each parameter of the 9-element MaRV state
vector which is not to be included in the model, the diagonal
element of the initial state transition matrix corresponding
to that parameter is set to zero. This allows much greater
flexibility than was actually demonstrated in this report.
It means that any combination of the nine-elements may be
used as the state vector of parameters to be determined. As
an example, if the position and velocity of the RV were ac-
curately known at reentry as might be provided by a long
free-flight track, one could conceivably solve only for the

111

aerodynamic parameters while propagating position and velocity according to the models given in Chapter II. This could be done in either the batch or sequential modes. A recommendation for future research is to compare the results of such a technique to those given in this report.

The batch weighted least squares method which was presented in Example One of Chapter IV, offers such attractive features when compared with the sequential estimator that one concludes that when the dynamic and measurement models are accurately known, the batch method is preferred. The attractive features mentioned above include:

(a) running time for the batch estimator is considerably less than that required for the sequential estimator,

(b) the estimator uncertainties are much smaller for the batch estimator as indicated by a comparison of Examples One and Two of Chapter IV, and

(c) programming of the batch estimator is much simpler and therefore less time consuming with few chances of making errors.

These features of the batch estimator, motivate one to look for ways of improving models, so that the batch estimator is applicable. This is probably not possible for the MaRV since there is no accurate general model of maneuvering flight; however, for BRV flight, it should be possible to come up with some analytic model, perhaps based on wind tunnel data, to model accurately atmospheric drag. One such model was

suggested in Chapter II where C_D was given as a function of
Mach number

$$C_D = k_1 + \frac{k_2}{M} + \frac{k_3}{M^2}$$ (II-71)

In the batch mode k_1, k_2 and k_3 could be included as param-
eters to be determined in the estimation process. The drag
model given by Eq (II-71) may not be the best model in gen-
eral. A recommendation for further study is to investigate
models like Eq (II-71) for the BRV case to see under what
circumstances the batch estimator would give reasonable re-
sults. It seems that this could only be done using real
data.

A final recommendation for future study is in the area
of sequential estimation with small batch sizes. It was
mentioned earlier that for small batch sizes, a priori sta-
tistics had to be used to keep $(P_0^{-1} + H^T Q^{-1} H)$ non-singular and
therefore invertible. It would appear that for very large
maneuvers or where C_T and C_C vary with time, small batch
sizes must be considered. When they were considered briefly
in this study it appeared that there was an inverse relation-
ship between the batch size and a weighting factor applied
to the inverse of the a priori covariance, P_0^{-1}. More re-
search may reveal a relationship so that the weighting can
be applied automatically by the program from the batch size.
This investigation could also look at adaptively optimizing

113

and changing the batch size as a function of time. As an example, it may be advantageous to use smaller batch sizes in regions of high deceleration and larger batch sizes in regions where the deceleration is not as high.

Bibliography

1. Aerospace TOR-0066(9320)-2, "TRACE66 Vol III: Trajectory Generation Equations and Methods," Apr 1970 (AD 870790).

2. ----- "TRACE66 Vol V: Differential Correction Procedure and Technique," Apr 1970.

3. Athans, M. et al. "A Suboptimal Estimation Algorithm With Probabilistic Editing for False Measurements With Application to Target Tracking With Wake Phenomena," IEEE Transaction on Automatic Control, Vol. AC-22, No 3, pp 372-384, June, 1977.

4. Barker, R.H., "Estimation of Decayed Satellite Reentry Trajectories," Ph.D. dissertation, Air Force Institute of Technology, Wright-Patterson AFB, Ohio, Dec 1981.

5. Bate, R.R. et al. Fundamentals of Astrodynamics, Dover Publications, Inc, New York, 1971.

6. Bryson, A.E. and Y.C. Ho. Applied Optimal Control (Revised Printing), Hemisphere Publishing Corp, 1975.

7. Buning, H. Elements of Space and Reentry Mechanics, The University of Michigan Engineering Summer Conference, 1964.

8. Chang, C.B. et al. "Application of the Fixed Interval Smoother to Maneuvering Trajectory Estimation," IEEE Transaction on Automatic Control AC-22, p 876, 1977.

9. -----. "On the State and Parameter Estimation for Maneuvering Vehicles," Proc Symposium on Nonlinear Estimation Theory, Sep 1975.

10. -----. Application of Adaptive Filtering Methods to Maneuvering Trajectory Estimation, Technical Note 1975-59, Lincoln Laboratory, MIT, 24 Nov 1975.

11. Day, K.S. and P.O. Schibe, "Least Squares Estimation in the Presence of Model Uncertainties," Second Symposium on Nonlinear Estimation Theory, September, 1971.

12. -----. Trajectory Reconstruction by the Method of Weighted Least Squares, Report No SYA-06, Signal Sciences, Inc, Santa Clara, Calif., 8 Oct 1976.

13. Gelb, A. et al. Applied Optimal Estimation, MIT Press, 1974.

14. Gruber, M. _An Approach to Target Tracking_, Technical Note 1967-8, Lincoln Laboratory, MIT, 10 Feb 1967 (AD 654727).

15. Ho, Y.C. _The Method of Least Squares and Optimal Filtering Theory_, The RAND Corp Memo RM-3329-PR, Oct 1962 (AD 286742).

16. Jazwinski, A.H. _Stochastic Processes and Filtering Theory_, Academic Press, 1970.

17. Johnson, L.W. and R.D.Riess, _Numerical Analysis_, Addison-Wesley, 1982.

18. Junkins, J.L., _An Introduction to Optimal Estimation of Dynamical Systems_, Sisthoff and Nordhoff Publishers, The Netherlands, 1978.

19. Kailath, T., "A View of Three Decades of Linear Filtering Theory," _IEEE Transaction on Information Theory_, March 1974, pp 146-181.

20. Kalman, R.E. and R.S. Bucy, "New Results in Linear Filtering and Prediction Theory," J. Basic Eng Vol 83, 1961, pp 95-108.

21. Kreyszig, E. _Advanced Engineering Mathematics_ (Fourth Edition), John Wiley and Sons, 1979.

22. Larson, R.E. _et al_. "Application of the Extended Kalman Filter to Ballistic Trajectory Estimation," Stanford Research Institute, Menlo Park, Calif. Final Report, Jan 1967 (AD 815377).

23. Liebelt, P.B. _An Introduction to Optimal Estimation_, Addison-Wesley Publishing Co., 1967.

24. Maybeck, P.S. _Stochastic Models, Estimation and Control_ Vol 1 (1979) and Vol 2 (1982), Academic Press.

25. Mehra, R.K., "A Comparison of Several Nonlinear Filters for Reentry Vehicle Tracking," _IEEE Transaction on Automatic Control_ AC-16 307-319, 1971.

26. Mikhail, E.M. _Observations and Least Squares_, New York: IEP-A Dun-Donnelly Publisher, 1976.

27. O'Connor, J., _Methods of Trajectory Mechanics_, ESMC-TR-80-45, ESMC, Patrick AFB, Fla, 1981 (ADB 059497).

28. Orwat, J.C. and D.K. Potter,"Application of the Extended Kalman Filter to Ballistic Trajectory Estimation and Prediction," M.S. Thesis, Air Force Institute of Technology, Wright-Patterson AFB, Ohio, June 1969 (AD 875083).

29. SAMSO-TR-77-36, "TRACE Vol VI: Orbital Statistics via Covariance Analysis," June 1977 (ADB 020557).

30. Sorenson, H.W.,"Least Squares Estimation: From Gauss to Kalman," IEEE Spectrum, July 1970, pp 63-68.

31. Swerling, P. "Modern State Estimation Methods from the Viewpoint of the Method of Least Squares," IEEE Trans on Automatic Control, Vol. AC-16, No. 6, December 1971.

32. Toines, C.C. et al. TRACE Orbit Determination Program Version D, Report No. TR-669(9990)-3 Aerospace Corp, Sep 1966.

33. TRW Systems Group, Analytical Studies and Programming in Support of Tracking and Data Reduction Techniques, Final Report No. 09127-6002-RO-00, Nov 1968 (AD 846 428).

34. Wickett, S. Metric Procedures and Wake Analysis, AERL Report F33657-75-C-0306, Everett Mass, 1976.

35. -----. Specialized Data Report-NRV, Research Note 973, AVCO Everett Research Lab, Inc, Dec 1975 (ADB 020166).

36. Wiesel, W. Lecture notes for MC 7.31, Modern Methods of Orbit Determination, School of Engineering, Air Force Institute of Technology, Wright-Patterson AFB, 1982.

37. Wishner, R.P. et al. "Status of Radar Tracking Algorithms," Proceedings of Symposium on Nonlinear Estimation Theory and its Application, IEEE, September 1970.

38. Wolaver, L.E. Modern Techniques in Astrodynamics - An Introduction, Clearinghouse, U.S. Dept of Commerce, Springfield Virginia 22151, 1970.

APPENDIX A The Geometrical Shape of the Earth

This appendix describes the model used for the shape of the earth and developes the relationships necessary in some of the transformations involved in the trajectory estimation problem.

The geometrical shape of the earth is modeled as an ellipsoid of revolution with the revolution being taken about the minor axis which coincides with the earth's axis of rotation. This ellipsoid of revolution, which differs only slightly from a sphere, is used to locate positions on, or above, the earth in a geodetic (or geographic) coordinate system. Figure A-1 is a graphic portrayal of the reference ellipsoid with the eccentricity greatly exaggerated showing the parameters associated with the ellipsoid. The values given for the semi-major and semi-minor axes are from the World Geodetic System (WGS-72) reference ellipsoid. From the geometry shown in figure A-2, the relationship between geodetic and geocentric latitude is determined. In the local cartesian coordinate system of Fig A-2, the equation of the ellipse is

$$\frac{x'^2}{a^2} + \frac{y'^2}{b^2} = 1 \tag{A-1}$$

The geodetic latitude line is perpendicular to the tangent plane at the earth's surface as shown, so that
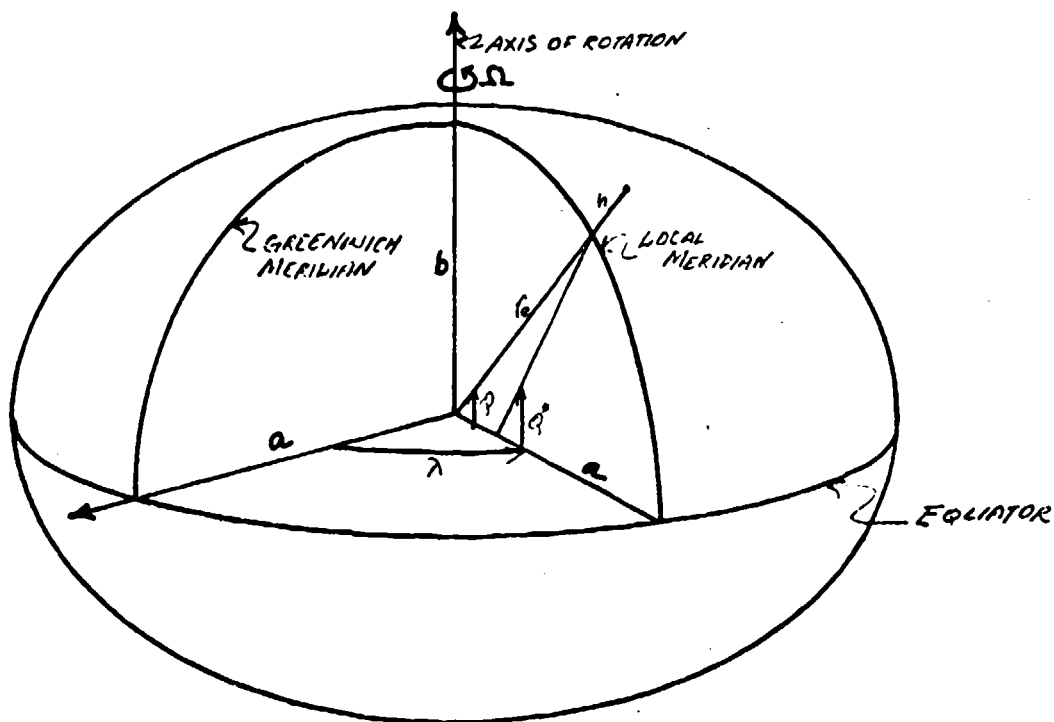
a – SEMI-MAJOR AXIS, 6378135(M)

b – SEMI-MINOR AXIS, 6356750(M)

h – GEOCENTRIC ALTITUDE

r_e – LOCAL RADIUS OF THE EARTH

λ – LONGITUDE

φ' – GEODETIC LATITUDE

φ – GEOCENTRIC LATITUDE

FIG A-1   PARAMETERS ASSOCIATED WITH REFERENCE ELLIPSOID
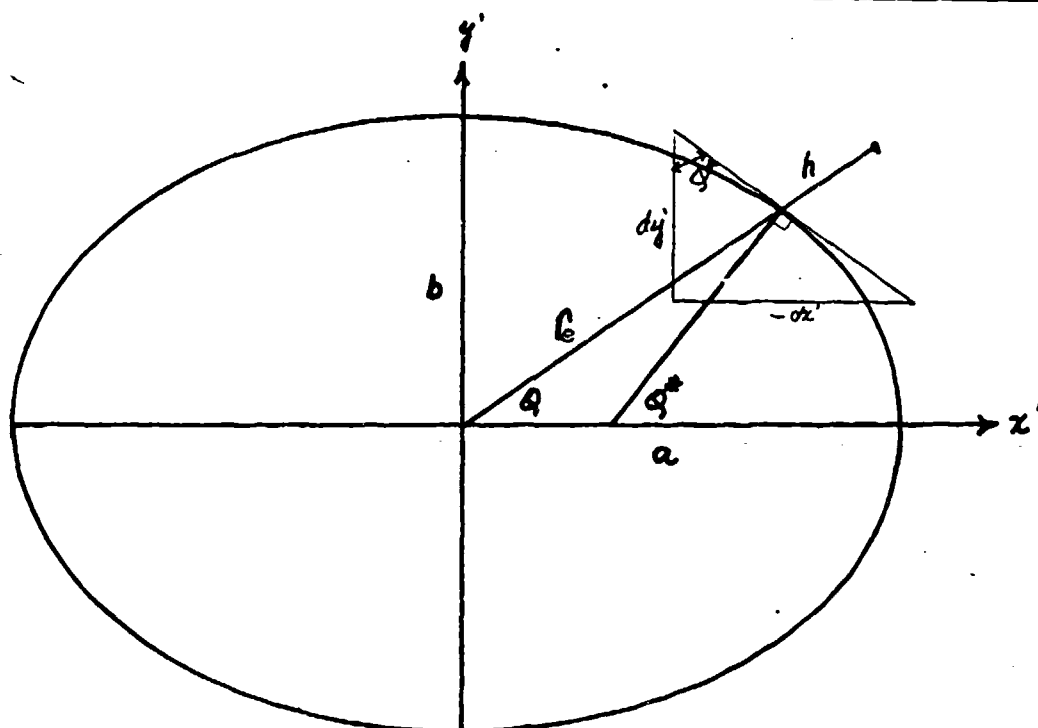
a - SEMI-MAJOR AXIS, 6378135(M)

b - SEMI-MINOR AXIS, 6356750(M)

h - GEOCENTRIC ALTITUDE

ℓ_e - LOCAL RADIUS OF THE EARTH

λ - LONGITUDE

φ' - GEODETIC LATITUDE

φ - GEOCENTRIC LATITUDE

FIG A-2   CROSS SECTION OF THE REFERENCE ELLIPSOID
USED FOR DETERMINING THE RELATIONSHIP BETWEEN
GEODETIC AND GEOCENTRIC LATITUDE

$$TAN\,\varphi^* = -\,dx'/dy' \tag{A-2}$$

Differentiating equation (A-1) we get

$$\frac{dx'}{dy'} = -\frac{y'}{x'}\frac{a^2}{b^2} \tag{A-3}$$

Substituting (A-2) in (A-3), we obtain

$$TAN\,\varphi^* = \frac{y'}{x'}\frac{a^2}{b^2} \tag{A-4}$$

From the geometry of figure (A-2), we have

$$TAN\,\varphi = \frac{y'}{x'} \tag{A-5}$$

Putting (A-5) into (A-4) we obtain

$$b^2\,TAN\,\varphi^* = a^2\,TAN\,\varphi \tag{A-6}$$

which is the relationship between geodetic and geocentric latitude which was sought.

The radius of the earth at φ is also determined from the geometry of Fig A-2.

$$r_e^2 = x'^2 + y'^2 \tag{A-7}$$

121

Solve (A-1) for y and substitute in (A-7) to obtain

$$r_e^2 = x'^2 + \left(1 - \frac{x'^2}{a^2}\right) b^2 = b^2 + x'^2 \left(1 - \frac{b^2}{a^2}\right) \tag{A-8}$$

Divide through by r_e^2 to obtain

$$1 = \frac{b^2}{r_e^2} + \frac{x'^2}{r_e^2}\left(1 - \frac{b^2}{a^2}\right) \tag{A-9}$$

Rearranging (A-9) and recognizing

$$\frac{x'^2}{r_e^2} = \cos^2 \varphi \tag{A-10}$$

we obtain

$$r_e = b \Big/ \left(1 - e^2 \cos^2 \varphi\right)^{\frac{1}{2}} \tag{A-11}$$

which gives the local radius of the earth for any geocentric latitude where e is the eccentricity given by

$$e^2 = \left(1 - \frac{b^2}{a^2}\right) \tag{A-12}$$

APPENDIX B <u>Partials Required in the Differential</u>
<u>Correction Process</u>

Central to the working of the differential correction process are the partial derivatives of the observations - in this case range (R), azimuth (A), and elevation (E) - with respect to the parameters to be estimated, in this case the elements of the state vector at some epoch time, t_o. The most general state vector for a MaRV is nine dimensional. Let the state vector at the epoch time be defined as

$$\underline{X}_o = (X_o, Y_o, Z_o, \dot{X}_o, \dot{Y}_o, \dot{Z}_o, \beta_o, C_T, C_c)^T \tag{B-1}$$

where the nine elements are as previously defined. No o subscript is required for C_T and C_c since they are modeled as constants. The partials required for the differential correction process then may be symbolized as

$$\frac{\partial R_i}{\partial X_o}, \frac{\partial R_i}{\partial Y_o}, \frac{\partial R_i}{\partial Z_o}, \frac{\partial R_i}{\partial \dot{X}_o}, \frac{\partial R_i}{\partial \dot{Y}_o}, \frac{\partial R_i}{\partial \dot{Z}_o}, \frac{\partial R_i}{\partial \beta_o}, \frac{\partial R_i}{\partial C_T}, \frac{\partial R_i}{\partial C_c}$$

$$\frac{\partial A_i}{\partial X_o}, \frac{\partial A_i}{\partial Y_o}, \frac{\partial A_i}{\partial Z_o}, \frac{\partial A_i}{\partial \dot{X}_o}, \frac{\partial A_i}{\partial \dot{Y}_o}, \frac{\partial A_i}{\partial \dot{Z}_o}, \frac{\partial A_i}{\partial \beta_o}, \frac{\partial A_i}{\partial C_T}, \frac{\partial A_i}{\partial C_c}$$

$$\frac{\partial E_i}{\partial X_o}, \frac{\partial E_i}{\partial Y_o}, \frac{\partial E_i}{\partial Z_o}, \frac{\partial E_i}{\partial \dot{X}_o}, \frac{\partial E_i}{\partial \dot{Y}_o}, \frac{\partial E_i}{\partial \dot{Z}_o}, \frac{\partial E_i}{\partial \beta_o}, \frac{\partial E_i}{\partial C_T}, \frac{\partial E_i}{\partial C_c}$$

where the subscript i is used to denote the time, t_i of the ith measurement i.e., $R_i = R(t_i)$. If there are n measurements, then i = 1, 2, 3, ... n. t_1 may or may not equal t_0. In this developme.. t t_i is always greater than or equal t_0.

The radar range, azimuth, and elevation at t_i are all functions of the RV's position at t_i.

$$R_i = R_i(X_i, Y_i, Z_i) \tag{B-2}$$

$$A_i = A_i(X_i, Y_i, Z_i) \tag{B-3}$$

$$E_i = E_i(X_i, Y_i, Z_i) \tag{B-4}$$

where X_i, Y_i, and Z_i are elements of the state a t_i in the ECI coordinate system.

(B-2) is determined from (B-3) by the chain rule for partial derivatives given by the following matrix equation

$$
\begin{bmatrix}
\partial R_i/\partial X_0 \\
\partial R_i/\partial Y_0 \\
\partial R_i/\partial Z_0 \\
\partial R_i/\partial \dot{X} \\
\partial R_i/\partial \dot{Y} \\
\partial R_i/\partial \dot{Z} \\
\partial E_i/\partial \beta \\
\partial R_i/\partial C_T \\
\partial R_i/\partial C_c
\end{bmatrix}
\begin{bmatrix}
\partial X_i/\partial X_0 & \partial Y_i/\partial X_0 & \partial Z_i/\partial X_0 \\
\partial X_i/\partial Y_0 & \partial Y_i/\partial Y_0 & \partial Z_i/\partial Y_0 \\
\partial X_i/\partial Z_0 & \partial Y_i/\partial Z_0 & \partial Z_i/\partial Z_0 \\
\partial X_i/\partial \dot{X}_0 & \partial Y_i/\partial \dot{X}_0 & \partial Z_i/\partial \dot{X}_0 \\
\partial X_i/\partial \dot{Y}_0 & \partial Y_i/\partial \dot{Y}_0 & \partial Z_i/\partial \dot{Z}_0 \\
\partial X_i/\partial \dot{Z}_0 & \partial Y_i/\partial \dot{Z} & \partial Z_i/\partial \dot{Z}_0 \\
\partial X_i/\partial \beta_0 & \partial Y_i/\partial \beta_0 & \partial Z_i/\partial \beta_0 \\
\partial X_i/\partial C_T & \partial Y_i/\partial C_T & \partial Z_i/\partial C_T \\
\partial X_i/\partial C_c & \partial Y_i/\partial C_c & \partial Z_i/\partial C_c
\end{bmatrix}
\begin{bmatrix}
\partial R_i/\partial X_i \\
\partial R_i/\partial Y_i \\
\partial R_i/\partial Z_i
\end{bmatrix}
\tag{B-5}
$$

where the matrix is a partitian of the state transition matrix $\Phi(t_i, t_0)$ to be developed on the next few pages.

Azimuth and elevation partials are calculated similar to (B-4) using the same partition of $\Phi(t_i, t_0)$.

124

The State Transition Matrix

The state transition matrix is defined as

$$\Phi(t_i, t_o) = \begin{bmatrix}
\frac{\partial X_i}{\partial X_o} & \frac{\partial Y_i}{\partial X_o} & \frac{\partial Z_i}{\partial X_o} & \frac{\partial \dot{X}_i}{\partial X_o} & \frac{\partial \dot{Y}_i}{\partial X_o} & \frac{\partial \dot{Z}_i}{\partial X_o} & \frac{\partial \rho_i}{\partial X_o} & \frac{\partial C_T}{\partial X_o} & \frac{\partial C_c}{\partial X_o} \\[4pt]
\frac{\partial X_i}{\partial Y_o} & \frac{\partial Y_i}{\partial Y_o} & \frac{\partial Z_i}{\partial Y_o} & \frac{\partial \dot{X}_i}{\partial Y_o} & \frac{\partial \dot{Y}_i}{\partial Y_o} & \frac{\partial \dot{Z}_i}{\partial Y_o} & \frac{\partial \rho_i}{\partial Y_o} & \frac{\partial C_T}{\partial Y_o} & \frac{\partial C_c}{\partial Y_o} \\[4pt]
\frac{\partial X_i}{\partial Z_o} & \frac{\partial Y_i}{\partial Z_o} & \frac{\partial Z_i}{\partial Z_o} & \frac{\partial \dot{X}_i}{\partial Z_o} & \frac{\partial \dot{Y}_i}{\partial Z_o} & \frac{\partial \dot{Z}_i}{\partial Z_o} & \frac{\partial \rho_i}{\partial Z_o} & \frac{\partial C_T}{\partial Z_o} & \frac{\partial C_c}{\partial Z_o} \\[4pt]
\frac{\partial X_i}{\partial \dot{X}_o} & \frac{\partial Y_i}{\partial \dot{X}_o} & \frac{\partial Z_i}{\partial \dot{X}_o} & \frac{\partial \dot{X}_i}{\partial \dot{X}_o} & \frac{\partial \dot{Y}_i}{\partial \dot{X}_o} & \frac{\partial \dot{Z}_i}{\partial \dot{X}_o} & \frac{\partial \rho_i}{\partial \dot{X}_o} & \frac{\partial C_T}{\partial \dot{X}_o} & \frac{\partial C_c}{\partial \dot{X}_o} \\[4pt]
\frac{\partial X_i}{\partial \dot{Y}_o} & \frac{\partial Y_i}{\partial \dot{Y}_o} & \frac{\partial Z_i}{\partial \dot{Y}_o} & \frac{\partial \dot{X}_i}{\partial \dot{Y}_o} & \frac{\partial \dot{Y}_i}{\partial \dot{Y}_o} & \frac{\partial \dot{Z}_i}{\partial \dot{Y}_o} & \frac{\partial \rho_i}{\partial \dot{Y}_o} & \frac{\partial C_T}{\partial \dot{Y}_o} & \frac{\partial C_c}{\partial \dot{Y}_o} \\[4pt]
\frac{\partial X_i}{\partial \dot{Z}_o} & \frac{\partial Y_i}{\partial \dot{Z}_o} & \frac{\partial Z_i}{\partial \dot{Z}_o} & \frac{\partial \dot{X}_i}{\partial \dot{Z}_o} & \frac{\partial \dot{Y}_i}{\partial \dot{Z}_o} & \frac{\partial \dot{Z}_i}{\partial \dot{Z}_o} & \frac{\partial \rho_i}{\partial \dot{Z}_o} & \frac{\partial C_T}{\partial \dot{Z}_o} & \frac{\partial C_c}{\partial \dot{Z}_o} \\[4pt]
\frac{\partial X_i}{\partial \rho_o} & \frac{\partial Y_i}{\partial \rho_o} & \frac{\partial Z_i}{\partial \rho_o} & \frac{\partial \dot{X}_i}{\partial \rho_o} & \frac{\partial \dot{Y}_i}{\partial \rho_o} & \frac{\partial \dot{Z}_i}{\partial \rho_o} & \frac{\partial \rho_i}{\partial \rho_o} & \frac{\partial C_T}{\partial \rho_o} & \frac{\partial C_c}{\partial \rho_o} \\[4pt]
\frac{\partial X_i}{\partial C_T} & \frac{\partial Y_i}{\partial C_T} & \frac{\partial Z_i}{\partial C_T} & \frac{\partial \dot{X}_i}{\partial C_T} & \frac{\partial \dot{Y}_i}{\partial C_T} & \frac{\partial \dot{Z}_i}{\partial C_T} & \frac{\partial \rho_i}{\partial C_T} & \frac{\partial C_T}{\partial C_T} & \frac{\partial C_c}{\partial C_T} \\[4pt]
\frac{\partial X_i}{\partial C_c} & \frac{\partial Y_i}{\partial C_c} & \frac{\partial Z_i}{\partial C_c} & \frac{\partial \dot{X}_i}{\partial C_c} & \frac{\partial \dot{Y}_i}{\partial C_c} & \frac{\partial \dot{Z}_i}{\partial C_c} & \frac{\partial \rho_i}{\partial C_c} & \frac{\partial C_T}{\partial C_c} & \frac{\partial C_c}{\partial C_c}
\end{bmatrix}$$

The state transition is propagated to the time of each observation by the matrix chain rule equation

$$\Phi(t_{i+1}, t_o) = \Phi(t_i, t_o)\,\Phi(t_{i+1}, t_i) \tag{B-7}$$

$$\Phi(t_o, t_o) = I \tag{B-8}$$

where I is the identity matrix and the elements of $\Phi(t_{i+1}, t_i)$ are determined from the truncated Taylor's series[*]

$$X_{i+1} = X_i + \dot{X}_i \Delta t + \ddot{X}_i \frac{\Delta t^2}{2} \tag{B-9}$$

---

[*]These simplifying approximations are used only for partial calculations and not for propagating the state.

$$\dot{X}_{i+1} = \dot{X}_i + \ddot{X}_i \Delta t \tag{B-10}$$

$$Y_{i+1} = Y_i + \dot{Y}_i \Delta t + \frac{1}{2} \ddot{Y}_i \Delta t^2 \tag{B-11}$$

$$\dot{Y}_{i+1} = \dot{Y}_i + \ddot{Y}_i \Delta t \tag{B-12}$$

$$Z_{i+1} = Z_i + \dot{Z}_i \Delta t + \frac{1}{2} \ddot{Z}_i \Delta t^2 \tag{B-13}$$

$$\dot{Z}_{i+1} = \dot{Z}_i + \ddot{Z}_i \Delta t \tag{B-14}$$

$$\beta_{i+1} = \beta_i \tag{B-15}$$

$$C_{T_{i+1}} = C_{T_i} \tag{B-16}$$

$$C_{c_{i+1}} = C_{c_i} \tag{B-17}$$

where $\ddot{X}$, $\ddot{Y}$, and $\ddot{Z}$ are the components of the total accelera-
tion due to gravity, drag, turn, and climb given in Chapter
II and

$$\Delta t = t_{i+1} - t_i \tag{B-18}$$

Partials of Gravity Acceleration

The earth's gravity model which is used in propagating
the state vector is given in Chapter II; however, a simpler

approximation is sufficiently accurate for calculating the
partials

$$\ddot{X}_{q_i} = -\frac{\mu X_i}{r_i^3} \tag{B-19}$$

$$\ddot{Y}_{q_i} = -\frac{\mu Y_i}{r_i^3} \tag{B-20}$$

$$\ddot{Z}_{q_i} = -\frac{\mu Z_i}{r_i^3} \tag{B-21}$$

where

$$r_i = (X_i^2 + Y_i^2 + Z_i^2)^{\frac{1}{2}} \tag{B-22}$$

Then

$$\partial \ddot{X}_{q_i}/\partial X_i = \frac{\mu}{r_i^3}\left(\frac{3X_i^2}{r_i^2} - 1\right) \tag{B-23}$$

$$\partial \ddot{X}_{q_i}/\partial Y_i = \frac{3\mu X_i Y_i}{r_i^5} \tag{B-24}$$

$$\partial \ddot{X}_{q_i}/\partial Z_i = \frac{\partial \ddot{X}_{q_i}}{\partial Y_i}\frac{Z_i}{Y_i} \tag{B-25}$$

$$\partial \ddot{Y}_{q_i}/\partial X_i = \partial \ddot{X}_{q_i}/\partial Y_i \tag{B-26}$$

$$\partial \ddot{Y}_{q_i}/\partial Y_i = \frac{\mu}{r_i^3}\left(\frac{3Y_i^2}{r_i^2} - 1\right) \tag{B-27}$$

$$\partial \ddot{Y}_{q_i}/\partial Z_i = \frac{\partial \ddot{Y}_{q_i}}{\partial X_i}\frac{Z_i}{X_i} \tag{B-28}$$

127

$$\partial \ddot{Z}_{g_i}/\partial x_i = \partial \ddot{X}_{g_i}/\partial z_i \tag{B-29}$$

$$\partial \ddot{Z}_{g_i}/\partial y_i = \partial \ddot{Y}_{g_i}/\partial z_i \tag{B-30}$$

$$\partial \ddot{Z}_{g_i}/\partial z_i = \frac{\mathscr{A}}{\eta_i^3}\left(\frac{3 z_i^2}{\eta_i^2} - 1\right) \tag{B-31}$$

All other partials of the gravity acceleration with respect to the state are zero.

Partials of Drag Acceleration

The partials of acceleration due to drag are determined from the following equations

$$\ddot{X}_{D_i} = - \frac{\rho_i V_{a_i} C_{d_i}}{\beta_b} \dot{X}_{a_i} \tag{B-32}$$

$$\ddot{Y}_{D_i} = \ddot{X}_{D_i} \frac{\dot{Y}_{a_i}}{\dot{X}_{a_i}} \tag{B-33}$$

$$\ddot{Z}_{D_i} = \ddot{X}_{D_i} \frac{\dot{Z}_{a_i}}{\dot{X}_{a_i}} \tag{B-34}$$

$$\rho_i = \beta \, e^{-\frac{h_i}{1000}} \tag{B-35}$$

$$V_{a_i} = \left[(\dot{X}_i + \Omega Y_i)^2 + (\dot{Y}_i - \Omega X_i)^2 + \dot{Z}_i^2\right]^{\frac{1}{2}} \tag{B-36}$$

$$h_i = (X_i^2 + Y_i^2 + Z_i^2)^{\frac{1}{2}} - \frac{b}{\sqrt{1 - e^2(X_i^2 + Y_i^2)/r_i^2}} \tag{B-37}$$

128

$$C_{D_i} = k_1 + \frac{k_2}{M_i} + \frac{k_3}{M_i^2} \tag{B-38}$$

The twenty-seven partials of drag acceleration with respect to the state elements are then

$$\frac{\partial \ddot{X}_{D_i}}{\partial X_i} = \frac{\rho C_{D_i}}{2\beta_o} \dot{X}_{a_i} \left[\frac{\dot{Y}_{a_i} \Omega}{V_{a_i}} + \frac{V_{a_i} X_i}{7000 \, r_i} \right] \tag{B-39}$$

$$\frac{\partial \ddot{Y}_{D_i}}{\partial X_i} = \frac{\partial \ddot{X}_{D_i}}{\partial X_i} \frac{\dot{Y}_{a_i}}{\dot{X}_{a_i}} + \frac{\rho C_{D_i}}{2\beta_o} V_{a_i} \Omega \tag{B-40}$$

$$\frac{\partial \ddot{Z}_{D_i}}{\partial X_i} = \frac{\partial \ddot{X}_{D_i}}{\partial X_i} \frac{\dot{Z}_i}{\dot{X}_{a_i}} \tag{B-41}$$

$$\frac{\partial \ddot{X}_{D_i}}{\partial Y_i} = -\frac{\rho C_{D_i}}{2\beta_o} V_{a_i} \Omega - \dot{X}_{a_i} \frac{\rho C_{D_i}}{2\beta_o} \left[\frac{\dot{X}_a \Omega}{V_{a_i}} - \frac{V_{a_i} Y_i}{7000 \, r_i} \right] \tag{B-42}$$

$$\frac{\partial \ddot{Y}_{D_i}}{\partial Y_i} = -\dot{Y}_{a_i} \frac{\rho C_{D_i}}{2\beta_o} \left[\frac{\dot{X}_a \Omega}{V_{a_i}} - \frac{V_{a_i} Y_i}{7000 \, r_i} \right] \tag{B-43}$$

$$\frac{\partial \ddot{Z}_{D_i}}{\partial Y_i} = \frac{\partial \ddot{Y}_{D_i}}{\partial Y_i} \frac{\dot{Z}_i}{\dot{Y}_{a_i}} \tag{B-44}$$

$$\frac{\partial \ddot{X}_{D_i}}{\partial Z_i} = \dot{X}_{a_i} \frac{\rho C_{D_i}}{2\beta_o} \frac{V_{a_i} Z_i}{7000 \, r_i} \tag{B-45}$$

$$\frac{\partial \ddot{Y}_{D_i}}{\partial Z_i} = \frac{\partial \ddot{X}_{D_i}}{\partial Z_i} \frac{\dot{Y}_{a_i}}{\dot{X}_{a_i}} \tag{B-46}$$

$$\frac{\partial \ddot{Z}_{D_i}}{\partial Z_i} = \frac{\partial \ddot{X}_{D_i}}{\partial Z_i} \frac{\dot{Z}_i}{\dot{X}_{a_i}} \tag{B-47}$$

$$\frac{\partial \ddot{X}_{D_i}}{\partial \dot{X}_i} = \frac{\partial \ddot{Y}_{D_i}}{\partial \dot{X}_i} \frac{\dot{X}_{a_i}}{\dot{Y}_{a_i}} - V_{a_i} \frac{\rho C_{D_i}}{2\beta_o} \tag{B-48}$$

129

$$\frac{\partial \ddot{Y}_{D_i}}{\partial \dot{X}_i} = -\frac{\dot{X}_i \dot{Y}_i \rho_i}{2\beta_o}\left[\frac{1}{340}\frac{\partial C_{D_i}}{\partial M_i} + \frac{C_{D_i}}{V_{a_i}}\right] \qquad (B-49)$$

$$\frac{\partial \ddot{Z}_{D_i}}{\partial \dot{X}_i} = \frac{\partial \ddot{Y}_i}{\partial \dot{X}_i}\frac{\dot{Z}_i}{\dot{Y}_{a_i}} \qquad (B-50)$$

$$\frac{\partial \ddot{X}_{D_i}}{\partial \dot{Y}_i} = \frac{\partial \ddot{Y}_i}{\partial \dot{X}_i} \qquad (B-51)$$

$$\frac{\partial \ddot{Y}_{D_i}}{\partial \dot{Y}_i} = \frac{\partial \ddot{X}_{D_i}}{\partial \dot{Y}_i}\frac{\dot{Y}_{a_i}}{\dot{X}_{a_i}} - \frac{V_{a_i}\rho C_{D_i}}{2\beta_o} \qquad (B-52)$$

$$\frac{\partial \ddot{Z}_{D_i}}{\partial \dot{Y}_i} = \frac{\partial \ddot{X}_{D_i}}{\partial \dot{Y}_i}\frac{\dot{Z}_i}{\dot{X}_{a_i}} \qquad (B-53)$$

$$\frac{\partial \ddot{X}_{D_i}}{\partial \dot{Z}_i} = \frac{\partial \ddot{Z}_{D_i}}{\partial \dot{X}_i} \qquad (B-54)$$

$$\frac{\partial \ddot{Y}_{D_i}}{\partial \dot{Z}_i} = \frac{\partial \ddot{Z}_{D_i}}{\partial \dot{Y}_i} \qquad (B-55)$$

$$\frac{\partial \ddot{Z}_{D_i}}{\partial \dot{Z}_i} = \frac{\partial \ddot{X}_{D_i}}{\partial \dot{Z}_i}\frac{\dot{Z}_i}{\dot{X}_{a_i}} - \frac{V_{a_i}\rho C_{D_i}}{2\beta_o} \qquad (B-56)$$

$$\frac{\partial \ddot{X}_{D_i}}{\partial \beta_o} = -\frac{\ddot{X}_{D_i}}{\beta_o} \qquad (B-57)$$

$$\frac{\partial \ddot{Y}_{D_i}}{\partial \beta_o} = -\frac{\ddot{Y}_{D_i}}{\beta_o} \qquad (B-58)$$

$$\frac{\partial \ddot{Z}_{D_i}}{\partial \beta_o} = -\frac{\ddot{Z}_{D_i}}{\beta_o} \qquad (B-59)$$

Partials of Turn Acceleration

The components of the acceleration due to turn were developed in Chapter II as

$$\ddot{X}_{T_i} = C_T \rho_i V_{a_i}^2 \frac{\left[Y_i \dot{Z}_i - Z_i(\dot{Y}_i - \Omega X_i) \right]}{T_i}$$ (B-60)

$$\ddot{Y}_{T_i} = C_T \rho_i V_{a_i}^2 \frac{\left[Z_i(\dot{X}_i + \Omega Y_i) - X_i \dot{Z}_i \right]}{T_i}$$ (B-61)

$$\ddot{Z}_{T_i} = C_T \rho_i V_{a_i}^2 \frac{\left[X_i(\dot{Y}_i - \Omega X_i) - Y_i(\dot{X}_i + \Omega Y_i) \right]}{T_i}$$ (B-62)

$$T_i = \left[(Y_i \dot{Z}_i - Z_i \dot{Y}_{a_i})^2 + (Z_i \dot{X}_{a_i} - X_i \dot{Z}_i)^2 + (X_i \dot{Y}_{a_i} - Y_i \dot{X}_{a_i})^2 \right]^{\frac{1}{2}}$$ (B-63)

In an effort to simplify the notation in the rather complicated turn partials, the i subscript which denotes those parameters which vary with time, will be dropped. Then the partials of turn acceleration with respect to the nine state elements are

$$\frac{\partial \ddot{X}_T}{\partial X} = C_T \left\{ \rho V_a^2 \left[\frac{TZ\Omega - (Y\dot{Z} - Z\dot{Y}_a)\frac{\partial T}{\partial X}}{T^2} \right] + \frac{Y\dot{Z} - Z\dot{Y}_a}{T} \frac{\partial(\rho V_a^2)}{\partial X} \right\}$$ (B-64)

$$\frac{\partial \ddot{Y}_T}{\partial X} = C_T \left\{ \rho V_a^2 \left[\frac{-T\dot{Z} - (Z\dot{X}_a - X\dot{Z})\frac{\partial T}{\partial X}}{T^2} \right] + \frac{Z\dot{X}_a - X\dot{Z}}{T} \frac{\partial(\rho V_a^2)}{\partial X} \right\}$$ (B-65)

$$\frac{\partial \ddot{Z}_T}{\partial X} = C_T \left\{ \rho V_a^2 \left[\frac{T(\dot{Y}_a - \Omega X) - (X\dot{Y}_a - Y\dot{X}_a)\frac{\partial T}{\partial X}}{T^2} \right] + \frac{X\dot{Y}_a - Y\dot{X}_a}{T} \frac{\partial(\rho V_a^2)}{\partial X} \right\}$$ (B-66)

$$\frac{\partial \ddot{X}_T}{\partial Y} = C_T \left\{ \rho V_a^2 \left[\frac{T\dot{Z} - (Y\dot{Z} - Z\dot{Y}_a)\frac{\partial T}{\partial Y}}{T^2} \right] + \frac{Y\dot{Z} - Z\dot{Y}_a}{T} \frac{\partial(\rho V_a^2)}{\partial Y} \right\}$$ (B-67)

$$\frac{\partial \ddot{Y}_T}{\partial Y} = C_T \left\{ \rho V_a^2 \left[\frac{TZ\Omega - (Z\dot{X}_a - X\dot{Z})\frac{\partial T}{\partial Y}}{T^2} \right] + \frac{Z\dot{X}_a - X\dot{Z}}{T} \frac{\partial(\rho V_a^2)}{\partial Y} \right\}$$ (B-68)

$$\frac{\partial \ddot{Z}_T}{\partial Y} = C_T \left\{ \rho V_a^2 \left[\frac{-T(\ddot{x}_a + \Omega Y) - (x\dot{y}_a - y\dot{x}_a)\frac{\partial T}{\partial Y}}{T^2} \right] + \frac{x\dot{y}_a - y\dot{x}_a}{T} \frac{\partial(\rho V_a^2)}{\partial Y} \right\} \qquad \text{(B-69)}$$

$$\frac{\partial \ddot{X}_T}{\partial Z} = C_T \left\{ \rho V_a^2 \left[\frac{-T\dot{y}_a - (y\dot{Z} - Z\dot{y}_a)\frac{\partial T}{\partial Z}}{T^2} \right] + \frac{y\dot{Z} - Z\dot{y}_a}{T} \frac{\partial(\rho V_a^2)}{\partial Z} \right\} \qquad \text{(B-70)}$$

$$\frac{\partial \ddot{Z}_T}{\partial Z} = C_T \left\{ \rho V_a^2 \left[\frac{-(x\dot{y}_a - y\dot{x}_a)\frac{\partial T}{\partial Z}}{T^2} \right] + \frac{x\dot{y}_a - y\dot{x}_a}{T} \frac{\partial(\rho V_a^2)}{\partial Z} \right\} \qquad \text{(B-71)}$$

$$\frac{\partial \ddot{Y}_T}{\partial Z} = C_T \left\{ \rho V_a^2 \left[\frac{T\dot{x}_a - (Z\dot{x}_a - x\dot{Z})\frac{\partial T}{\partial Z}}{T^2} \right] + \frac{Z\dot{x}_a - x\dot{Z}}{T} \frac{\partial(\rho V_a^2)}{\partial Z} \right\} \qquad \text{(B-72)}$$

$$\frac{\partial \ddot{X}_T}{\partial X} = C_T \left\{ \rho V_a^2 \left[\frac{-(y\dot{Z} - Z\dot{y})\frac{\partial T}{\partial X}}{T^2} \right] + \frac{y\dot{Z} - Z\dot{y}_a}{T} \frac{\partial(\rho V_a^2)}{\partial \dot{X}} \right\} \qquad \text{(B-73)}$$

$$\frac{\partial \ddot{Y}_T}{\partial X} = C_T \left\{ \rho V_a^2 \left[\frac{TZ - (Z\dot{x}_a - x\dot{Z})\frac{\partial T}{\partial X}}{T^2} \right] + \frac{Z\dot{x}_a - x\dot{Z}}{T} \frac{\partial(\rho V_a^2)}{\partial X} \right\} \qquad \text{(B-74)}$$

$$\frac{\partial \ddot{Z}_T}{\partial X} = C_T \left\{ \rho V_a^2 \left[\frac{-TY - (x\dot{y}_a - y\dot{x}_a)\frac{\partial T}{\partial X}}{T^2} \right] + \frac{x\dot{y}_a - y\dot{x}_a}{T} \frac{\partial(\rho V_a^2)}{\partial X} \right\} \qquad \text{(B-75)}$$

$$\frac{\partial \ddot{X}_T}{\partial \dot{Y}} = C_T \left\{ \rho V_a^2 \left[\frac{-TZ - (y\dot{Z} - Z\dot{y})\frac{\partial T}{\partial \dot{Y}}}{T^2} \right] + \frac{y\dot{Z} - Z\dot{y}_a}{T} \frac{\partial(\rho V_a^2)}{\partial \dot{Y}} \right\} \qquad \text{(B-76)}$$

$$\frac{\partial \ddot{Y}_T}{\partial \dot{Y}} = C_T \left\{ \rho V_a^2 \left[\frac{-(Z\dot{x}_a - x\dot{Z})\frac{\partial T}{\partial \dot{Y}}}{T^2} \right] + \frac{Z\dot{x}_a - x\dot{Z}}{T} \frac{\partial(\rho V_a^2)}{\partial \dot{Y}} \right\} \qquad \text{(B-77)}$$

$$\frac{\partial \ddot{Z}_T}{\partial \dot{Y}} = C_T \left\{ \rho V_a^2 \left[\frac{TX - (x\dot{y}_a - y\dot{x}_a)\frac{\partial T}{\partial \dot{Y}}}{T^2} \right] + \frac{x\dot{y}_a - y\dot{x}_a}{T} \frac{\partial(\rho V_a^2)}{\partial \dot{Y}} \right\} \qquad \text{(B-78)}$$

$$\frac{\partial \ddot{X}_T}{\partial \dot{Z}} = C_T \left\{ \rho V_a^2 \left[\frac{TY - (y\dot{Z} - Z\dot{y})\frac{\partial T}{\partial \dot{Z}}}{T^2} \right] + \frac{y\dot{Z} - Z\dot{y}_a}{T} \frac{\partial(\rho V_a^2)}{\partial \dot{Z}} \right\} \qquad \text{(B-79)}$$

$$\frac{\partial \ddot{Y}_T}{\partial \dot{Z}} = C_T \left\{ \rho V_a^2 \left[\frac{-TX - (Z\dot{x}_a - x\dot{Z})\frac{\partial T}{\partial \dot{Z}}}{T^2} \right] + \frac{Z\dot{x}_a - x\dot{Z}}{T} \frac{\partial(\rho V_a^2)}{\partial \dot{Z}} \right\} \qquad \text{(B-80)}$$

132

$$\frac{\partial \ddot{Z}_T}{\partial \dot{Z}} = G_r \left\{ \rho k_a^2 \left[\frac{-(X\dot{Y}_a - Y\dot{X}_a)\frac{\partial T}{\partial Z}}{T^2} \right] + \frac{X\dot{Y}_a - Y\dot{X}_a}{T} \frac{\partial (\rho k_a^2)}{\partial \dot{Z}} \right\} \tag{B-81}$$

where

$$\frac{\partial T}{\partial X} = \frac{(Y\dot{Z} - Z\dot{Y})Z\Omega - (Z\dot{X}_a - X\dot{Z})\dot{Z} + (X\dot{Y}_a - Y\dot{X}_a)(\dot{Y}_a - X\Omega)}{T} \tag{B-82}$$

$$\frac{\partial T}{\partial Y} = \frac{(Y\dot{Z} - Z\dot{Y})\dot{Z} + (Z\dot{X}_a - X\dot{Z}_a)Z\Omega - (X\dot{Y}_a - Y\dot{X}_a)(\dot{X}_a + \Omega Y)}{T} \tag{B-83}$$

$$\frac{\partial T}{\partial Z} = \frac{-(Y\dot{Z} - Z\dot{Y})\dot{Y}_a + (Z\dot{X}_a - X\dot{Z})\dot{X}_a}{T} \tag{B-84}$$

$$\frac{\partial T}{\partial \dot{X}} = \frac{(Z\dot{X}_a - X\dot{Z})Z - (X\dot{Y}_a - Y\dot{X}_a)Y}{T} \tag{B-85}$$

$$\frac{\partial T}{\partial \dot{Y}} = \frac{-(Y\dot{Z} - Z\dot{Y})Z + (X\dot{Y}_a - Y\dot{X}_a)X}{T} \tag{B-86}$$

$$\frac{\partial T}{\partial \dot{Z}} = \frac{(Y\dot{Z} - Z\dot{Y})Y - (Z\dot{X}_a - X\dot{Z})X}{T} \tag{B-87}$$

and where

$$\frac{\partial (\rho k_a^2)}{\partial X} = -\rho \left(2\dot{Y}_a \Omega + \frac{X V_a^2}{7000 r} \right) \tag{B-88}$$

$$\frac{\partial (\rho k_a^2)}{\partial Y} = \rho \left(2\dot{X}_a \Omega - \frac{Y V_a^2}{7000 r} \right) \tag{B-89}$$

$$\frac{\partial (\rho k_a^2)}{\partial Z} = -\frac{\rho Z V_a^2}{7000 r} \tag{B-90}$$

$$\frac{\partial(\rho V_a^2)}{\partial \ddot{X}} = 2\rho \qquad\qquad\text{(B-91)}$$

$$\frac{\partial(\rho V_a^2)}{\partial \dot{Y}} = 2\rho \dot{Y}_a \qquad\qquad\text{(B-92)}$$

$$\frac{\partial(\rho V_a^2)}{\partial \dot{Z}} = 2\rho \dot{Z} \qquad\qquad\text{(B-93)}$$

Additionally

$$\frac{\partial \ddot{X}_T}{\partial C_T} = \rho V_a^2 \frac{(Y\dot{Z} - Z\dot{Y}_a)}{T} \qquad\qquad\text{(B-94)}$$

$$\frac{\partial \ddot{Y}_T}{\partial C_T} = \rho V_a^2 \frac{(Z\dot{X}_a - X\dot{Z})}{T} \qquad\qquad\text{(B-95)}$$

$$\frac{\partial \ddot{Z}_T}{\partial C_T} = \rho V_a^2 \frac{(X\dot{Y}_a - Y\dot{X}_a)}{T} \qquad\qquad\text{(B-96)}$$

Partials of $\ddot{X}_T$, $\ddot{Y}_T$, and $\ddot{Z}_T$ wrt β_o and C_c are all zero.

Partials of Climb Acceleration

The components of the acceleration due to climb from Chapter II are

$$\ddot{X}_c = C_c \rho V_a \left[\frac{\dot{Y}_a(X\dot{Y}_a - Y\dot{X}_a) - \dot{Z}(Z\dot{X}_a - X\dot{Z})}{T} \right] \qquad\qquad\text{(B-97)}$$

$$\ddot{Y}_c = C_c \rho V_a \left[\frac{\dot{Z}(Y\dot{Z} - Z\dot{Y}_a) - \dot{X}_a(X\dot{Y}_a - Y\dot{X}_a)}{T} \right] \qquad\qquad\text{(B-98)}$$

134

$$\ddot{Z}_c = C_c \rho V_a \left[\frac{\dot{X}_a(Z\dot{X}_a - X\dot{Z}) - \dot{Y}_a(Y\dot{Z} - Z\dot{Y}_a)}{T} \right] \qquad (B\text{-}99)$$

from which the partials of the climb acceleration with respect to the state elements are

$$\frac{\partial \ddot{X}_c}{\partial X} = C_c \left\{ \rho V_a \left[\frac{T\left[\dot{Y}_a^2 + \dot{Z}^2 - \Omega\left(2X\dot{Y}_a - Y\dot{X}_a\right)\right] - \left[\dot{Y}_a(X\dot{Y}_a - Y\dot{X}_a) - \dot{Z}(Z\dot{X}_a - X\dot{Z})\right]\frac{\partial T}{\partial X}}{T^2} \right] \right.$$
$$\left. + \frac{\dot{Y}_a(X\dot{Y}_a - Y\dot{X}_a) - \dot{Z}(Z\dot{X}_a - X\dot{Z})}{T} \frac{\partial(\rho V_a)}{\partial X} \right\} \qquad (B\text{-}100)$$

$$\frac{\partial \ddot{Y}_c}{\partial X} = C_c \left\{ \rho V_a \left[\frac{T\left[-\dot{X}_a\dot{Y}_a + \Omega\left(Z\dot{Z} + X\dot{X}_a\right)\right] - \left[\dot{Z}(Y\dot{Z} - Z\dot{Y}_a) - \dot{X}_a(X\dot{Y}_a - Y\dot{X}_a)\right]\frac{\partial T}{\partial X}}{T^2} \right] \right.$$
$$\left. + \frac{\dot{Z}(Y\dot{Z} - Z\dot{Y}_a) - \dot{X}_a(X\dot{Y}_a - Y\dot{X}_a)}{T} \frac{\partial(\rho V_a)}{\partial X} \right\} \qquad (B\text{-}101)$$

$$\frac{\partial \ddot{Z}_c}{\partial X} = C_c \left\{ \rho V_a \left[\frac{T\left[-\dot{X}_a\dot{Y}_a - \Omega\left(2Z\dot{Y}_a - Y\dot{Z}\right)\right] - \left[\dot{X}_a(Z\dot{X}_a - X\dot{Z}) - (Y\dot{Z} - Z\dot{Y}_a)\dot{Y}_a\right]\frac{\partial T}{\partial X}}{T^2} \right] \right.$$
$$\left. + \frac{\dot{X}_a(Z\dot{X}_a - X\dot{Z}) - \dot{Y}_a(Y\dot{Z} - Z\dot{Y}_a)}{T} \frac{\partial(\rho V_a)}{\partial X} \right\} \qquad (B\text{-}102)$$

$$\frac{\partial \ddot{X}_c}{\partial Y} = C_c \left\{ \rho V_a \left[\frac{T\left[-\dot{X}_a\dot{Y}_a - \Omega\left(\dot{Y}Y + Z\dot{Z}\right)\right] - \left[\dot{Y}_a(X\dot{Y}_a - Y\dot{X}_a) - \dot{Z}(Z\dot{X}_a - X\dot{Z})\right]\frac{\partial T}{\partial Y}}{T^2} \right] \right.$$
$$\left. + \frac{\dot{Y}_a(X\dot{Y}_a - Y\dot{X}_a) - \dot{Z}(Z\dot{X}_a - X\dot{Z})}{T} \frac{\partial(\rho V_a)}{\partial Y} \right\} \qquad (B\text{-}103)$$

$$\frac{\partial \ddot{Y}_c}{\partial Y} = C_c \left\{ \rho V_a \left[\frac{T\left[-\dot{x}_a \dot{y}_a - \Omega(y\dot{y}_a + z\dot{z})\right] - \left[\dot{y}_a(x\dot{y}_a - y\dot{x}_a) - \dot{z}(z\dot{x}_a - x\dot{z})\right]\frac{\partial T}{\partial Y}}{T^2} \right] \right.$$

$$\left. + \frac{\dot{z}(y\dot{z} - z\dot{y}_a) - \dot{x}_a(x\dot{y}_a - y\dot{x}_a)}{T} \frac{\partial(\rho V_a)}{\partial Y} \right\} \qquad \text{(B-104)}$$

$$\frac{\partial \ddot{Z}_c}{\partial Y} = C_c \left\{ \rho V_a \left[\frac{T\left[-\dot{y}_a Z + \Omega(2z\dot{x}_a - x\dot{z})\right] - \left[\dot{x}_a(z\dot{x}_a - x\dot{z}) - \dot{y}_a(y\dot{z} - z\dot{y}_a)\right]\frac{\partial T}{\partial Y}}{T^2} \right] \right.$$

$$\left. + \frac{\dot{x}_a(z\dot{x}_a - x\dot{z}) - \dot{y}_a(y\dot{z} - z\dot{y}_a)}{T} \frac{\partial(\rho V_a)}{\partial Y} \right\} \qquad \text{(B-105)}$$

$$\frac{\partial \ddot{X}_c}{\partial Z} = C_c \left\{ \rho V_a \left[\frac{-T\dot{x}_a \dot{z} - \left[\dot{y}_a(x\dot{y}_a - y\dot{x}_a) - \dot{z}(z\dot{x}_a - x\dot{z})\right]\frac{\partial T}{\partial Z}}{T^2} \right] \right.$$

$$\left. + \frac{\dot{y}_a(x\dot{y}_a - y\dot{x}_a) - \dot{z}(z\dot{x}_a - x\dot{z})}{T} \frac{\partial(\rho V_a)}{\partial Z} \right\} \qquad \text{(B-106)}$$

$$\frac{\partial \ddot{Y}_c}{\partial Z} = C_c \left\{ \rho V_a \left[\frac{-T\dot{y}_a \dot{z} - \left[\dot{z}(y\dot{z} - \dot{y}_a z) - \dot{x}_a(x\dot{y}_a - y\dot{x}_a)\right]\frac{\partial T}{\partial Z}}{T^2} \right] \right.$$

$$\left. + \frac{\dot{z}(y\dot{z} - z\dot{y}_a) - \dot{x}_a(x\dot{y}_a - y\dot{x}_a)}{T} \frac{\partial(\rho V_a)}{\partial Z} \right\} \qquad \text{(B-107)}$$

$$\frac{\partial \ddot{Z}_c}{\partial Z} = C_c \left\{ \rho V_a \left[\frac{T(\dot{x}_a^2 + \dot{y}_a^2) - \left[\dot{x}_a(z\dot{x}_a - x\dot{z}) - \dot{y}_a(y\dot{z} - z\dot{y}_a)\right]\frac{\partial T}{\partial Z}}{T^2} \right] \right.$$

$$\left. + \frac{\dot{x}_a(z\dot{x}_a - x\dot{z}) - \dot{y}_a(y\dot{z} - z\dot{y}_a)}{T} \frac{\partial(\rho V_a)}{\partial Z} \right\} \qquad \text{(B-108)}$$

$$\frac{\partial \ddot{X}_c}{\partial \dot{X}} = C_c \left\{ \rho V_a \left[\frac{T(-y\dot{y}_a - z\dot{z}) - \left[\dot{y}_a(x\dot{y}_a - y\dot{x}_a) - \dot{z}(z\dot{x}_a - x\dot{z})\right]\frac{\partial T}{\partial \dot{X}}}{T^2} \right] \right.$$

$$\left. + \frac{\dot{y}_a(x\dot{y}_a - y\dot{x}_a) - z(z\dot{x}_a - x\dot{z})}{T} \frac{\partial(\rho V_a)}{\partial \dot{X}} \right\} \qquad \text{(B-109)}$$

136

$$\frac{\partial \ddot{Y}_c}{\partial X} = C_c \left\{ \rho V_a \left[\frac{T(-X\dot{Y}_a + 2Y\dot{X}_a) - [\dot{Z}(Y\dot{Z} - Z\dot{Y}_a) - \dot{X}_a(X\dot{Y}_a - Y\dot{X}_a)]\frac{\partial T}{\partial X}}{T^2} \right] \right.$$

$$\left. + \frac{\dot{Z}(Y\dot{Z} - Z\dot{Y}_a) - \dot{X}_a(X\dot{Y}_a - Y\dot{X}_a)}{T} \frac{\partial(\rho V_a)}{\partial X} \right\} \quad \text{(B-110)}$$

$$\frac{\partial \ddot{Z}_c}{\partial X} = C_c \left\{ \rho V_a \left[\frac{T(2Z\dot{X}_a - X\dot{Z}) - [\dot{X}_a(Z\dot{X}_a - X\dot{Z}) - \dot{Y}_a(Y\dot{Z} - Z\dot{Y}_a)]\frac{\partial T}{\partial X}}{T^2} \right] \right.$$

$$\left. + \frac{\dot{X}_a(Z\dot{X}_a - X\dot{Z}) - \dot{Y}_a(Y\dot{Z} - Z\dot{Y}_a)}{T} \frac{\partial(\rho V_a)}{\partial X} \right\} \quad \text{(B-111)}$$

$$\frac{\partial \ddot{X}_c}{\partial Y} = C_c \left\{ \rho V_a \left[\frac{T(2X\dot{Y}_a - Y\dot{X}_a) - [\dot{Y}_c(X\dot{Y}_a - Y\dot{X}_c) - \dot{Z}(Z\dot{X}_a - X\dot{Z})]\frac{\partial T}{\partial Y}}{T^2} \right] \right.$$

$$\left. + \frac{\dot{Y}_a(X\dot{Y}_a - Y\dot{X}_a) - \dot{Z}(Z\dot{X}_a - X\dot{Z})}{T} \frac{\partial(\rho V_a)}{\partial Y} \right\} \quad \text{(B-112)}$$

$$\frac{\partial \ddot{Y}_c}{\partial Y} = C_c \left\{ \rho V_a \left[\frac{T(Z\dot{Z} - X\dot{X}_a) - [\dot{Z}(Y\dot{Z} - Z\dot{Y}_a) - \dot{X}_a(X\dot{Y}_a - Y\dot{X}_a)]\frac{\partial T}{\partial Y}}{T^2} \right] \right.$$

$$\left. + \frac{\dot{Z}(Y\dot{Z} - Z\dot{Y}) - \dot{X}_a(X\dot{Y}_a - Y\dot{X}_a)}{T} \frac{\partial(\rho V_a)}{\partial Y} \right\} \quad \text{(B-113)}$$

$$\frac{\partial \ddot{Z}_c}{\partial Y} = C_c \left\{ \rho V_a \left[\frac{T(-Y\dot{Z} + 2Z\dot{Y}_a) - [\dot{X}(Z\dot{X}_a - X\dot{Z}) - \dot{Y}_a(Y\dot{Z} - Z\dot{Y}_a)]\frac{\partial T}{\partial Y}}{T^2} \right] \right.$$

$$\left. + \frac{\dot{X}_a(Z\dot{X}_a - X\dot{Z}) - \dot{Y}_a(Y\dot{Z} - Z\dot{Y}_a)}{T} \frac{\partial(\rho V_a)}{\partial Y} \right\} \quad \text{(B-114)}$$

$$\frac{\partial \ddot{X}_c}{\partial Z} = C_c \left\{ \rho V_a \left[\frac{T(-Z\dot{X}_a - 2X\dot{Z}) - [\dot{Y}_a(X\dot{Y}_a - Y\dot{X}_a) - \dot{Z}(Z\dot{X}_a - X\dot{Z})]\frac{\partial T}{\partial Z}}{T^2} \right] \right.$$

$$\left. + \frac{\dot{Y}_a(X\dot{Y}_a - Y\dot{X}_a) - \dot{Z}(Z\dot{X}_a - X\dot{Z})}{T} \frac{\partial(\rho V_a)}{\partial Z} \right\} \quad \text{(B-115)}$$

$$\frac{\partial \ddot{Y}_c}{\partial \dot{Z}} = C_c \left\{ \rho V_a \left[\frac{T(2Y\dot{Z} - Z\dot{Y}_a) - [\dot{Z}(Y\dot{Z} - Z\dot{Y}_a) - \dot{X}_a(X\dot{Y}_a - Y\dot{X}_a)]\frac{\partial T}{\partial \dot{Z}}}{T^2} \right] \right.$$

$$\left. + \frac{\dot{Z}(Y\dot{Z} - Z\dot{Y}) - \dot{X}_a(X\dot{Y}_a - Y\dot{X}_a)}{T} \frac{\partial(\rho V_a)}{\partial \dot{Z}} \right\} \quad \text{(B-116)}$$

$$\frac{\partial \ddot{Z}_c}{\partial \dot{Z}} = C_c \left\{ \rho V_a \left[\frac{T(-X\dot{X} - Y\dot{Y}) - [\dot{X}_a(Z\dot{X}_a - X\dot{Z}) - \dot{Y}_a(Y\dot{Z} - Z\dot{Y}_a)]\frac{\partial T}{\partial \dot{Z}}}{T^2} \right] \right.$$

$$\left. + \frac{\dot{X}_a(Z\dot{X}_a - X\dot{Z}) - \dot{Y}_a(Y\dot{Z} - Z\dot{Y})}{T} \frac{\partial(\rho V_a)}{\partial \dot{Z}} \right\} \quad \text{(B-117)}$$

where the partials of T are as given in the previous section and

$$\frac{\partial(\rho V_a)}{\partial X} = -\rho \frac{\dot{Y}_a \Omega}{V_a} - \frac{V_a \rho Y}{7000r} \quad \text{(B-118)}$$

$$\frac{\partial(\rho V_a)}{\partial Y} = \rho \frac{\dot{X}_a \Omega}{V_a} - \frac{V_a \rho Y}{7000r} \quad \text{(B-119)}$$

$$\frac{\partial(\rho V_a)}{\partial Z} = -\rho \frac{V_a Z}{7000r} \quad \text{(B-120)}$$

$$\frac{\partial(\rho V_a)}{\partial \dot{X}} = \rho \frac{\dot{X}_a}{V_a} \quad \text{(B-121)}$$

$$\frac{\partial(\rho V_a)}{\partial \dot{Y}} = \rho \frac{\dot{Y}_a}{V_a} \quad \text{(B-122)}$$

$$\frac{\partial(\rho V_a)}{\partial \dot{Z}} = \rho \frac{\dot{Z}_a}{V_a} \quad \text{(L-123)}$$

The partials of $\ddot{X}_c$, $\ddot{Y}_c$, and $\ddot{Z}_c$ wrt β_o and C_T are all zero and

138

$$\frac{\partial \ddot{X}}{\partial C_c} = \rho k_a \left[\frac{\dot{Y}_a (X\dot{Y}_a - Y\dot{X}_a) - \dot{Z}(Z\dot{X}_a - X\dot{Z})}{T} \right] \qquad \text{(B-124)}$$

$$\frac{\partial \ddot{Y}}{\partial C_c} = \rho k_a \left[\frac{\dot{Z}(Y\dot{Z} - Z\dot{Y}_a) - \dot{X}_a (X\dot{Y}_a - Y\dot{X}_a)}{T} \right] \qquad \text{(B-125)}$$

$$\frac{\partial \ddot{Z}}{\partial C_c} = \rho k_a \left[\frac{\dot{X}_a (Z\dot{X}_a - X\dot{Z}) - \dot{Y}_a (Y\dot{Z} - Z\dot{Y}_a)}{T} \right] \qquad \text{(B-126)}$$

With the partials of acceleration with respect to state elements given in this and previous sections and equations (B-9) through (B-18) all of the elements of $\Phi(t_{i+1}, t_i)$ are at hand.

Vita

Larry Neale Lillard was born on 22 September 1938 in Marked Tree, Arkansas. He attended public school graduating from Marked Tree High School in 1956. After spending two years in the Air Force from 1959 to 1961, he returned to Arkansas State College and graduated in 1964 with a Bachelor of Science degree with a major in Mathematics. After graduation, he was employed by the Aeronautical Chart and Information Center in St. Louis. While there he was selected to do graduate study at the University of Illinois. He graduated from the University of Illinois in 1966 with a Master of Science degree in Civil Engineering.

Since 1967, he has been employed by the Air Force Foreign Technology Division at Wright-Patterson AFB, Ohio. He is presently Team Leader of the Reentry Team of the Trajectory Analysis Group, Engineering Data Division.

Permanent address: 4357 Elmshaven Dr.
Dayton, Oh. 45424

This thesis was typed by Mrs. Sharon Maruna.

REPORT DOCUMENTATION PAGE	READ INSTRUCTIONS BEFORE COMPLETING FORM	
1. REPORT NUMBER AFIT/GA/AA/82D-5	2. GOVT ACCESSION NO. AD-A124 885	3. RECIPIENT'S CATALOG NUMBER
4. TITLE (and Subtitle) POST-FLIGHT TRAJECTORY RECONSTRUCTION OF A MANEUVERING REENTRY VEHICLE FROM RADAR MEASUREMENTS	5. TYPE OF REPORT & PERIOD COVERED MS Thesis	
	6. PERFORMING ORG. REPORT NUMBER	
7. AUTHOR(s) Larry N. Lillard	8. CONTRACT OR GRANT NUMBER(s)	
9. PERFORMING ORGANIZATION NAME AND ADDRESS Air Force Institute of Technology (AFIT-EN) Wright-Patterson AFB, Ohio 45433	10. PROGRAM ELEMENT. PROJECT. TASK AREA & WORK UNIT NUMBERS	
11. CONTROLLING OFFICE NAME AND ADDRESS	12. REPORT DATE Dec 1982	
	13. NUMBER OF PAGES 150	
14. MONITORING AGENCY NAME & ADDRESS(if different from Controlling Office)	15. SECURITY CLASS. (of this report) Unclassified	
	15a. DECLASSIFICATION/DOWNGRADING SCHEDULE	

16. DISTRIBUTION STATEMENT (of this Report)

Approved for public release; distribution unlimited.

17. DISTRIBUTION STATEMENT (of the abstract entered in Block 20, if different from Report)

18. SUPPLEMENTARY NOTES

Approved for Public release IAW AFR 190-17.

LYNN E. WOLAVER
Dean for Research and Professional Development
Air Force Institute of Technology (ATC)

4 JAN 1983

19. KEY WORDS (Continue on reverse side if necessary and identify by block number)

Maneuvering Reentry Vehicle
Weighted Least Squares

20. ABSTRACT (Continue on reverse side if necessary and identify by block number)

A technique for determining the aerodynamic parameters of a maneuvering reentry vehicle (MaRV) from post-flight analysis of radar tracking data was developed. The technique uses a sequential weighted least squares estimator which steps through the data processing batches of data sequentially. The observations consisted of angle and range measurements from a precision tracking radar located in the vicinity of the impact area.

DD FORM 1473 EDITION OF 1 NOV 65 IS OBSOLETE

A six dimension estimator consisting of three position and three velocity components was designed for estimating the state of the RV during free flight. Two reentry estimators were developed. One, a seven dimension estimator consisting of the six elements of the free-flight estimator plus the ballistic coefficient, was designed to estimate the state during ballistic reentry. The second is the nine element MaRV estimator used once a maneuver is begun. An algorithm based on measurement residual monitoring was developed to switch adaptively from the six-state estimator to the seven-state estimator and then to the nine-state estimator. A series of numerical simulations was performed to validate the technique and its programming. Monte Carlo simulations were used to verify the accuracy of the estimator covariance matrix.

END

FILMED

3-83

DTIC